

Supplementary File of “Evolutionary Many-Objective Optimization Based on Adversarial Decomposition”

Mengyuan Wu, Ke Li, Sam Kwong, *Fellow, IEEE*, and Qingfu Zhang, *Fellow, IEEE*

Abstract—The paper entitled “Evolutionary Many-Objective Optimization Based on Adversarial Decomposition” develops an adversarial decomposition method that leverages the complementary characteristics of two different scalarizing functions within a single paradigm. More specifically, we maintain two co-evolving populations simultaneously by using different scalarizing functions. In order to avoid allocating redundant computational resources to the same region of the Pareto front, we stably match these two co-evolving populations into one-one solution pairs according to their working regions upon the Pareto front. Then, each solution pair can at most contribute one principal mating parent during the mating selection process. Due to the page limits of the paper, we present some experimental studies in this supplementary file.

III. MANY-OBJECTIVE OPTIMIZATION ALGORITHM BASED ON ADVERSARIAL DECOMPOSITION

IV. EXPERIMENTAL SETUP

D. Peer Algorithms

Some further comments on the peer algorithms are listed as follows.

- *MOEA/D* uses the original PBI function with $\theta = 5.0$ for the DTLZ and WFG test problems. As for the $DTLZ^{-1}$ and WFG^{-1} test problems, it uses the inverted PBI function [1] with $\theta = 0.1$ as suggested in [2]. Note that the inverted PBI function replaces the ideal point with the nadir point in (3).
- *Global WASF-GA* is a decomposition-based algorithm that selects solutions to survive according to the rankings of solutions by each subproblem. It adopts the ideal and nadir points simultaneously for subproblem formulations. Instead of co-evolving two populations, Global WASF-GA only has a single population, where half of the solutions are evolved toward the ideal point, while the others are pushed backward from the nadir point.
- *PICEA-g* co-evolves a set of target vectors sampled in the objective space, which can be regarded as a second population. The second population act as goals to guide the environmental selection by setting the fitness of a solution based on the number of target vectors it dominates.

M. Wu, S. Kwong and Q. Zhang are with the Department of Computer Science, City University of Hong Kong, Kowloon, Hong Kong SAR (e-mail: mengyuan.wu@my.cityu.edu.hk, cssamk@cityu.edu.hk, qingfu.zhang@cityu.edu.hk).

K. Li is with the College of Engineering, Mathematics and Physical Sciences, University of Exeter, Exeter, EX4 4QF, UK (e-mail: k.li@exeter.ac.uk).

Algorithm 2: PopulationUpdate(S_c, S_d, \bar{x}, W)

```

Input:  $S_c, S_d, W$  and an offspring solution  $\bar{x}$ 
Output: Updated  $S_c$  and  $S_d$ 
1 for  $i \leftarrow 1$  to  $N$  do
2    $D_d[i] \leftarrow d_2(\bar{F}(\bar{x})|\mathbf{w}^i, \mathbf{0});$ 
3    $i_d \leftarrow \underset{0 \leq i \leq N}{\operatorname{argmin}} D_d[i]$ 
4   if  $\bar{g}^d(\bar{x}|\mathbf{w}^{i_d}) \leq \bar{g}^d(\mathbf{x}_d^{i_d}|\mathbf{w}^{i_d})$  then
5      $\mathbf{x}_d^{i_d} \leftarrow \bar{x};$ 
6   for  $i \leftarrow 1$  to  $N$  do
7      $D_c[i] \leftarrow d_2(\bar{F}(\bar{x})|\mathbf{w}^i, \mathbf{1});$ 
8    $I_c \leftarrow$  Sort  $D_c$  in ascending order and return the indexes;
9    $t \leftarrow 0;$ 
10  for  $i \leftarrow 1$  to  $N$  do
11    if  $\bar{g}^c(\bar{x}|\mathbf{w}^{I_c[i]}) \leq \bar{g}^c(\mathbf{x}_c^{I_c[i]}|\mathbf{w}^{I_c[i]})$  then
12       $\mathbf{x}_c^{I_c[i]} \leftarrow \bar{x}, t++;$ 
13       $\mathbf{x}_c^{I_c[i]}.closeness \leftarrow i, \mathbf{x}_c^{I_c[i]}.closestP \leftarrow I_c[0];$ 
14      if  $t == nr_c$  then
15        break;
16 return  $S_c, S_d;$ 

```

- *Two_Arch2* maintains two archives via indicator-based selection and Pareto-based selection separately. In particular, an L_p -norm-based diversity maintenance scheme is designed to maintain the diversity archive.

V. EXPERIMENTAL STUDIES

A. Comparisons on DTLZ and WFG Test Problems

The mean HV metric values with $\mathbf{z}^r = (2, \dots, 2)^T$ of different algorithms on DTLZ and WFG test problems are given in Table II and Table III.

B. Comparisons on DTLZ⁻¹ and WFG⁻¹ Test Problems

The mean HV metric values with $\mathbf{z}^r = (2, \dots, 2)^T$ of different algorithms on DTLZ⁻¹ and WFG⁻¹ test problems are presented in Table IV and Table V.

D. Comparisons on DTLZ and WFG Test Problems under HV Metric with $\mathbf{z}^r = (1.1, \dots, 1.1)^T$ and IGD Metric

The mean HV metric values with $\mathbf{z}^r = (1.1, \dots, 1.1)^T$ of different algorithms on DTLZ and WFG test problems are

Algorithm 3: Match(S_c, W)

Input: S_c, W
Output: Matching array M and sentinel array R

- 1 Calculate preference lists for S_c and P_d ;
- 2 Compute a two-level stable matching between S_c and P_d ;
- 3 **for** $i \leftarrow 1$ **to** N **do**
- 4 $M[i] \leftarrow$ Index of the matching mate in S_c of x_d^i ;
- 5 **if** x_d^i finds a stable matching mate in the first-level stable matching **then**
- 6 $R[i] \leftarrow 1$; // the i th pair has collaborative information
- 7 **else**
- 8 $R[i] \leftarrow 0$;
- 9 **return** M, R

Algorithm 4: PopSelection(S_c, S_d, i, M, W)

Input: S_c, S_d, W , matching array M and the subproblem index i
Output: population index pop

- 1 **if** $\Delta_d^i > \Delta_c^{M[i]}$ **then**
- 2 $pop \leftarrow 1$; // chosen from S_d
- 3 **else if** $\Delta_d^i < \Delta_c^{M[i]}$ **then**
- 4 $pop \leftarrow 2$; // chosen from S_c
- 5 **else**
- 6 **if** x_d^i is nondominated and $x_c^{M[i]}.closeness > m$ **then**
- 7 $pop \leftarrow 1$;
- 8 **else if** x_d^i is dominated and $x_c^{M[i]}.closeness \leq m$ **then**
- 9 $pop \leftarrow 2$;
- 10 **else**
- 11 $pop \leftarrow$ Randomly select from {1, 2};
- 12 **return** pop ;

given in Table VII and Table VIII. Generally speaking, the comparisons of HV metric values with $\mathbf{z}^r = (1.1, \dots, 1.1)^T$ are similar to those with $\mathbf{z}^r = (2, \dots, 2)^T$. Slight variances can be noticed on some test problems. For example, when using $\mathbf{z}^r = (1.1, \dots, 1.1)^T$, θ -DEA performs significantly better on DTLZ4 test problem, while MOEA/AD becomes the best algorithm on WFG6 test problem. The IGD results are given in Table IX and Table X. Different from the HV metric values, the comparisons of the IGD metric values vary quite much on different test problems with different number of objectives. On DTLZ test suites, MOEA/AD, θ -DEA, MOEA/D-IPBI and Two_Arch2 perform the best on different problems, whereas on WFG4 to WFG9 test problems, NSGA-III achieves comparable results with MOEA/AD and θ -DEA. Coincident with Table VIII, Two_Arch2 are less competitive on WFG6 to WFG9 test problems with regular PF shapes.

Algorithm 5: MatingSelection(S_c, S_d, i, M, R, W, B)

Input: S_c, S_d, W , matching array M and the subproblem index i , sentinel array R , neighborhood structure B
Output: mating parents \bar{S}

- 1 $pop \leftarrow$ PopSelection(S_c, S_d, i, M, W);
- 2 **if** $rand < \delta$ **then**
- 3 $S_p \leftarrow \emptyset$;
- 4 **if** $pop == 1$ **then**
- 5 **for** $j \leftarrow 1$ **to** T **do**
- 6 $S_p \leftarrow S_p \cup \{x_d^{B[i][j]}\}$;
- 7 **if** $R[B[i][j]] == 1$ **then**
- 8 $S_p \leftarrow S_p \cup \{x_c^{M[B[i][j]]}\}$;
- 9 $\mathbf{x}^r \leftarrow$ Randomly select a solution from S_p ;
- 10 $\bar{S} \leftarrow \{x_d^i, \mathbf{x}^r\}$;
- 11 **else**
- 12 **for** $j \leftarrow 1$ **to** T **do**
- 13 **if** $x_c^{B[M[i][j]]}.closestP \neq x_c^{M[i]}.closestP$ **then**
- 14 $S_p \leftarrow S_p \cup \{x_c^{B[M[i][j]]}\}$;
- 15 $\mathbf{x}^r \leftarrow$ Randomly select a solution from S_p ;
- 16 $\bar{S} \leftarrow \{x_c^{M[i]}, \mathbf{x}^r\}$;
- 17 **else**
- 18 $S_p \leftarrow S_c \cup S_d$;
- 19 $\mathbf{x}^r \leftarrow$ Randomly select a solution from S_p ;
- 20 **if** $pop == 1$ **then**
- 21 $\bar{S} \leftarrow \{x_d^i, \mathbf{x}^r\}$;
- 22 **else**
- 23 $\bar{S} \leftarrow \{x_c^{M[i]}, \mathbf{x}^r\}$;
- 24 **return** \bar{S}

E. Comparisons on DTLZ⁻¹ and WFG⁻¹ Test Problems under HV Metric with $\mathbf{z}^r = (1.1, \dots, 1.1)^T$ and IGD Metric

The HV metric values with $\mathbf{z}^r = (1.1, \dots, 1.1)^T$ on DTLZ⁻¹ and WFG⁻¹ test problems are presented in Table XI and Table XII. In this case, Two_Arch2 provides the best HV metric values on most of the minus test problems, which is conflict to the HV comparisons using $\mathbf{z}^r = (2, \dots, 2)^T$ shown in Table IV and Table V. We argue that the worst point $\mathbf{z}^r = (1.1, \dots, 1.1)^T$ is too close to the inverted PFs of the minus problems. As a result, the HV metric are in favor of the solutions located at the center of the PFs. The mean IGD metric values on DTLZ⁻¹ and WFG⁻¹ test problems given in Table XIII and Table XIV are coincident with our explanations, where MOEA/D obtains the best mean IGD metric values on 50 out of 55 test problems.

F. Performance Scores under HV Metric with $\mathbf{z}^r = (1.1, \dots, 1.1)^T$ and IGD Metric

The average performance score of each algorithm on different test problems under HV metric with $\mathbf{z}^r = (1.1, \dots, 1.1)^T$ are shown in Fig. 6. It can be seen from Fig. 6(a) that Two_Arch2 obtains the best average performance score on 3-objective

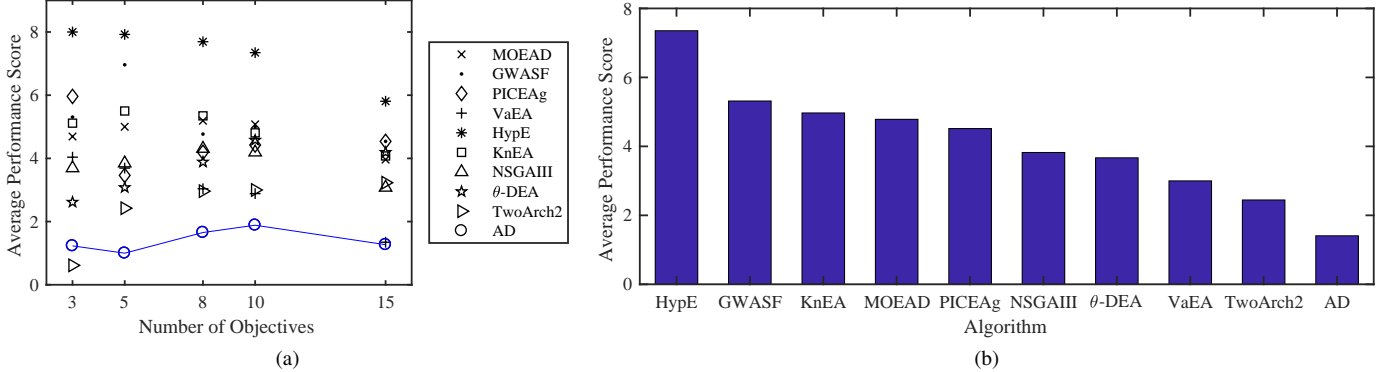


Fig. 6: Average performance scores under HV metric with $\mathbf{z}^r = (1.1, \dots, 1.1)^T$: (a) on test problems with different number of objectives; (b) over all test problems.

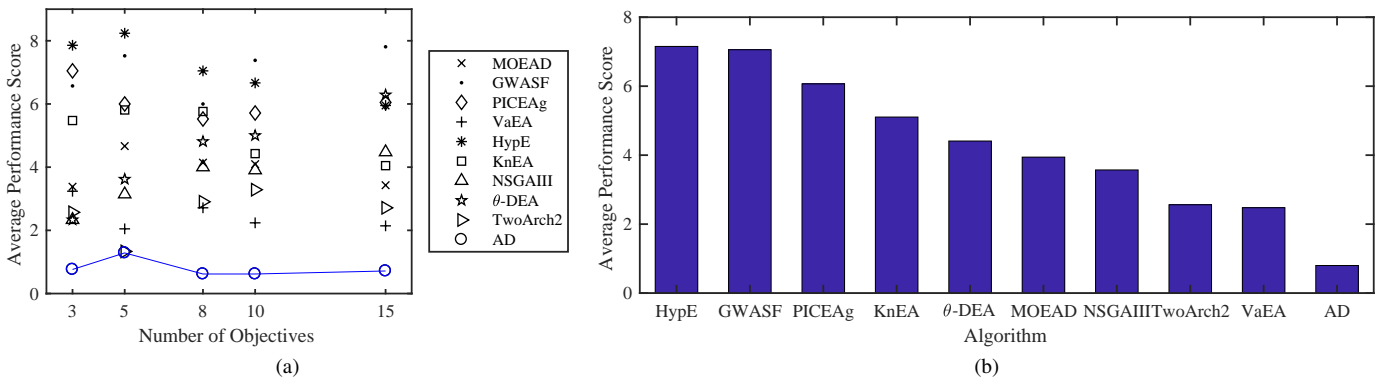


Fig. 7: Average performance scores under IGD metric: (a) on test problems with different number of objectives; (b) over all test problems.

are evolved toward ideal point while the others are evolved backward from the nadir point. Among them, only MOEA/AD employs different subproblem formulations for two populations that follow adversarial search directions. As a consequence, two populations are expected to have complementary search behaviors, i.e., one is diversity-oriented and the other is convergence-oriented. The comparison results under HV metric with $\mathbf{z}^r = (2, \dots, 2)^T$ are shown in Table XV and Table XVI. Due to limitation of the mechanism used to maintain the external population [5], MOEA/D-MR is only run on 3-objective test problems. For DTLZ1 to DTLZ4 test problems, MOEA/AD performs significantly better in 43 out of 44 comparisons. DBEA-DS, which co-evolves two populations using the same subproblem formulations, only outperforms MOEA/AD on 3-objective DTLZ1 test problem. The HV results on DTLZ⁻¹ test problems are similar. Although DBEA-DS obtains better mean metric values on 3 3-objective test problems, its superiority is only significant on 3-objective DTLZ4⁻¹ test problem. When the number of objectives is more than 3, MOEA/AD remains the best algorithms on all test problems.

2) *Adversarial Search Directions:* The adversarial search directions of the two populations in MOEA/AD make it adapt to problems with inverted PFs. In addition, they different search directions also add diversity to the mating process. In

TABLE XV: HV Results of Global WASF-GA, MOEA/D-MR, DBEA-DS and MOEA/AD on DTLZ Test Problems ($\mathbf{z}^r = (2, \dots, 2)^T$).

Problem	m	GWASF	MR	DBEA-DS	MOEA/AD
DTLZ1	3	7.134e+0†	4.562e+0†	7.788e+0‡	7.787e+0
	5	1.965e+1†	—	3.088e+1†	3.197e+1
	8	7.026e+1†	—	0.000e+0†	2.560e+2
	10	4.761e+2†	—	0.000e+0†	1.024e+3
	15	1.092e+3†	—	0.000e+0†	3.270e+4
DTLZ2	3	7.301e+0†	7.321e+0†	7.404e+0†	7.412e+0
	5	3.037e+1†	—	3.110e+1†	3.170e+1
	8	2.423e+2†	—	2.549e+2†	2.558e+2
	10	6.398e+2†	—	8.505e+2†	1.024e+3
	15	1.638e+4†	—	1.426e+4†	3.276e+4
DTLZ3	3	6.504e+0†	1.109e+0†	7.374e+0†	7.403e+0
	5	1.600e+1†	—	0.000e+0†	3.169e+1
	8	1.278e+2†	—	0.000e+0†	2.558e+2
	10	5.115e+2†	—	0.000e+0†	1.024e+3
	15	1.631e+4†	—	0.000e+0†	3.276e+4
DTLZ4	3	6.961e+0†	7.343e+0†	7.376e+0†	7.412e+0
	5	2.710e+1†	—	2.742e+1†	3.169e+1
	8	1.575e+2†	—	7.228e+0†	2.558e+2
	10	7.165e+2†	—	2.611e+1†	1.024e+3
	15	1.636e+4†	—	5.815e+2†	3.276e+4

According to Wilcoxon's rank sum test, † and ‡ indicates whether the corresponding algorithm is significantly worse or better than MOEA/AD respectively.

this experiment, we develop a variant of MOEA/AD, denoted

Algorithm 6: MatingSelectionV2($S_c, S_d, i, M, R, C, W, B$)

Input: S_c, S_d, W , matching array M and the subproblem index i , sentinel array R , neighborhood structure B

Output: mating parents \bar{S}

```

1  $pop \leftarrow \text{PopSelection}(S_c, S_d, i, M, W);$ 
2 if  $rand < \delta$  then
3    $S_p \leftarrow \emptyset;$ 
4   if  $pop == 1$  then
5     for  $j \leftarrow 1$  to  $T$  do
6        $S_p \leftarrow S_p \cup \{\mathbf{x}_d^{B[i][j]}\};$ 
7      $\mathbf{x}^r \leftarrow \text{Randomly select a solution from } S_p;$ 
8      $\bar{S} \leftarrow \{\mathbf{x}_d^i, \mathbf{x}^r\};$ 
9   else
10    for  $j \leftarrow 1$  to  $T$  do
11       $S_p \leftarrow S_p \cup \{\mathbf{x}_c^{B[M[i]][j]}\};$ 
12     $\mathbf{x}^r \leftarrow \text{Randomly select a solution from } S_p;$ 
13     $\bar{S} \leftarrow \{\mathbf{x}_c^{M[i]}, \mathbf{x}^r\};$ 
14 else
15   if  $pop == 1$  then
16      $\mathbf{x}^r \leftarrow \text{Randomly select a solution from } S_d;$ 
17      $\bar{S} \leftarrow \{\mathbf{x}_d^i, \mathbf{x}^r\};$ 
18   else
19      $\mathbf{x}^r \leftarrow \text{Randomly select a solution from } S_c;$ 
20      $\bar{S} \leftarrow \{\mathbf{x}_c^{M[i]}, \mathbf{x}^r\};$ 
21 return  $\bar{S}$ 
```

TABLE XIX: HV Results of MOEA/AD and its Three Variants on DTLZ Test Problems ($\mathbf{z}^r = (2, \dots, 2)^T$).

Problem	m	AD-v1	AD-v2	AD-v3	MOEA/AD
DTLZ1	3	7.785e+0†	7.785e+0†	7.777e+0†	7.787e+0
	5	3.197e+1†	3.196e+1†	3.191e+1†	3.197e+1
	8	2.560e+2†	2.491e+2†	2.499e+2†	2.560e+2
	10	1.008e+3†	9.767e+2†	1.006e+3†	1.024e+3
	15	3.055e+4†	3.186e+4†	3.098e+4†	3.270e+4
DTLZ2	3	7.412e+0	7.412e+0	7.411e+0†	7.412e+0
	5	3.170e+1	3.170e+1	3.170e+1†	3.170e+1
	8	2.558e+2†	2.558e+2†	2.558e+2†	2.558e+2
	10	1.024e+3†	1.024e+3†	1.024e+3†	1.024e+3
	15	3.276e+4	3.276e+4	3.276e+4	3.276e+4
DTLZ3	3	7.405e+0	7.239e+0	7.405e+0	7.403e+0
	5	3.097e+1†	2.877e+1†	3.092e+1†	3.169e+1
	8	2.125e+2†	2.330e+2†	2.058e+2†	2.558e+2
	10	8.783e+2†	8.356e+2†	6.739e+2†	1.024e+3
	15	2.761e+4†	2.574e+4†	2.681e+4†	3.276e+4
DTLZ4	3	7.410e+0†	7.411e+0	7.410e+0†	7.412e+0
	5	3.169e+1	3.169e+1	3.169e+1	3.169e+1
	8	2.558e+2	2.558e+2	2.558e+2	2.558e+2
	10	1.024e+3	1.024e+3	1.024e+3	1.024e+3
	15	3.276e+4	3.276e+4†	3.276e+4	3.276e+4

According to Wilcoxon's rank sum test, † and ‡ indicates whether the corresponding algorithm is significantly worse or better than MOEA/AD respectively.

- The collaboration between two populations help strengthen their complementary behaviors, i.e., one is diversity-oriented and the other is convergence-oriented.
- The three criteria together help to select a promising principal parent solution from a matching pair, which

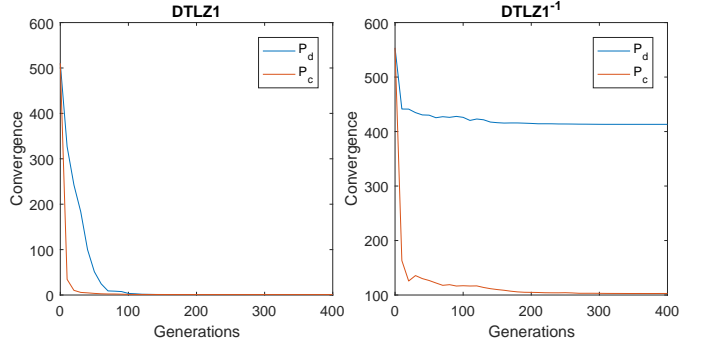


Fig. 8: Online convergence comparisons of two populations.

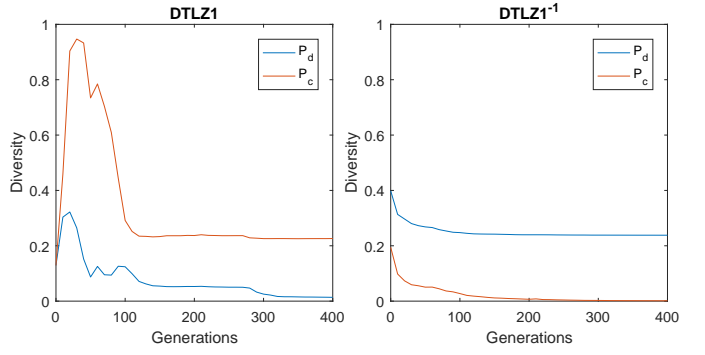


Fig. 9: Online diversity comparisons of two populations.

makes the reproduction more efficient.

H. Online Comparisons of Two Populations

In this subsection, we study the different properties of the two populations during the optimization of 3-objective DTLZ1 and DTLZ1⁻¹ test problems. According to [6], the $g(\mathbf{x})$ of the DTLZ test problem is adopted to assess the convergence of the two populations. A smaller $g(\mathbf{x})$ indicates better convergence of a population for a DTLZ test problem. As shown in Fig. 8(a), the mean $g(\mathbf{x})$ of P_c decreases much earlier than P_d , indicating the better convergence ability of the AASF subproblem formulation. Similar trends of $g(\mathbf{x})$ can be seen in Fig. 8(b). A difference between Fig. 8(a) and Fig. 8(b) is that the convergence of P_c can be as good as P_d on DTLZ1 test problem but not on DTLZ1⁻¹ test problem, which is caused by the limited convergence ability of the PBI subproblem formulation when the search directions are not suitable for the inverted PF. As for the diversity of the two populations, it is not only affected by the subproblem formulations but mainly depends on the search directions. Typically, the population that follows search directions suitable for the orientation of the PF is expected to achieve better diversity, which can be seen in Fig. 9. Note that the diversity measure in Fig. 9 is defined as the mean value of the angle between each reference direction and its closest objective vector in the solution set.

I. Comparisons on Time Complexity

In order to give a fair comparison on the running times of different algorithms, we also implement a MATLAB version

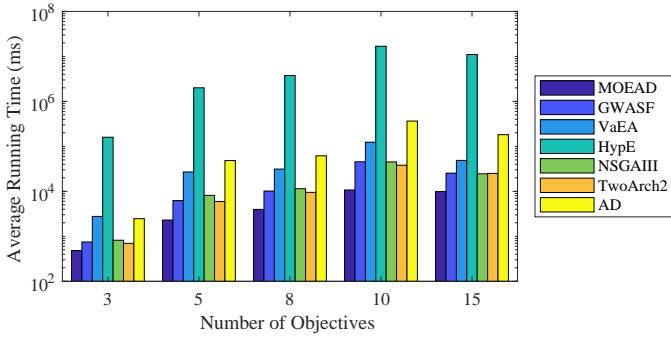


Fig. 10: Average running times of algorithms implemented in Java on WFG and WFG^{-1} test problems.

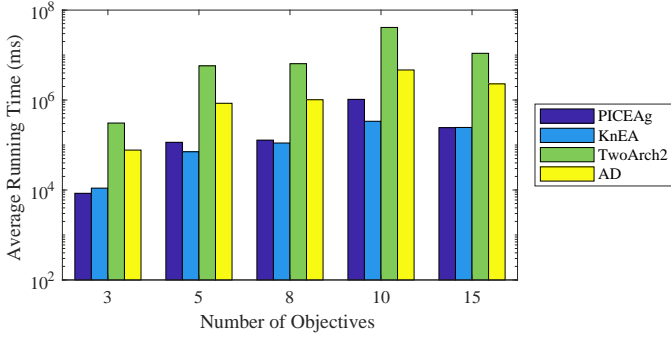


Fig. 11: Average running times of algorithms implemented in MATLAB on WFG and WFG^{-1} test problems.

of MOEA/AD. The average running times of the algorithms implemented in Java and algorithms implemented in MATLAB on WFG and WFG^{-1} test problems are presented in Fig. 10 and Fig. 11. Generally speaking, the average running times of different algorithms increase with the number of objectives and the population size. It can be seen that the deposition-based EMO algorithms tend to have lower running times than other types of algorithms. Compared with other deposition-based algorithms, the time complexity of the proposed MOEA/AD is moderately higher, which mainly comes from three factors: 1) two populations need to be maintained simultaneously; 2) the estimation of the nadir point requires to compute the current non-dominated solutions in each generation; and 3) the time complexity of the two-level one-one stable matching is $\mathcal{O}(N^2 \log N)$ [7].

J. Demonstration of Final Solution Sets

The final solution sets obtained by different algorithms in the run of median HV metric values with $\mathbf{z}^r = (2, \dots, 2)^T$ on each test instance are demonstrated in Fig. 12 to Fig. 141. It can be seen from the figures that MOEA/AD is very competitive on regular PF shapes such as hyperplanes and hyperspheres due to the evenly distributed weight vectors. Thanks to the complementary effects of the two subproblem formulations, it can achieve better convergence and diversity on other decomposition-based EMO algorithms, e.g., on 3-objective WFG8 test problem shown in Fig. 23. In contrast, the distribution of the final solution sets obtained by other types

of EMO algorithms, e.g., Two_Arch2, VaEA and PICEAg, are less uniform. However, MOEA/AD still suffers from a common issue of decomposition-based methods, i.e., the irregular PF shapes. The dealing with irregular PF shapes is out of the scope of this paper. Another strength of MOEA/AD is shown on problems with inverted PFs, which can be owed to the adversarial search directions of the two populations.

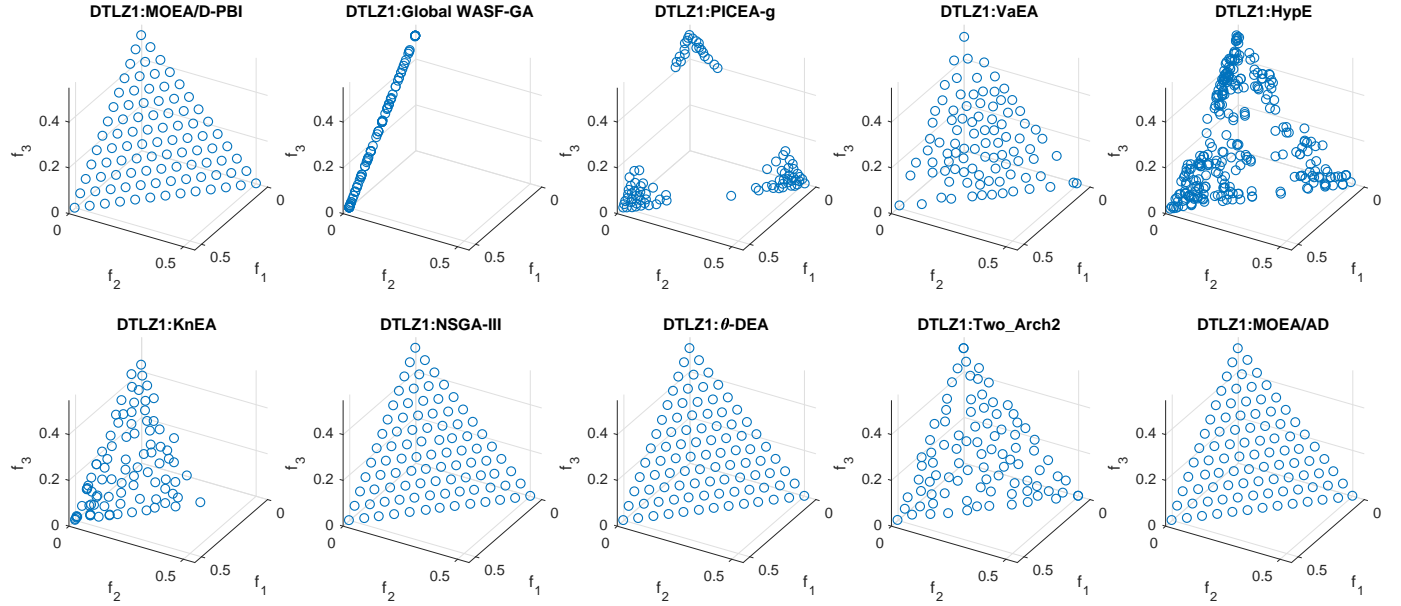


Fig. 12: Final solution sets on 3-objective DTLZ1 test problem obtained by 10 algorithms in the run of median HV metric values with $\mathbf{z}^r = (2, \dots, 2)^T$.

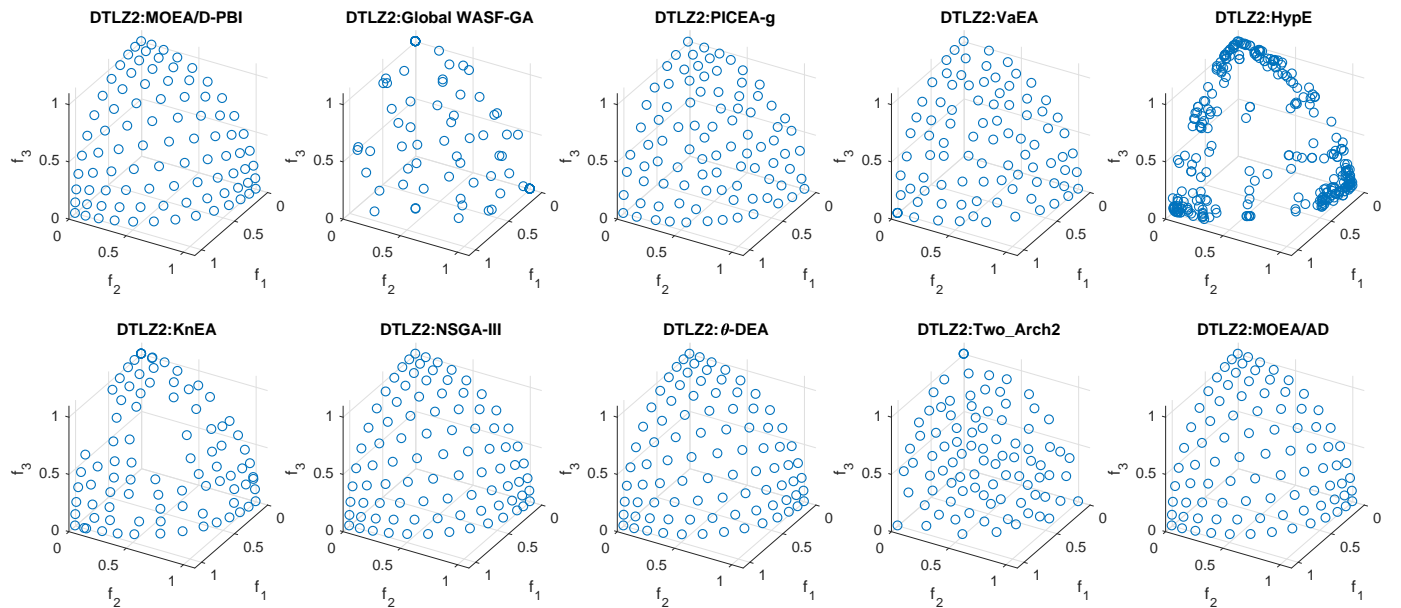


Fig. 13: Final solution sets on 3-objective DTLZ2 test problem obtained by 10 algorithms in the run of median HV metric values with $\mathbf{z}^r = (2, \dots, 2)^T$.

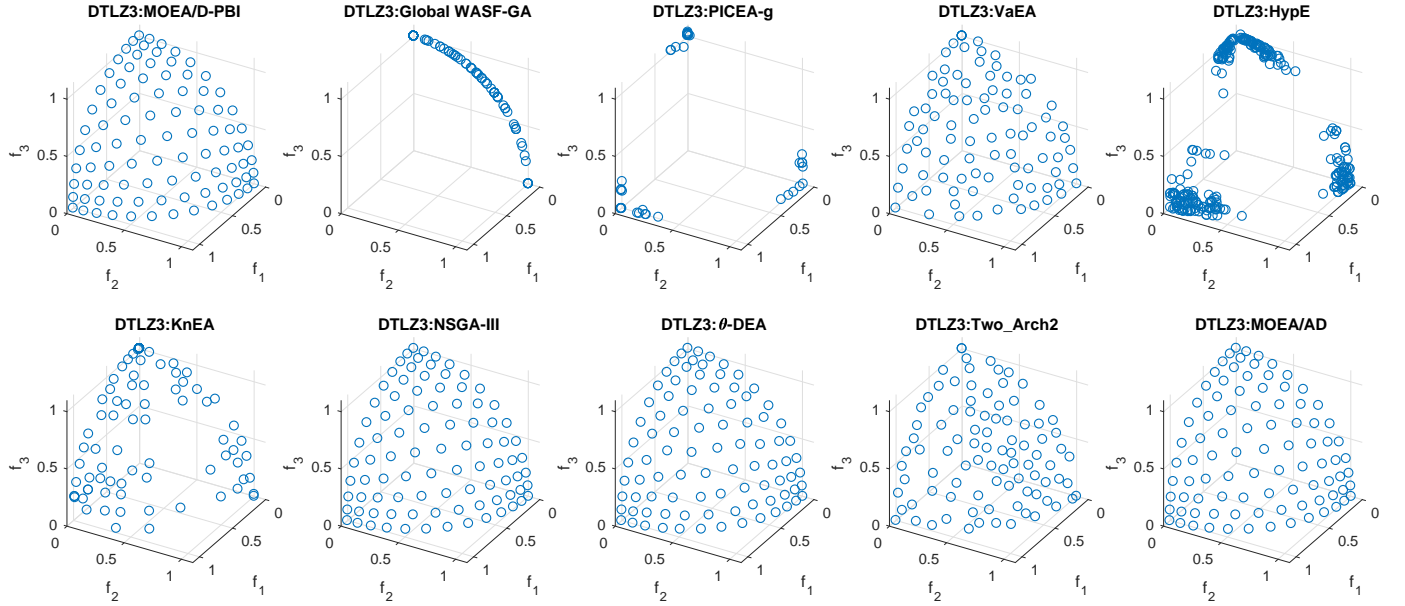


Fig. 14: Final solution sets on 3-objective DTLZ3 test problem obtained by 10 algorithms in the run of median HV metric values with $\mathbf{z}^r = (2, \dots, 2)^T$.

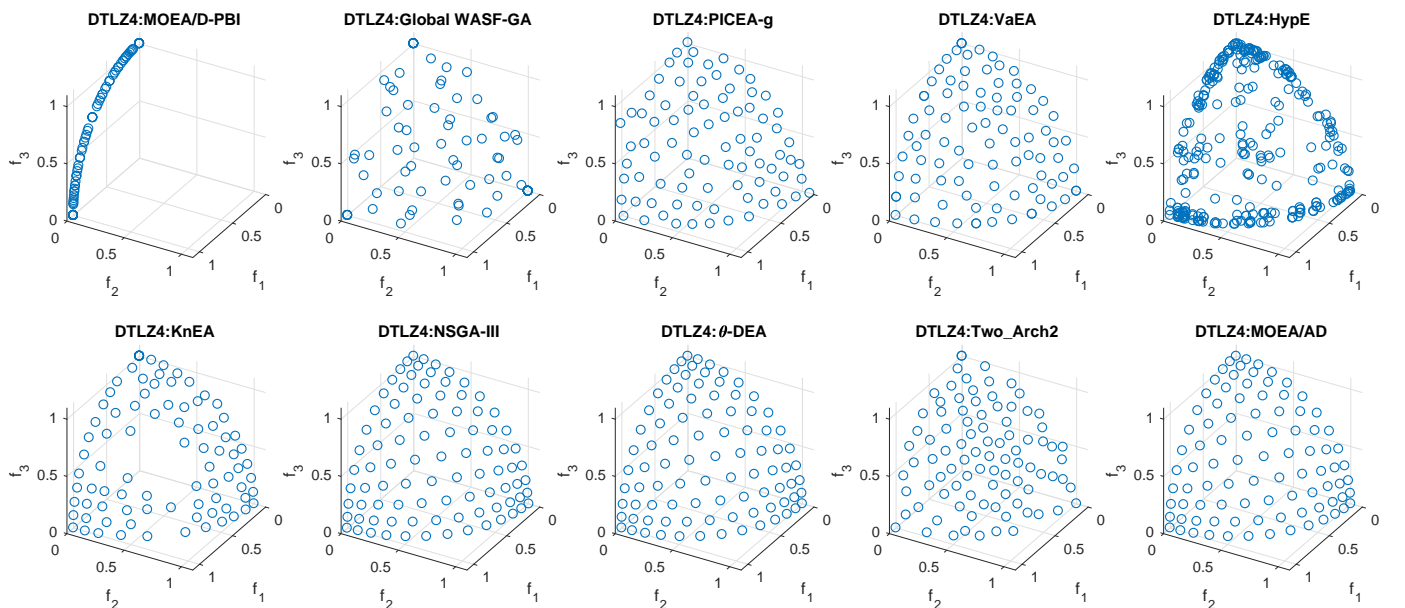


Fig. 15: Final solution sets on 3-objective DTLZ4 test problem obtained by 10 algorithms in the run of median HV metric values with $\mathbf{z}^r = (2, \dots, 2)^T$.

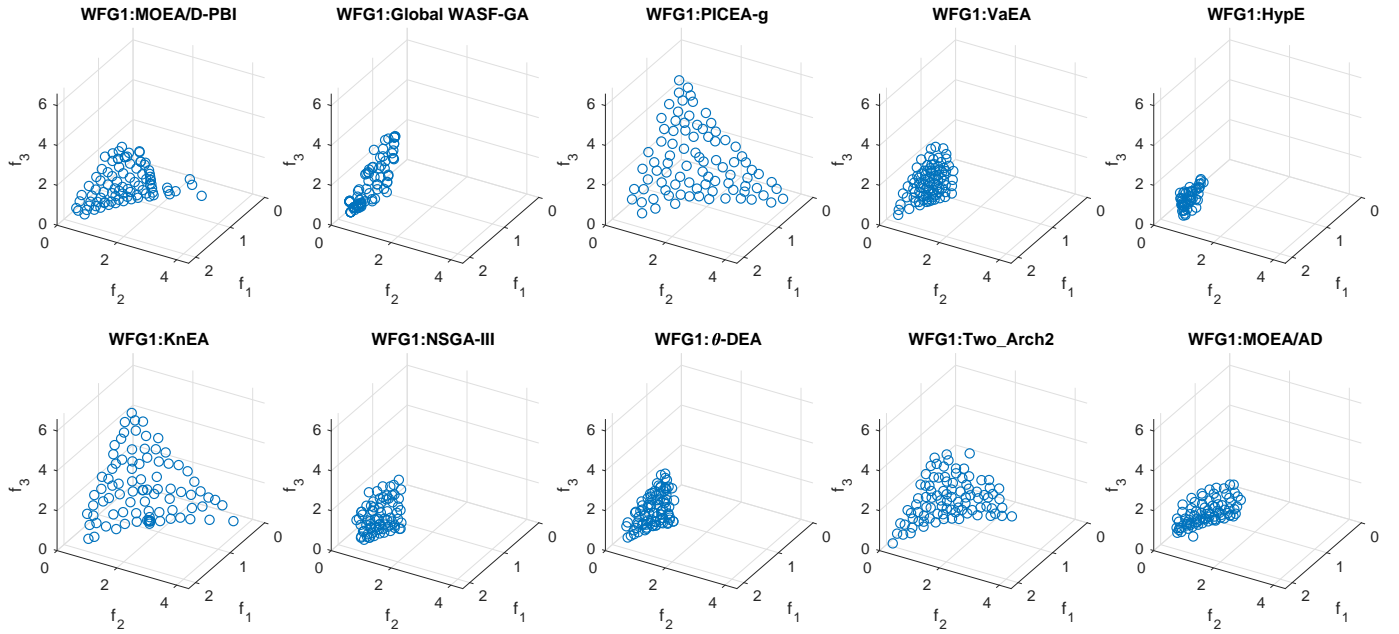


Fig. 16: Final solution sets on 3-objective WFG1 test problem obtained by 10 algorithms in the run of median HV metric values with $\mathbf{z}^r = (2, \dots, 2)^T$.

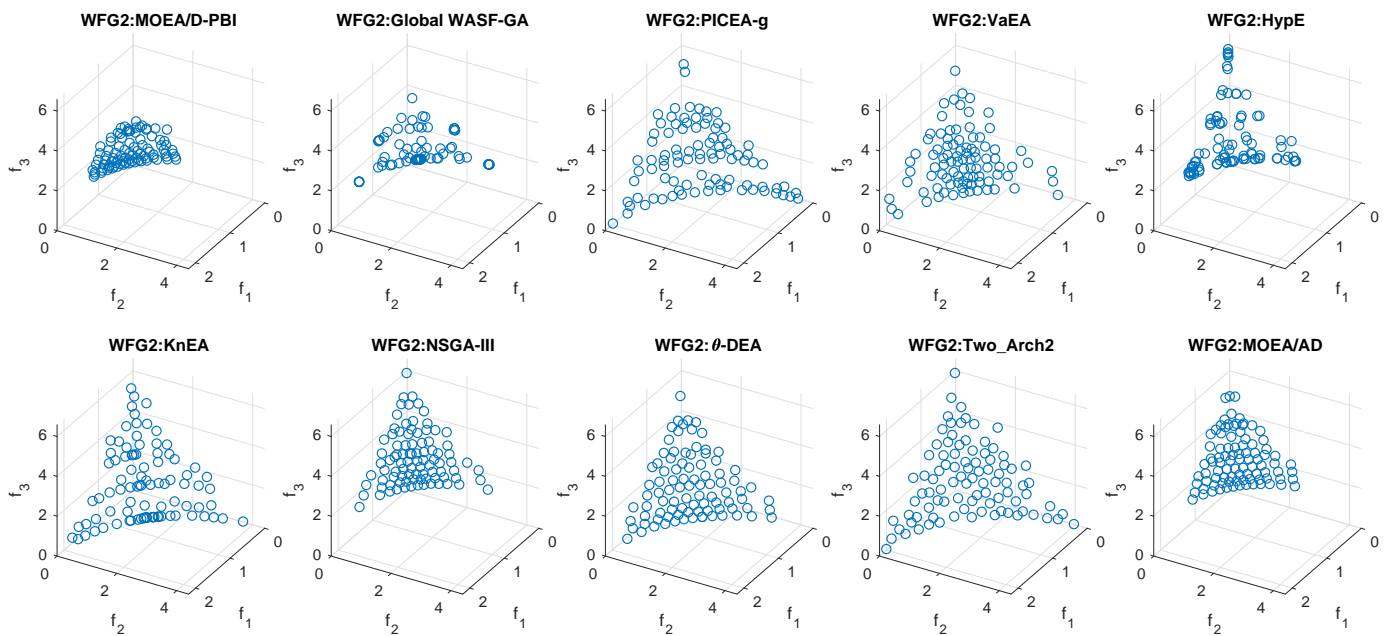


Fig. 17: Final solution sets on 3-objective WFG2 test problem obtained by 10 algorithms in the run of median HV metric values with $\mathbf{z}^r = (2, \dots, 2)^T$.

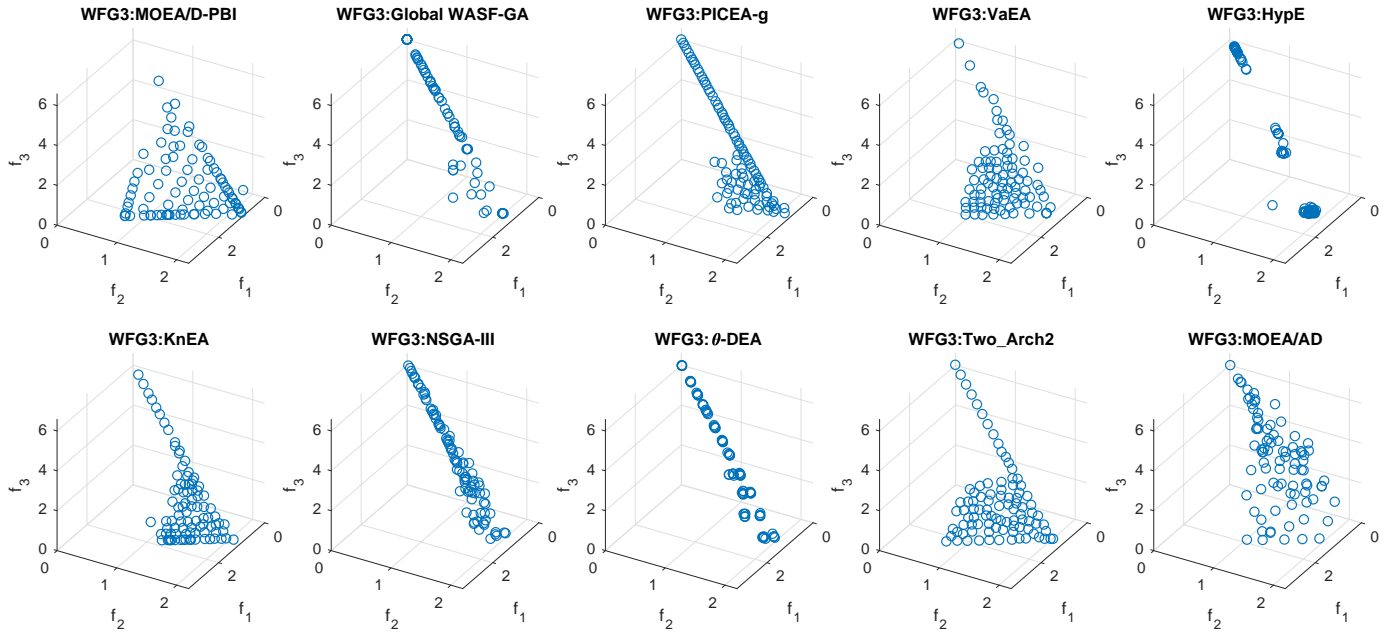


Fig. 18: Final solution sets on 3-objective WFG3 test problem obtained by 10 algorithms in the run of median HV metric values with $\mathbf{z}^r = (2, \dots, 2)^T$.

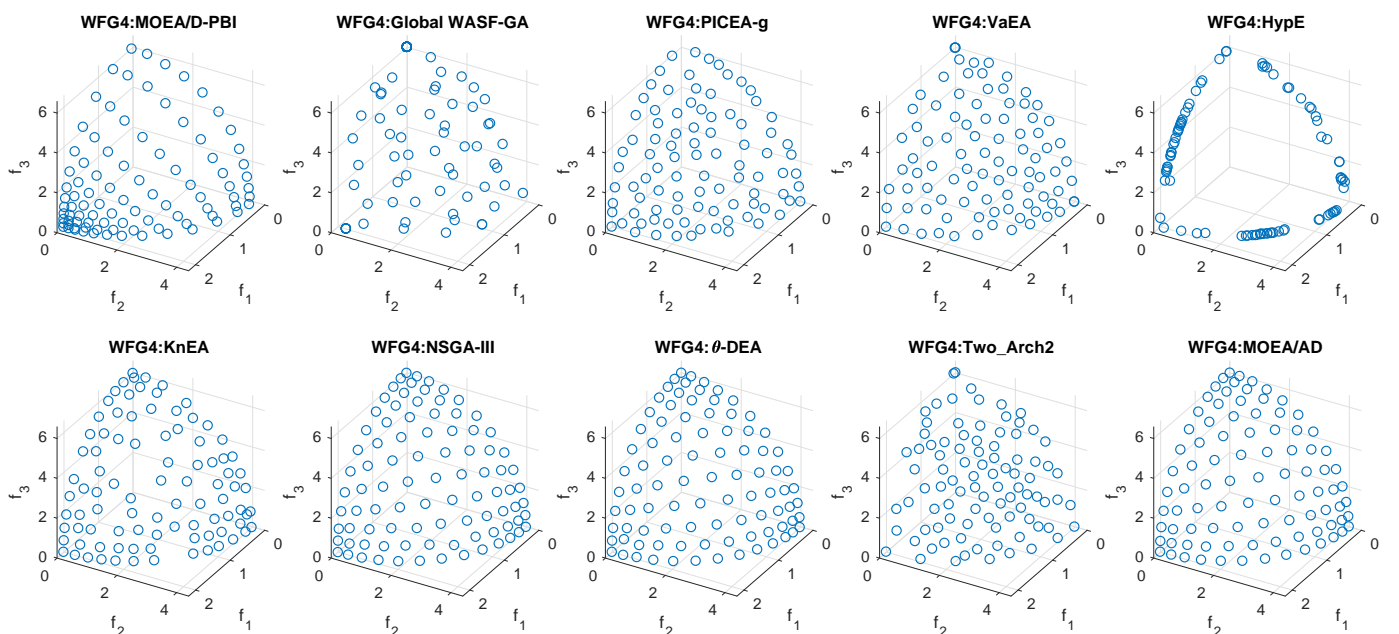


Fig. 19: Final solution sets on 3-objective WFG4 test problem obtained by 10 algorithms in the run of median HV metric values with $\mathbf{z}^r = (2, \dots, 2)^T$.

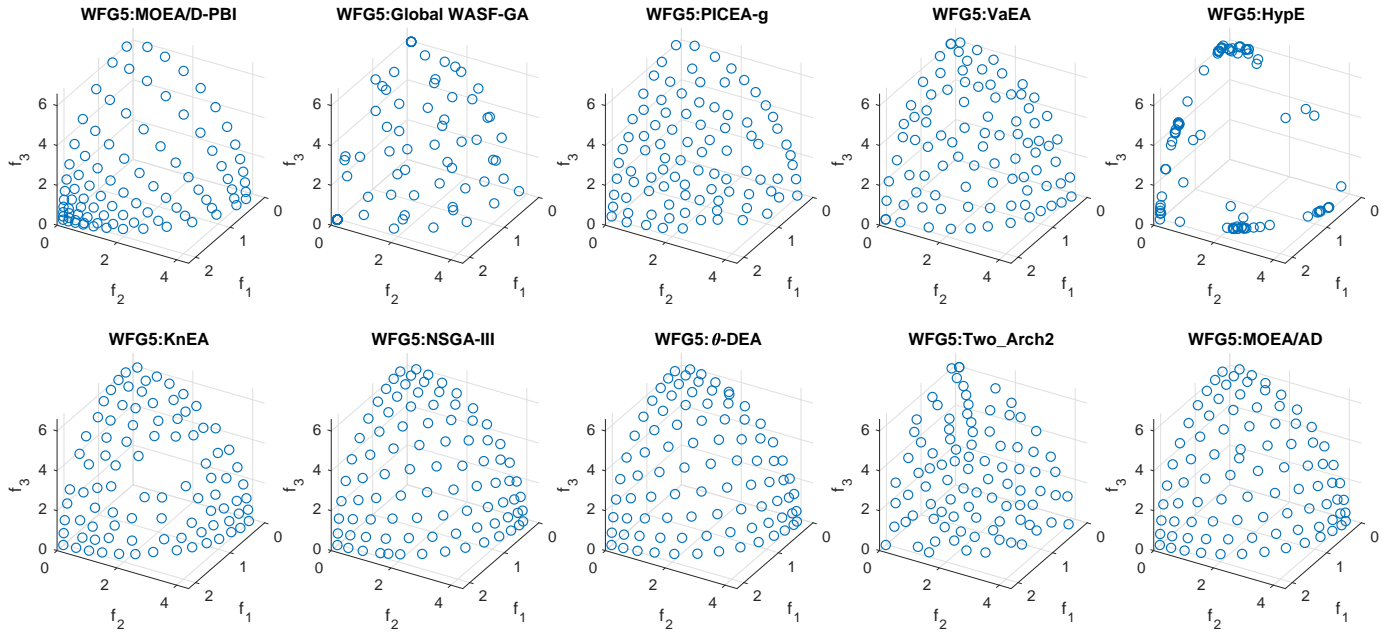


Fig. 20: Final solution sets on 3-objective WFG5 test problem obtained by 10 algorithms in the run of median HV metric values with $\mathbf{z}^r = (2, \dots, 2)^T$.

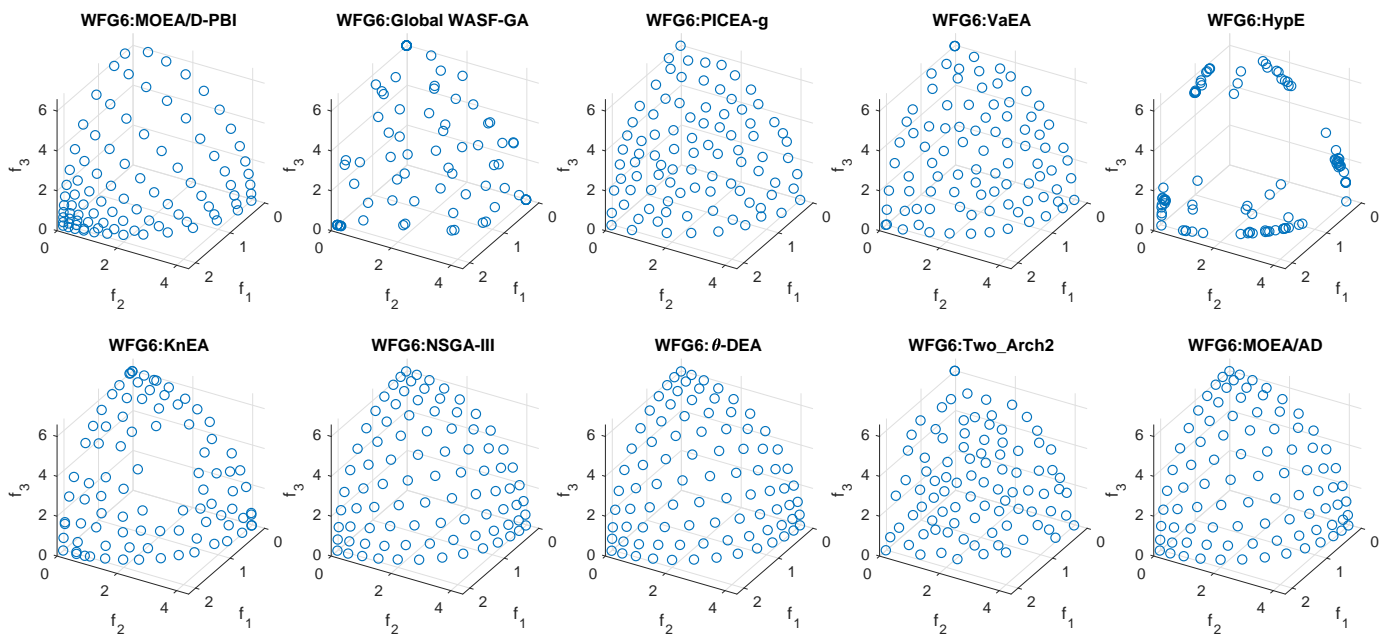


Fig. 21: Final solution sets on 3-objective WFG6 test problem obtained by 10 algorithms in the run of median HV metric values with $\mathbf{z}^r = (2, \dots, 2)^T$.

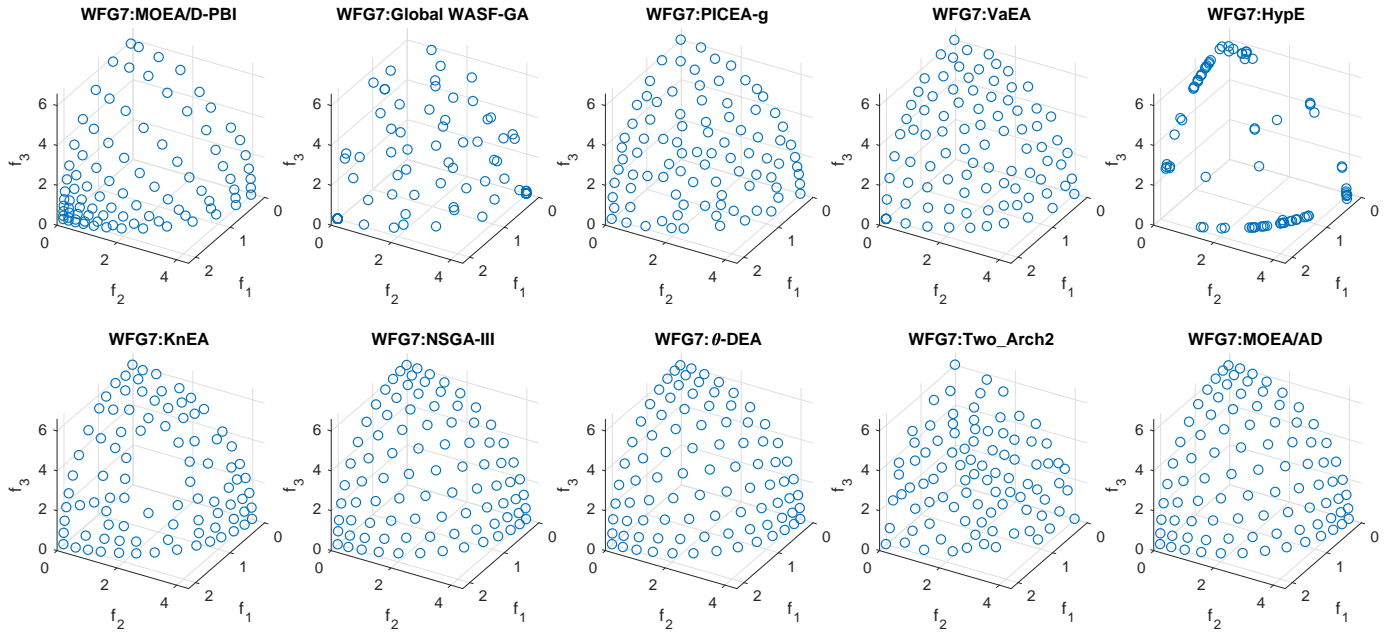


Fig. 22: Final solution sets on 3-objective WFG7 test problem obtained by 10 algorithms in the run of median HV metric values with $\mathbf{z}^r = (2, \dots, 2)^T$.

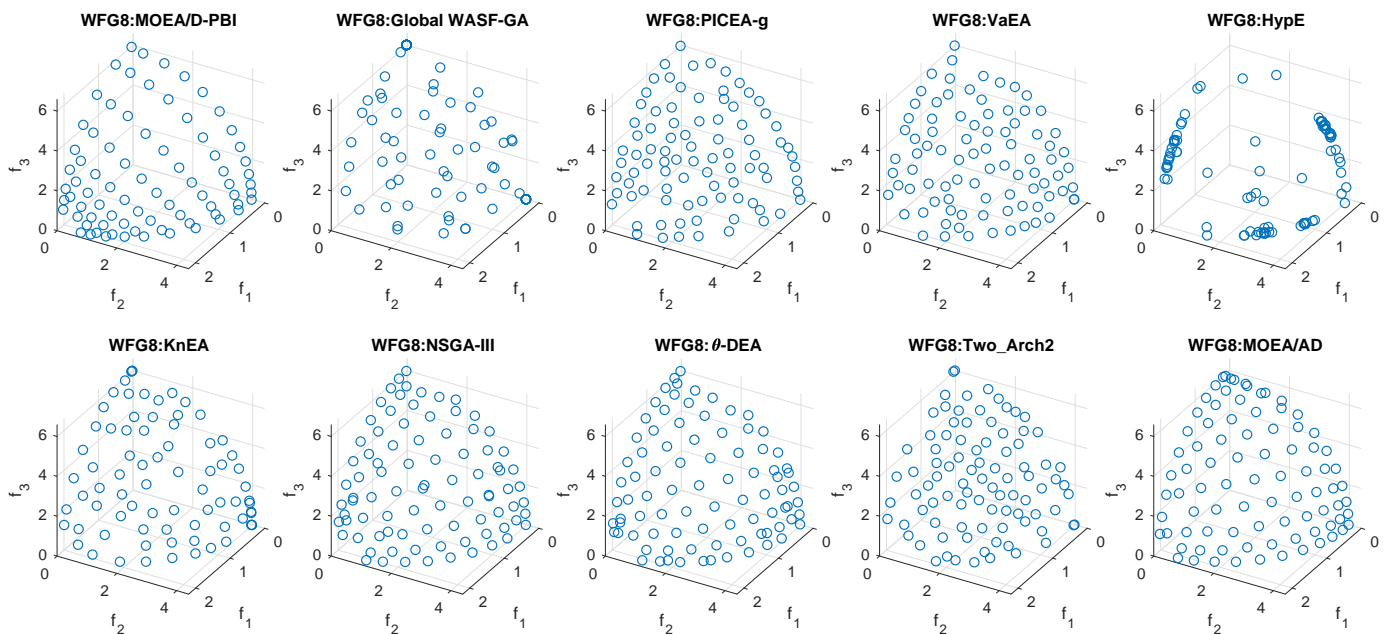


Fig. 23: Final solution sets on 3-objective WFG8 test problem obtained by 10 algorithms in the run of median HV metric values with $\mathbf{z}^r = (2, \dots, 2)^T$.

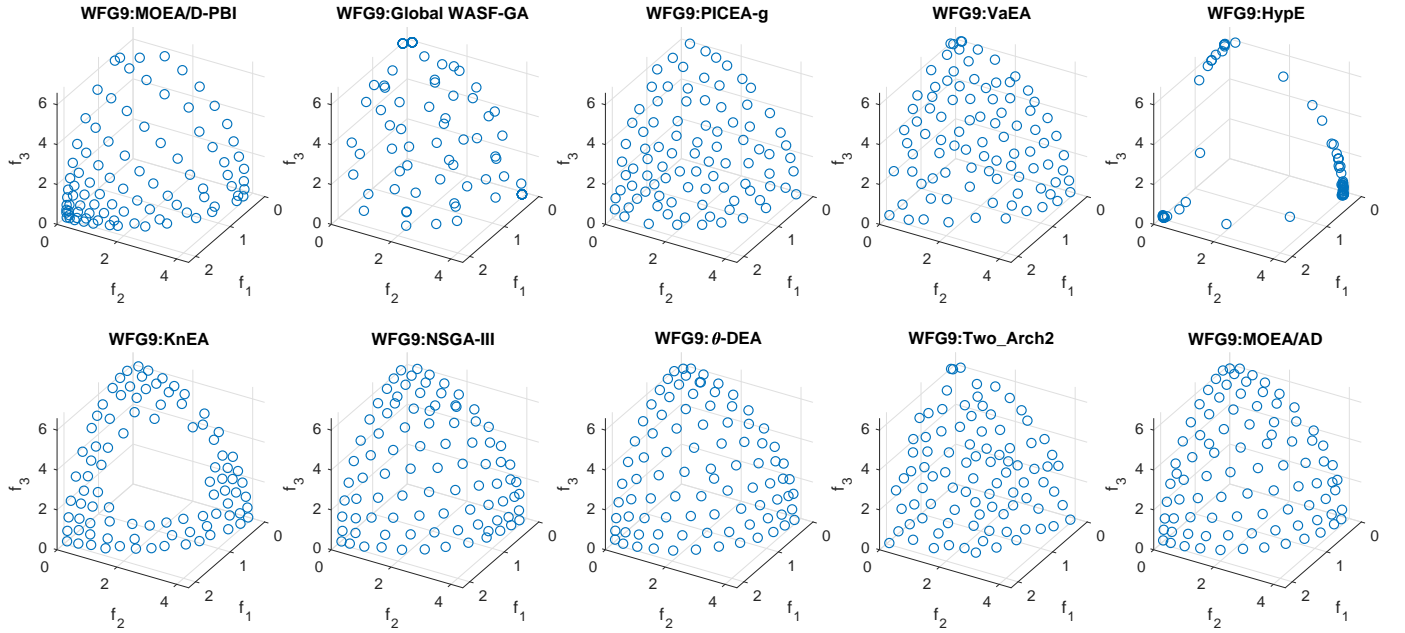


Fig. 24: Final solution sets on 3-objective WFG9 test problem obtained by 10 algorithms in the run of median HV metric values with $\mathbf{z}^r = (2, \dots, 2)^T$.

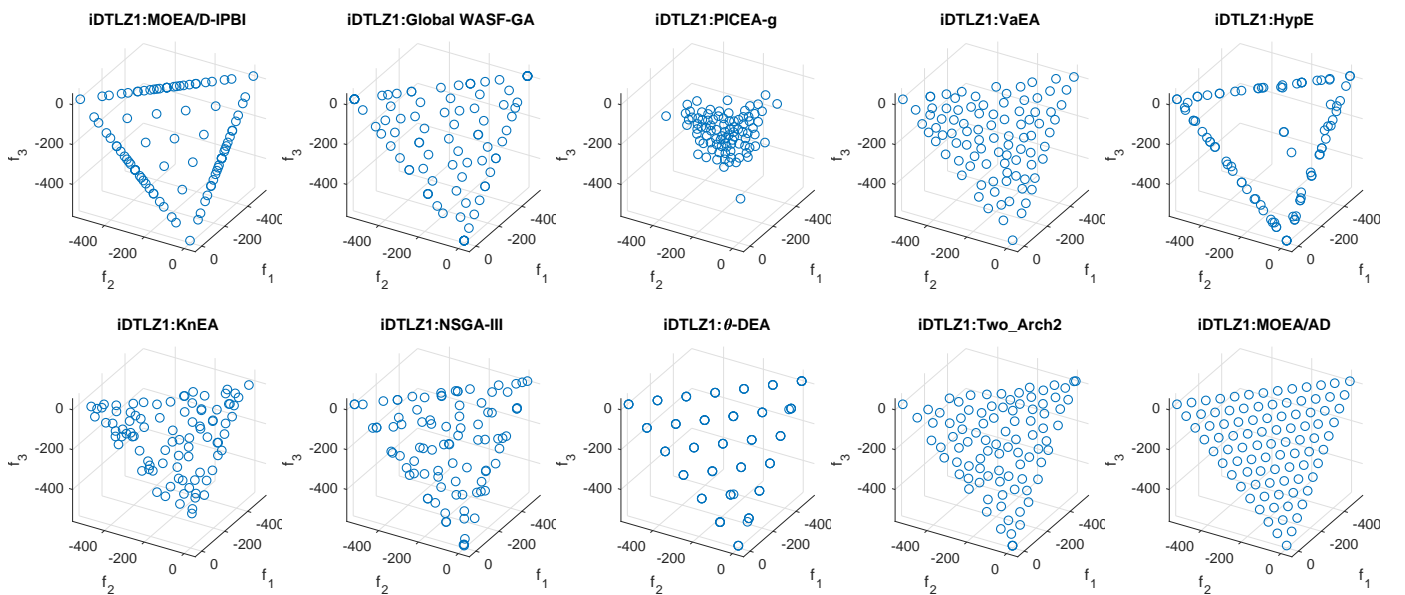


Fig. 25: Final solution sets on 3-objective DTLZ1 $^{-1}$ test problem obtained by 10 algorithms in the run of median HV metric values with $\mathbf{z}^r = (2, \dots, 2)^T$.

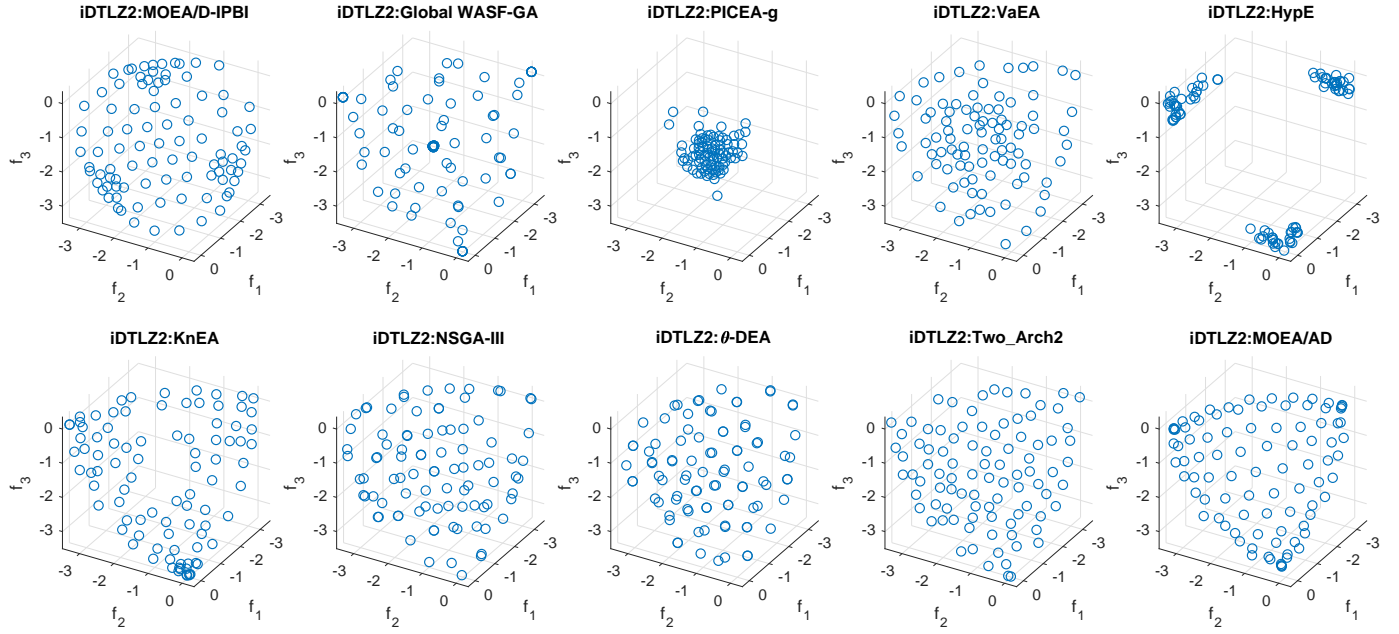


Fig. 26: Final solution sets on 3-objective DTLZ2⁻¹ test problem obtained by 10 algorithms in the run of median HV metric values with $\mathbf{z}^r = (2, \dots, 2)^T$.

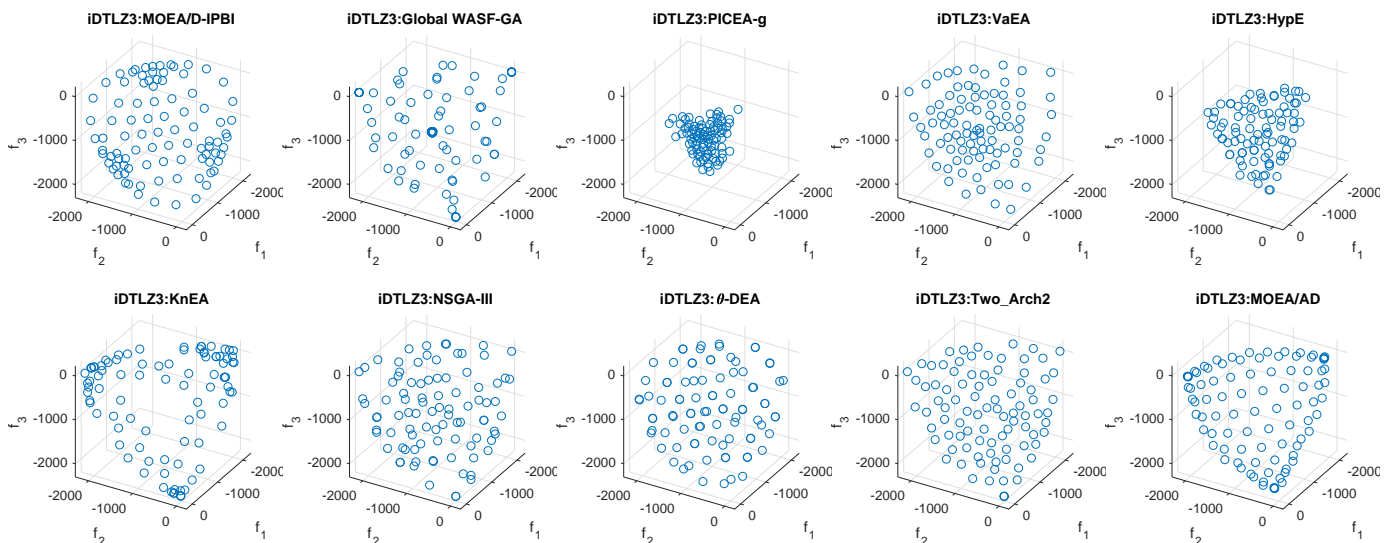


Fig. 27: Final solution sets on 3-objective DTLZ3⁻¹ test problem obtained by 10 algorithms in the run of median HV metric values with $\mathbf{z}^r = (2, \dots, 2)^T$.

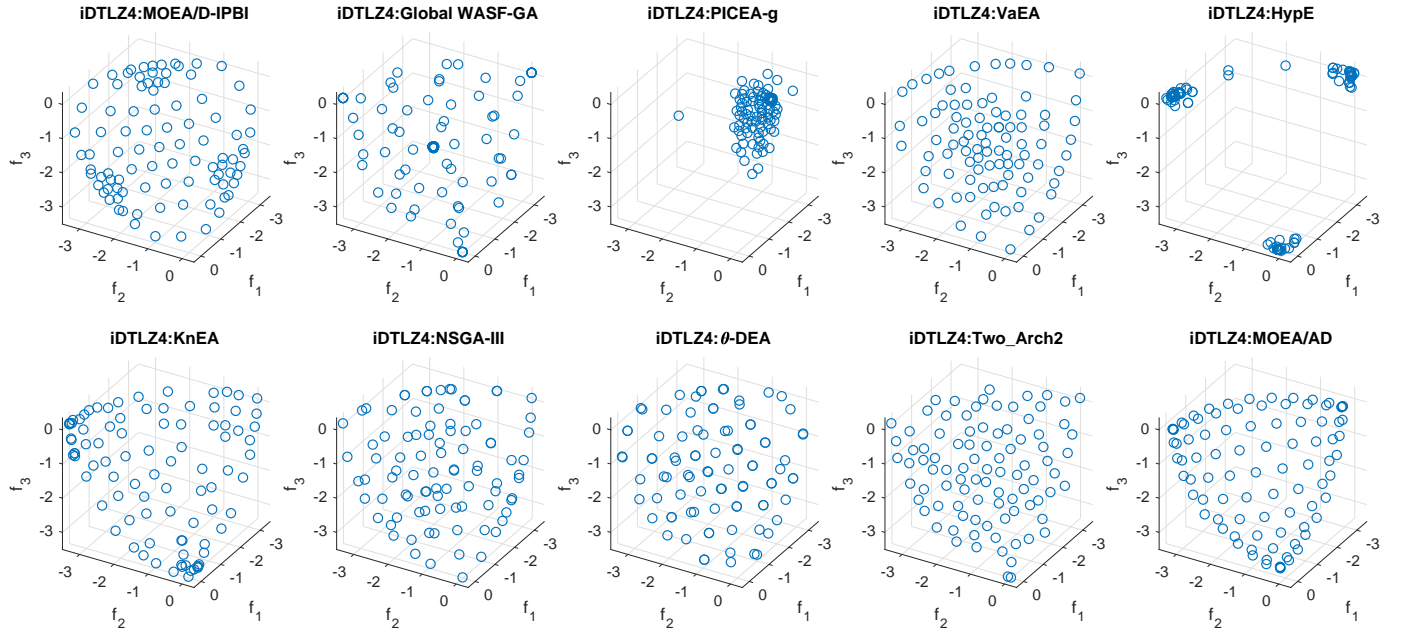


Fig. 28: Final solution sets on 3-objective $DTLZ4^{-1}$ test problem obtained by 10 algorithms in the run of median HV metric values with $\mathbf{z}^r = (2, \dots, 2)^T$.

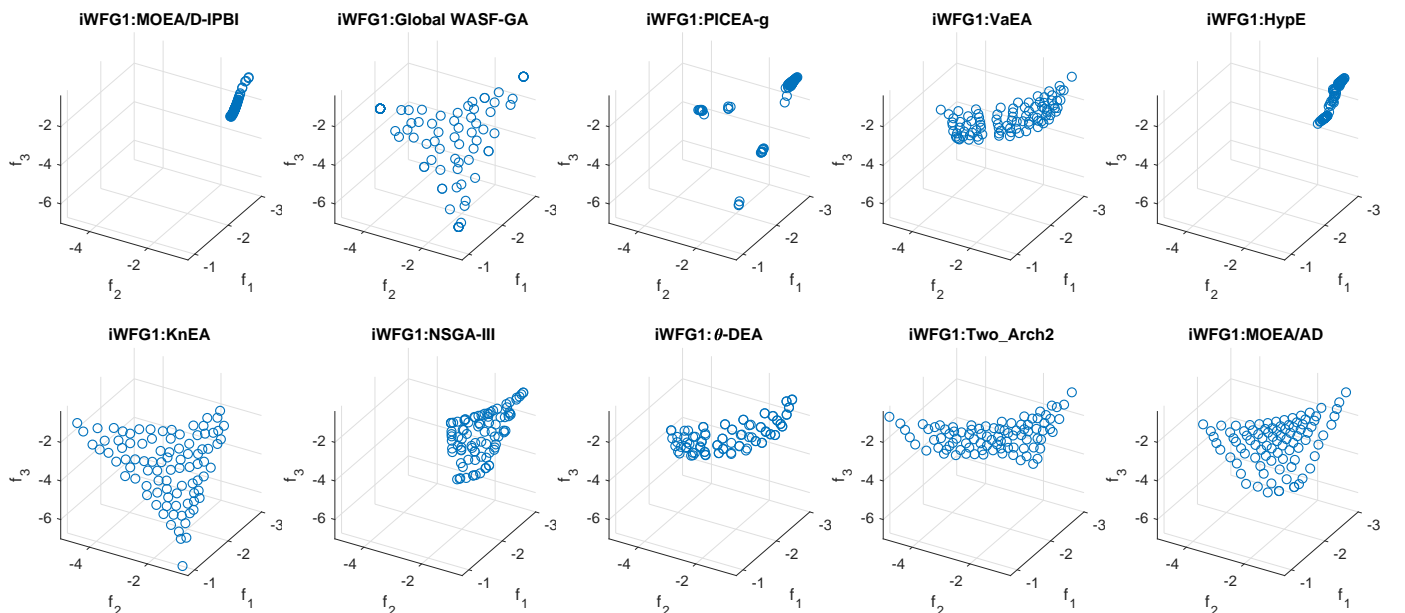


Fig. 29: Final solution sets on 3-objective $WFG1^{-1}$ test problem obtained by 10 algorithms in the run of median HV metric values with $\mathbf{z}^r = (2, \dots, 2)^T$.

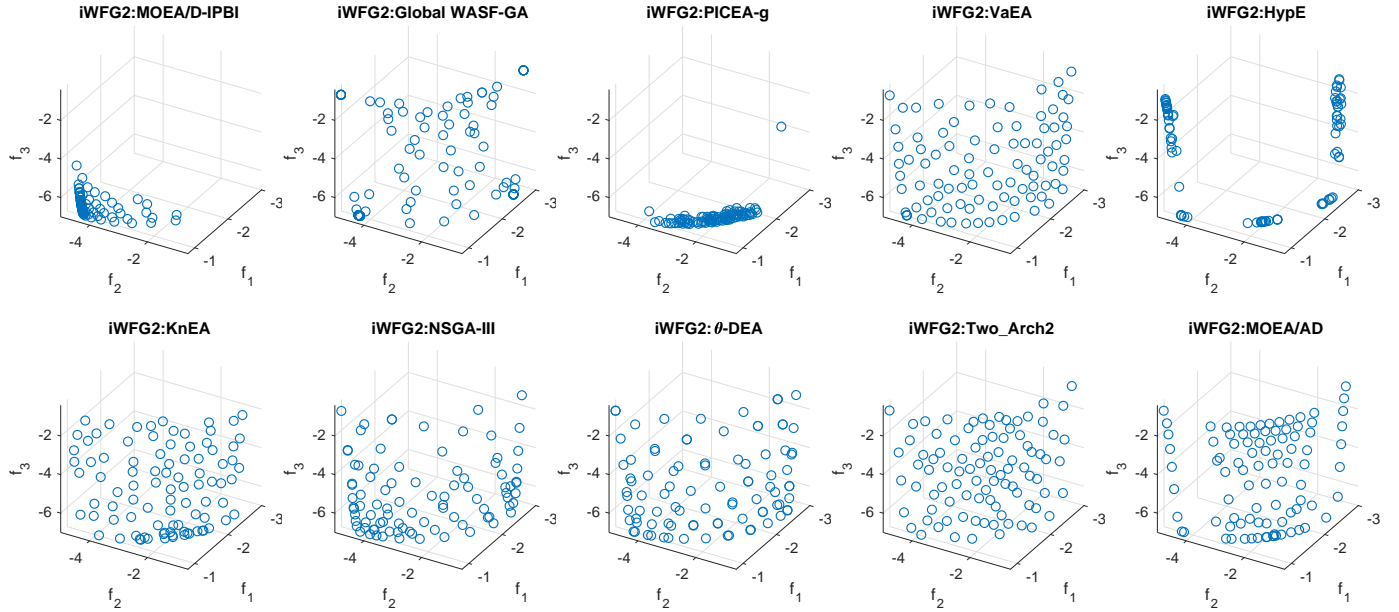


Fig. 30: Final solution sets on 3-objective WFG2⁻¹ test problem obtained by 10 algorithms in the run of median HV metric values with $\mathbf{z}^r = (2, \dots, 2)^T$.

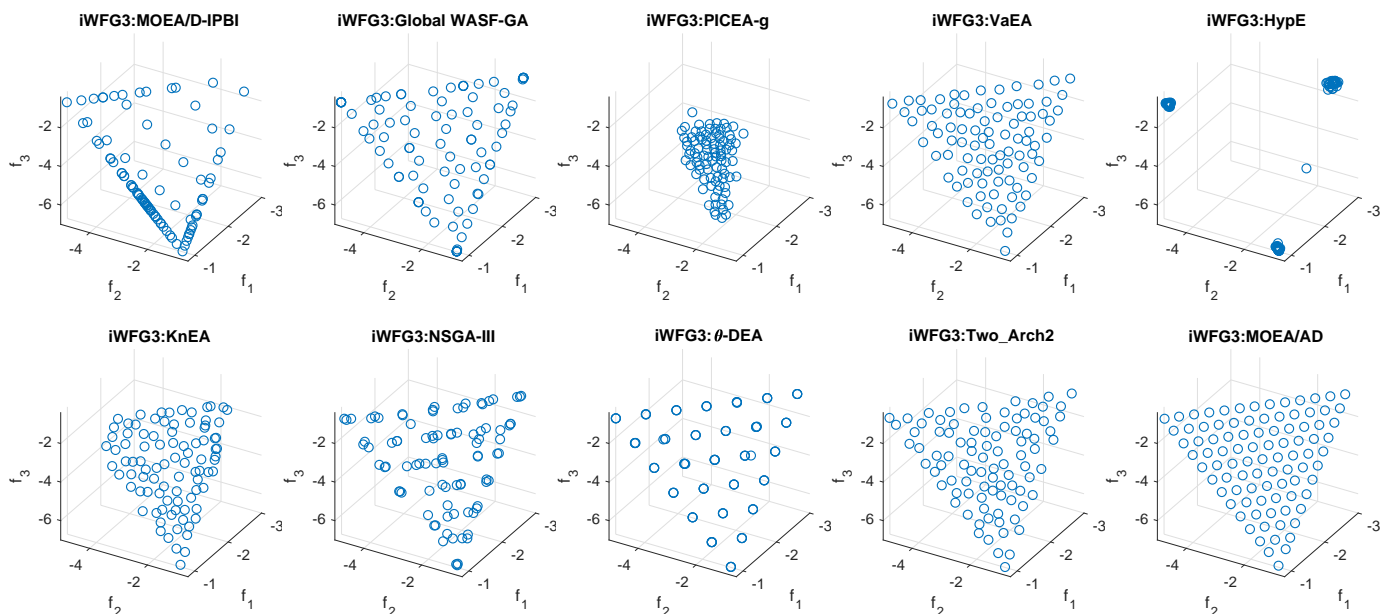


Fig. 31: Final solution sets on 3-objective WFG3⁻¹ test problem obtained by 10 algorithms in the run of median HV metric values with $\mathbf{z}^r = (2, \dots, 2)^T$.

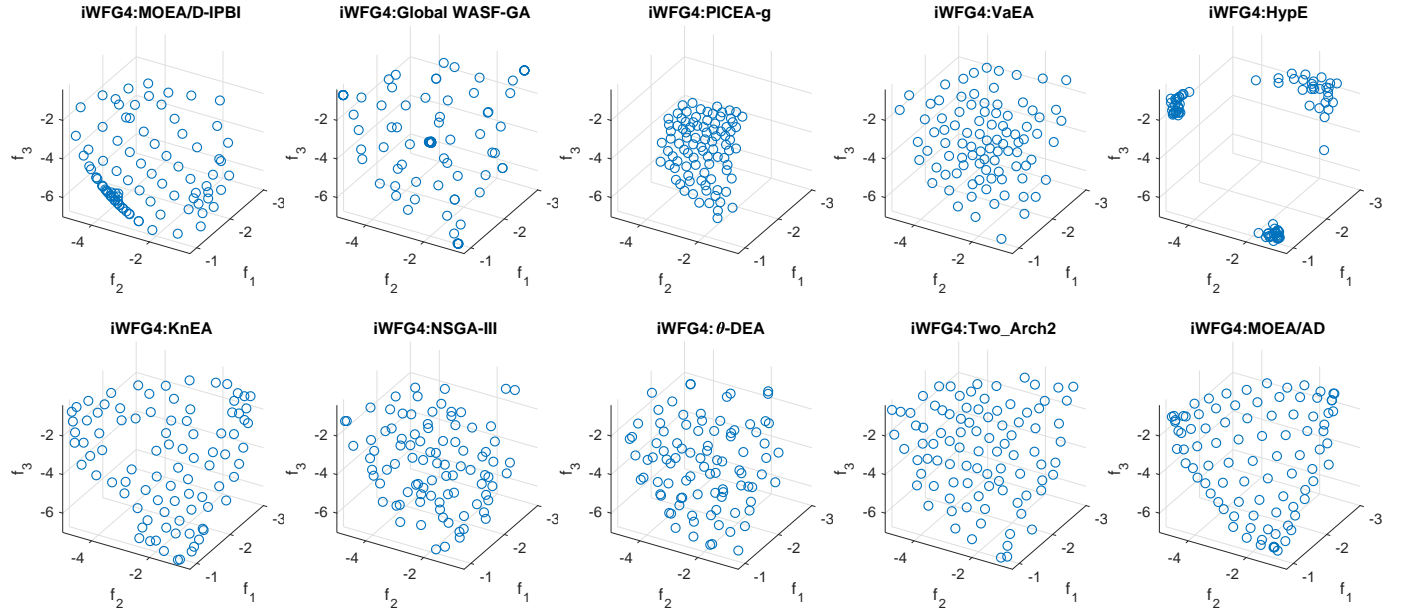


Fig. 32: Final solution sets on 3-objective WFG4⁻¹ test problem obtained by 10 algorithms in the run of median HV metric values with $\mathbf{z}^r = (2, \dots, 2)^T$.

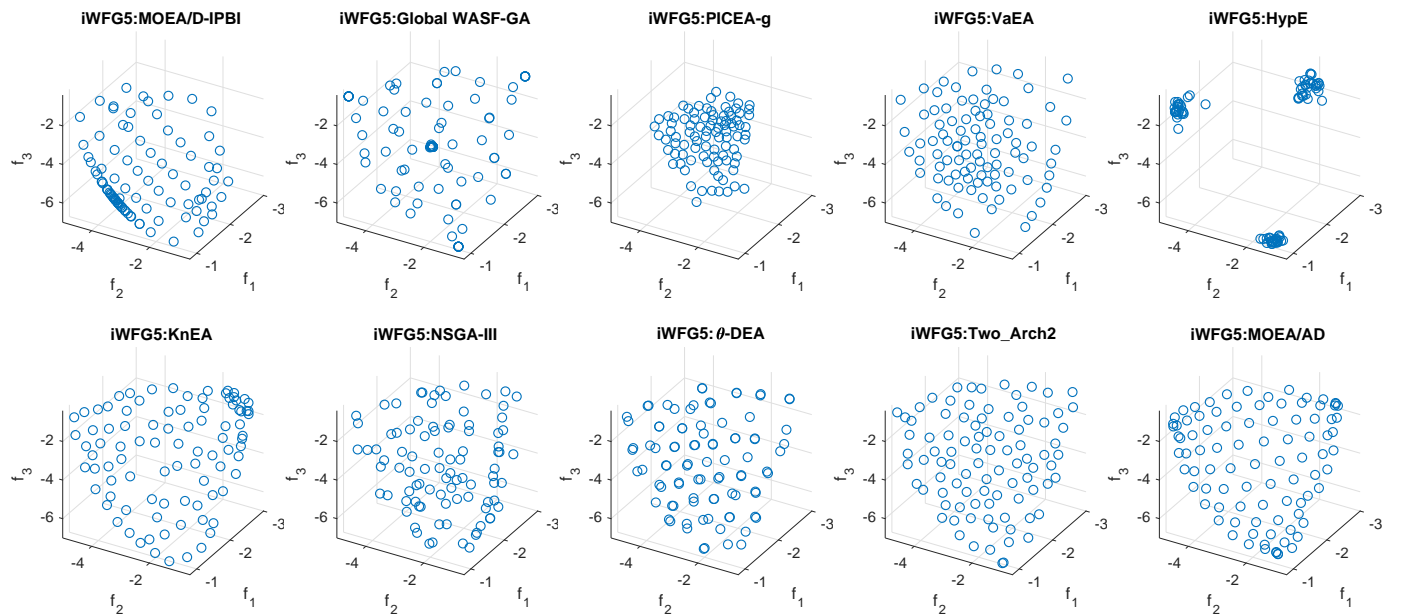


Fig. 33: Final solution sets on 3-objective WFG5⁻¹ test problem obtained by 10 algorithms in the run of median HV metric values with $\mathbf{z}^r = (2, \dots, 2)^T$.

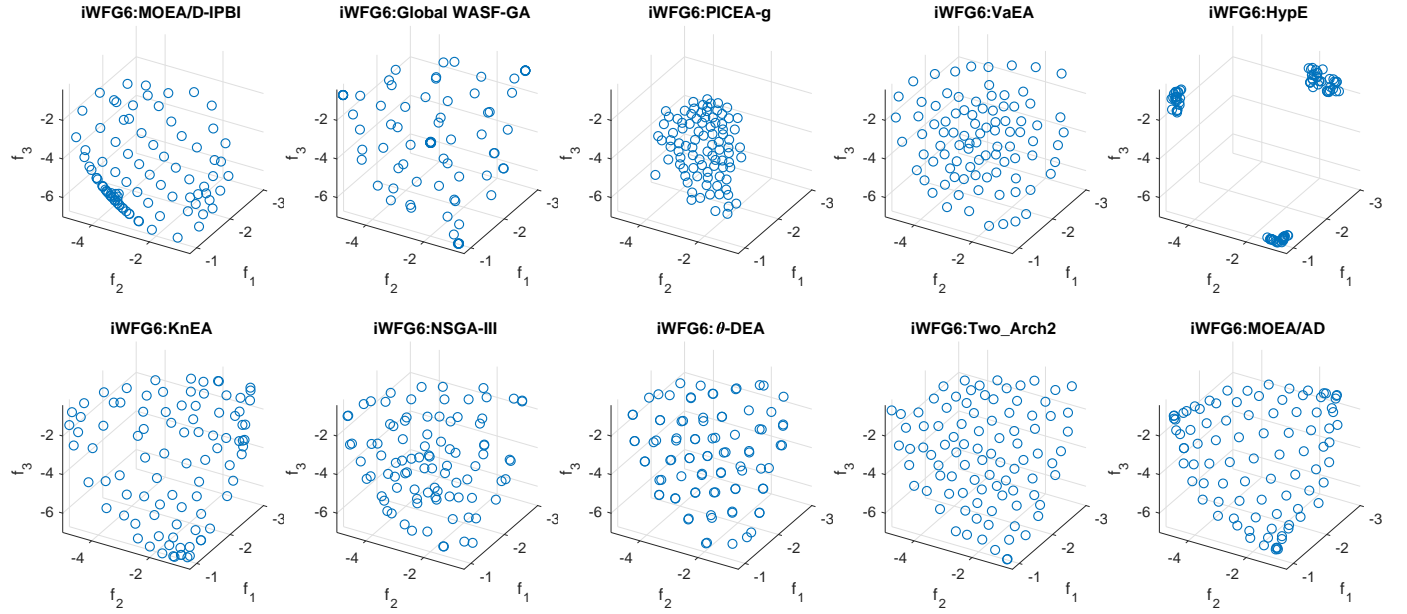


Fig. 34: Final solution sets on 3-objective WFG6⁻¹ test problem obtained by 10 algorithms in the run of median HV metric values with $\mathbf{z}^r = (2, \dots, 2)^T$.

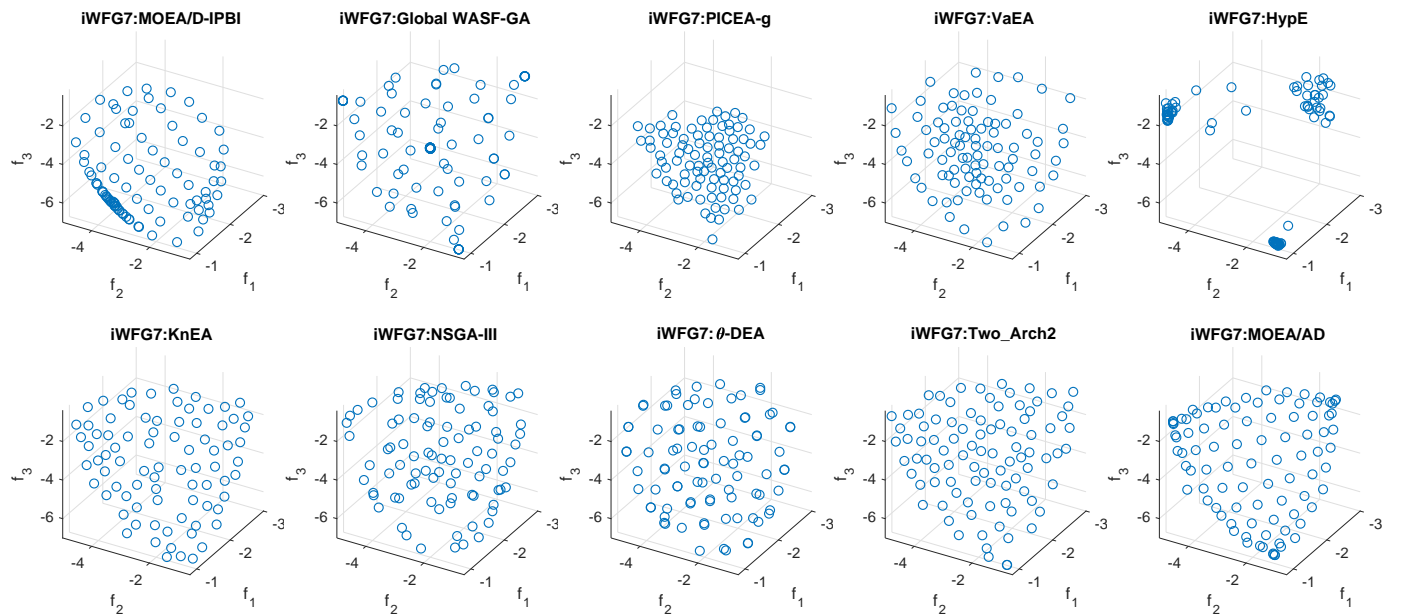


Fig. 35: Final solution sets on 3-objective WFG7⁻¹ test problem obtained by 10 algorithms in the run of median HV metric values with $\mathbf{z}^r = (2, \dots, 2)^T$.

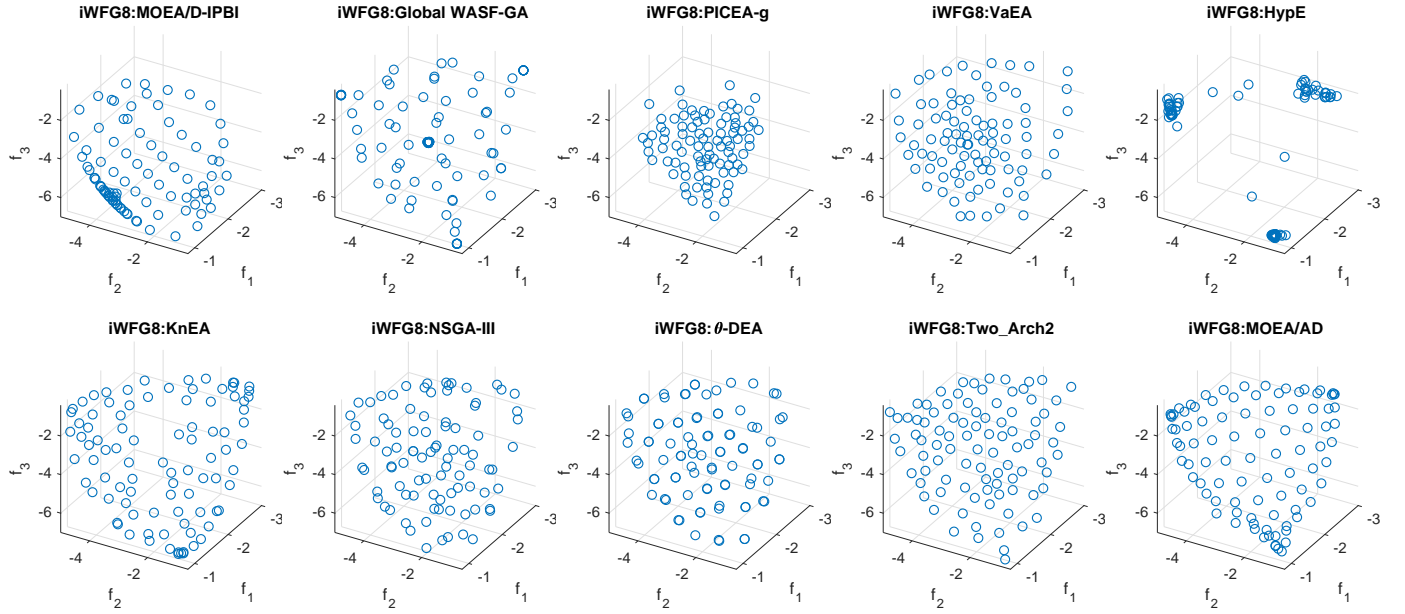


Fig. 36: Final solution sets on 3-objective WFG8⁻¹ test problem obtained by 10 algorithms in the run of median HV metric values with $\mathbf{z}^r = (2, \dots, 2)^T$.

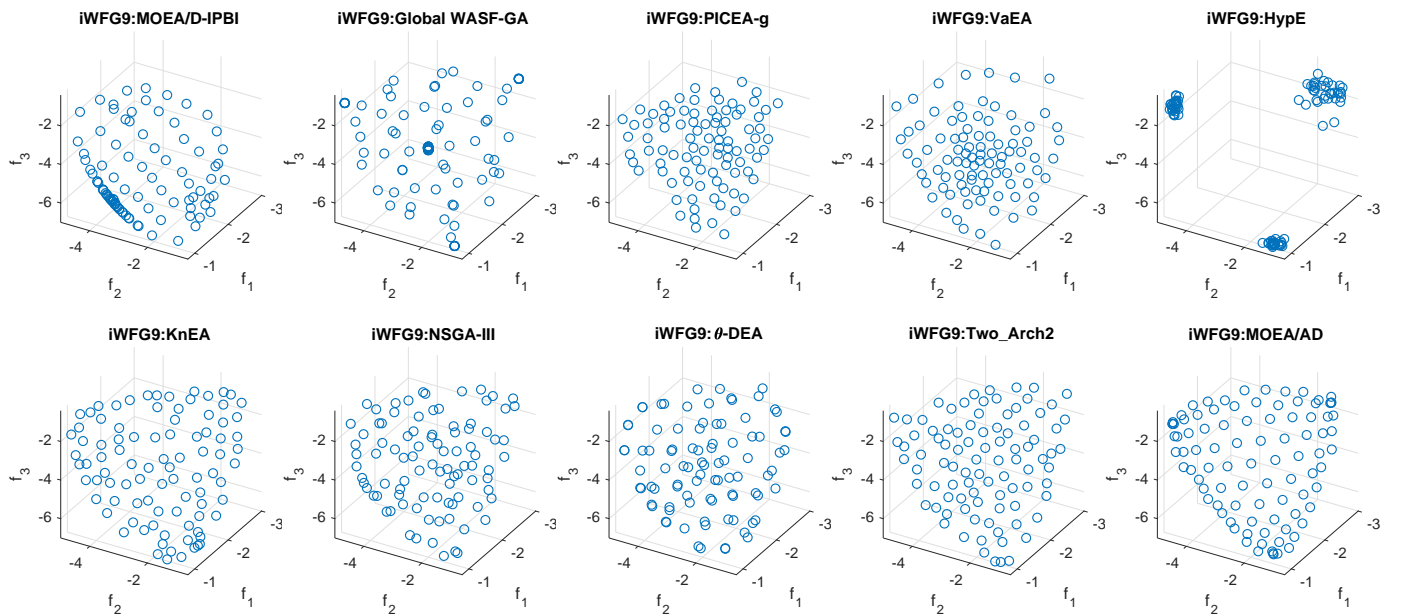


Fig. 37: Final solution sets on 3-objective WFG9⁻¹ test problem obtained by 10 algorithms in the run of median HV metric values with $\mathbf{z}^r = (2, \dots, 2)^T$.

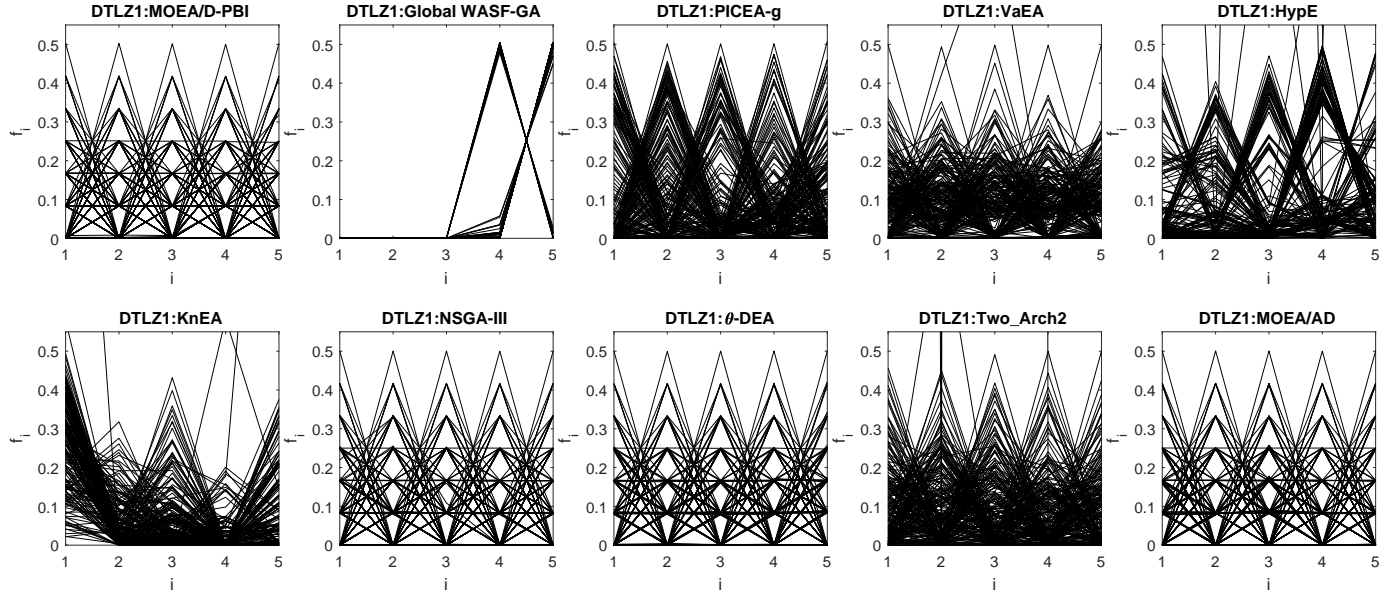


Fig. 38: Final solution sets on 5-objective DTLZ1 test problem obtained by 10 algorithms in the run of median HV metric values with $\mathbf{z}^r = (2, \dots, 2)^T$.

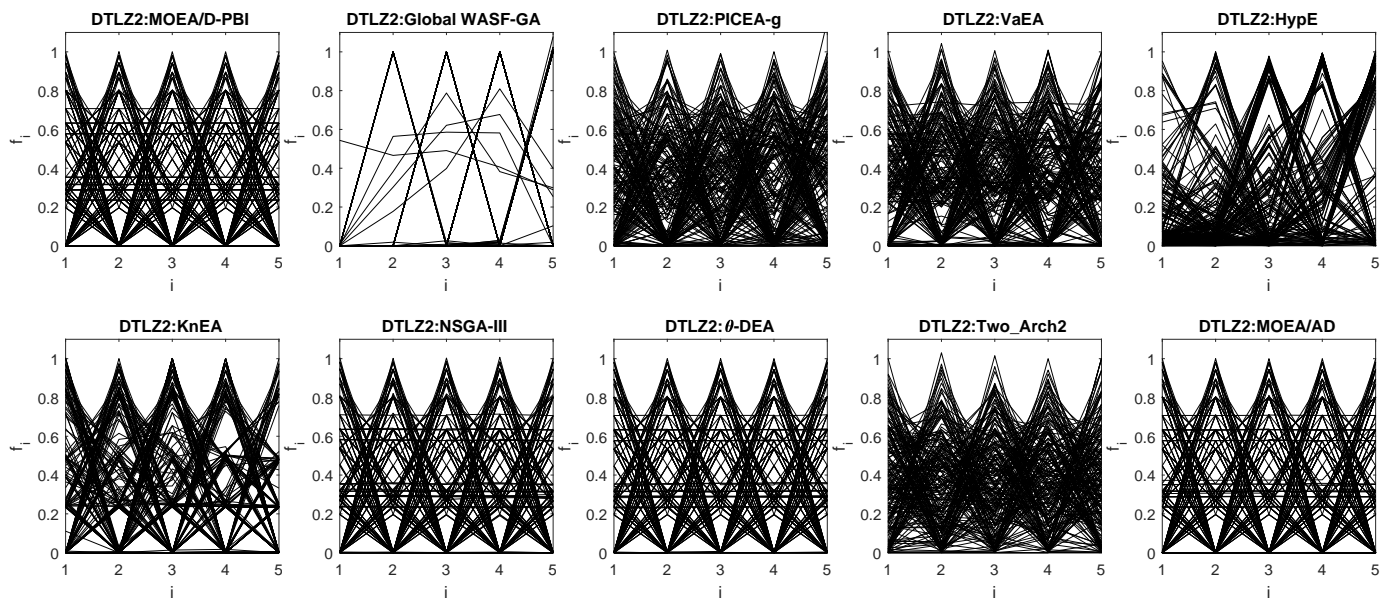


Fig. 39: Final solution sets on 5-objective DTLZ2 test problem obtained by 10 algorithms in the run of median HV metric values with $\mathbf{z}^r = (2, \dots, 2)^T$.

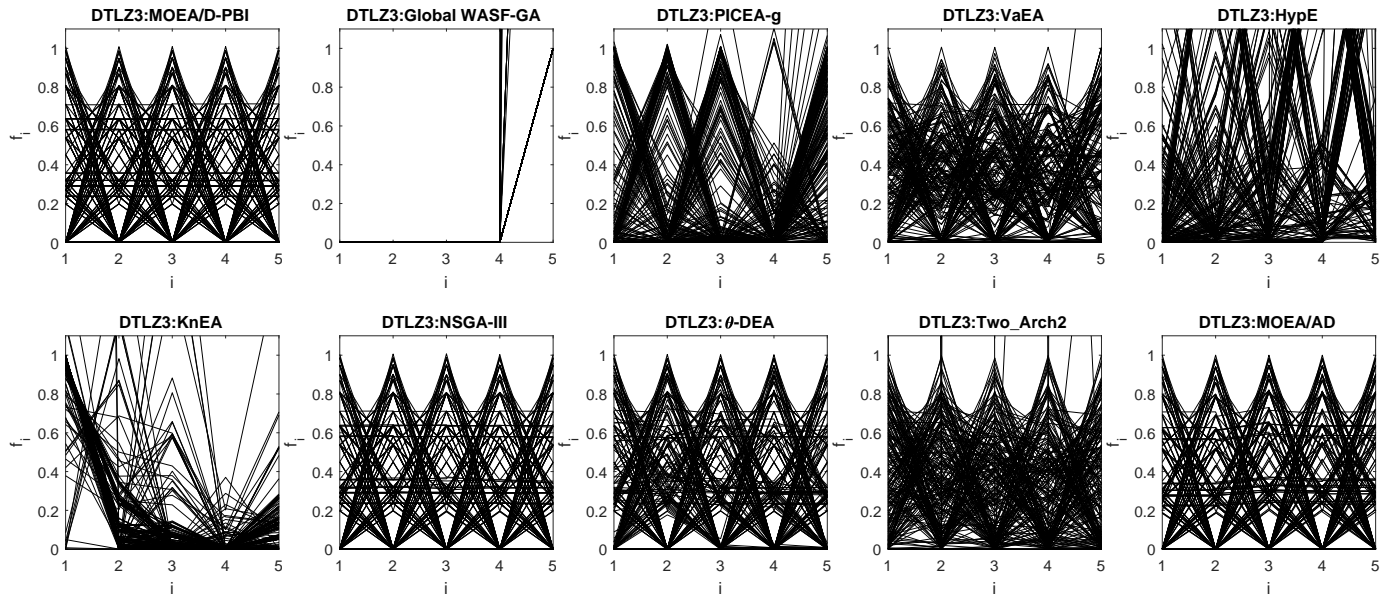


Fig. 40: Final solution sets on 5-objective DTLZ3 test problem obtained by 10 algorithms in the run of median HV metric values with $\mathbf{z}^r = (2, \dots, 2)^T$.

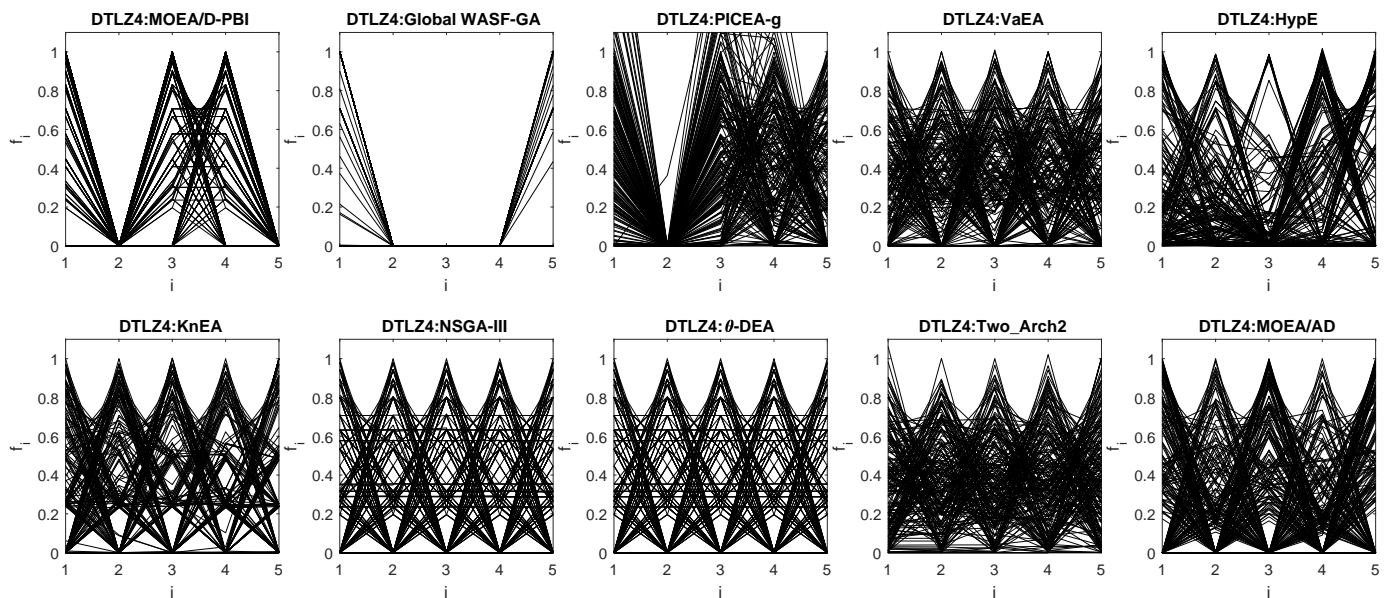


Fig. 41: Final solution sets on 5-objective DTLZ4 test problem obtained by 10 algorithms in the run of median HV metric values with $\mathbf{z}^r = (2, \dots, 2)^T$.

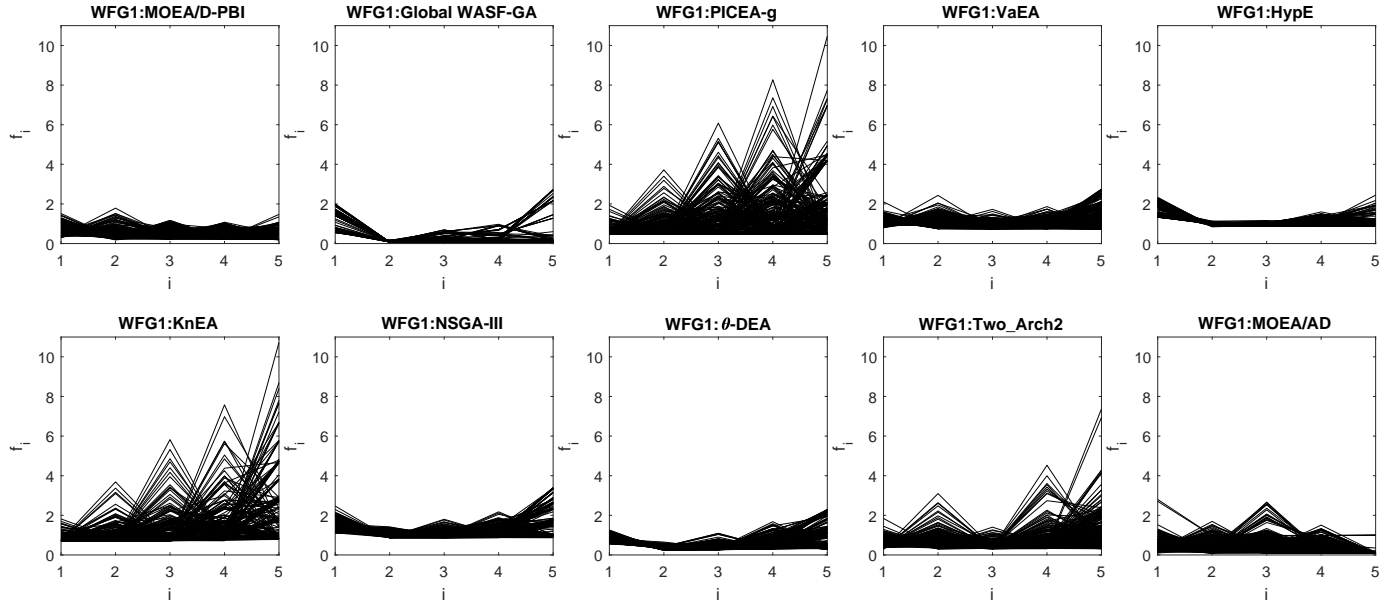


Fig. 42: Final solution sets on 5-objective WFG1 test problem obtained by 10 algorithms in the run of median HV metric values with $\mathbf{z}^r = (2, \dots, 2)^T$.

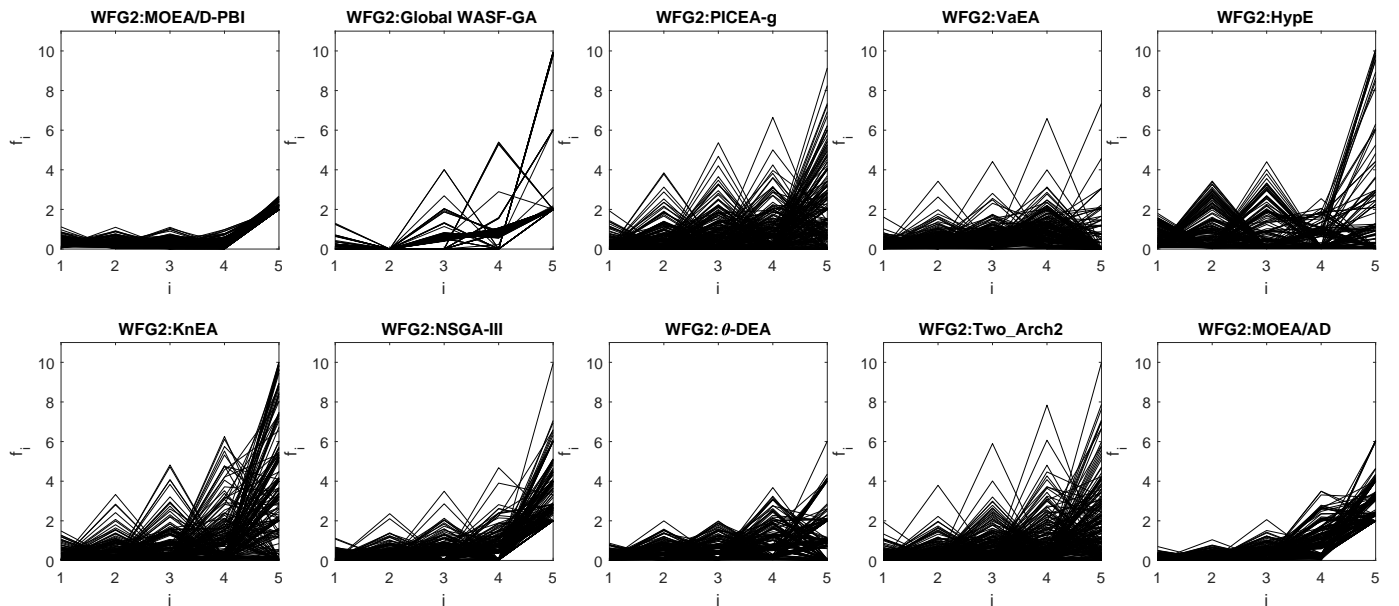


Fig. 43: Final solution sets on 5-objective WFG2 test problem obtained by 10 algorithms in the run of median HV metric values with $\mathbf{z}^r = (2, \dots, 2)^T$.

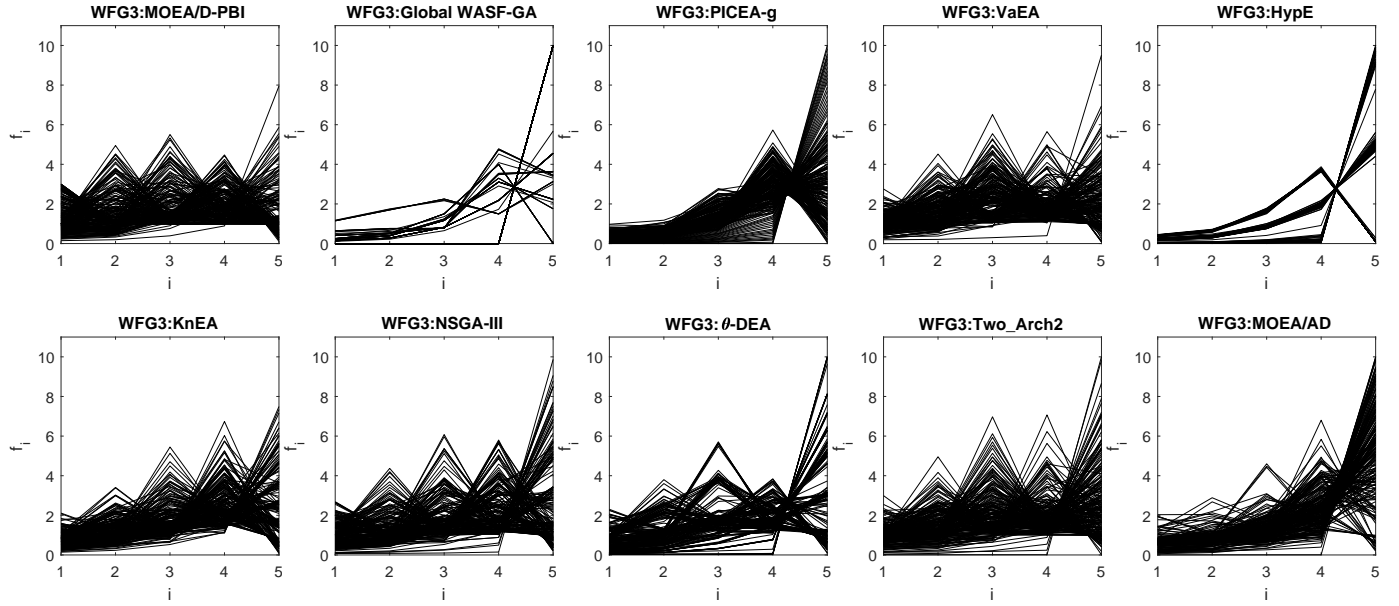


Fig. 44: Final solution sets on 5-objective WFG3 test problem obtained by 10 algorithms in the run of median HV metric values with $\mathbf{z}^r = (2, \dots, 2)^T$.

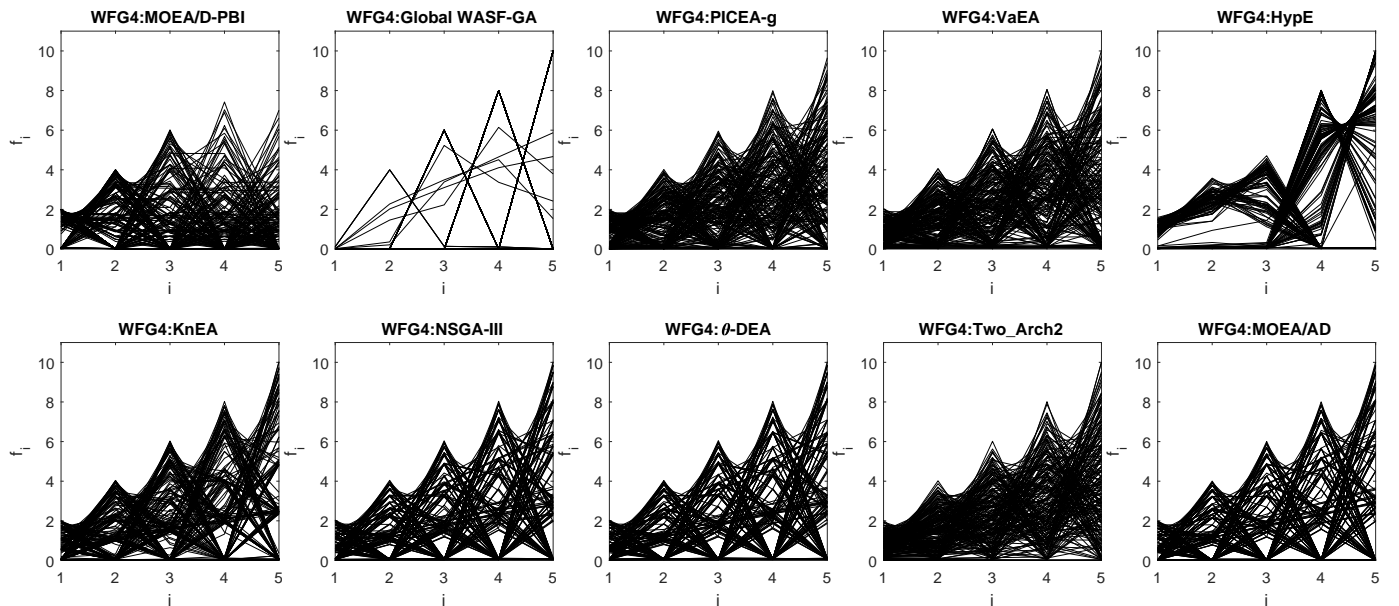


Fig. 45: Final solution sets on 5-objective WFG4 test problem obtained by 10 algorithms in the run of median HV metric values with $\mathbf{z}^r = (2, \dots, 2)^T$.

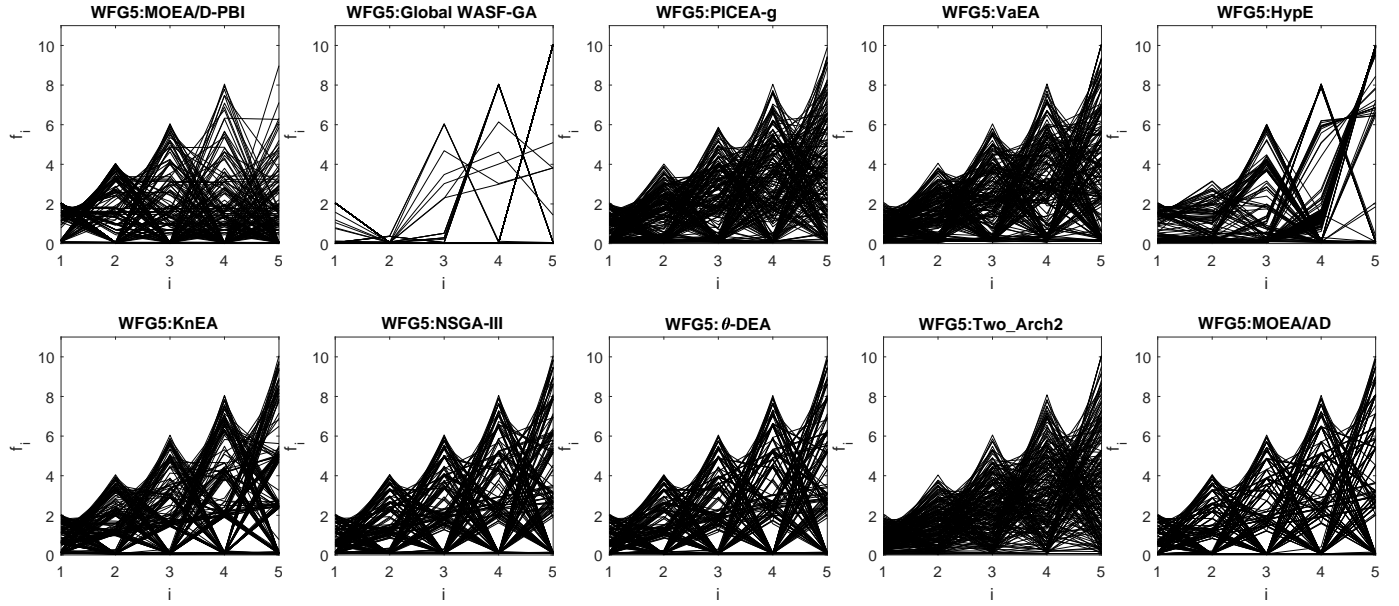


Fig. 46: Final solution sets on 5-objective WFG5 test problem obtained by 10 algorithms in the run of median HV metric values with $\mathbf{z}^r = (2, \dots, 2)^T$.

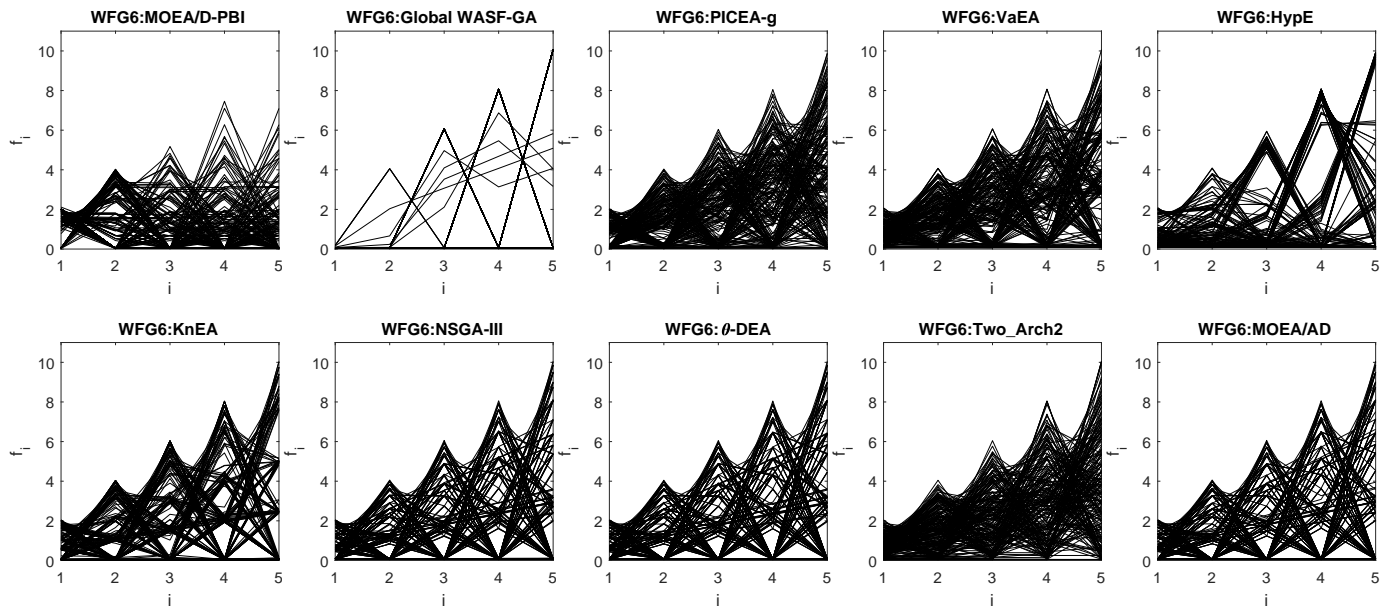


Fig. 47: Final solution sets on 5-objective WFG6 test problem obtained by 10 algorithms in the run of median HV metric values with $\mathbf{z}^r = (2, \dots, 2)^T$.

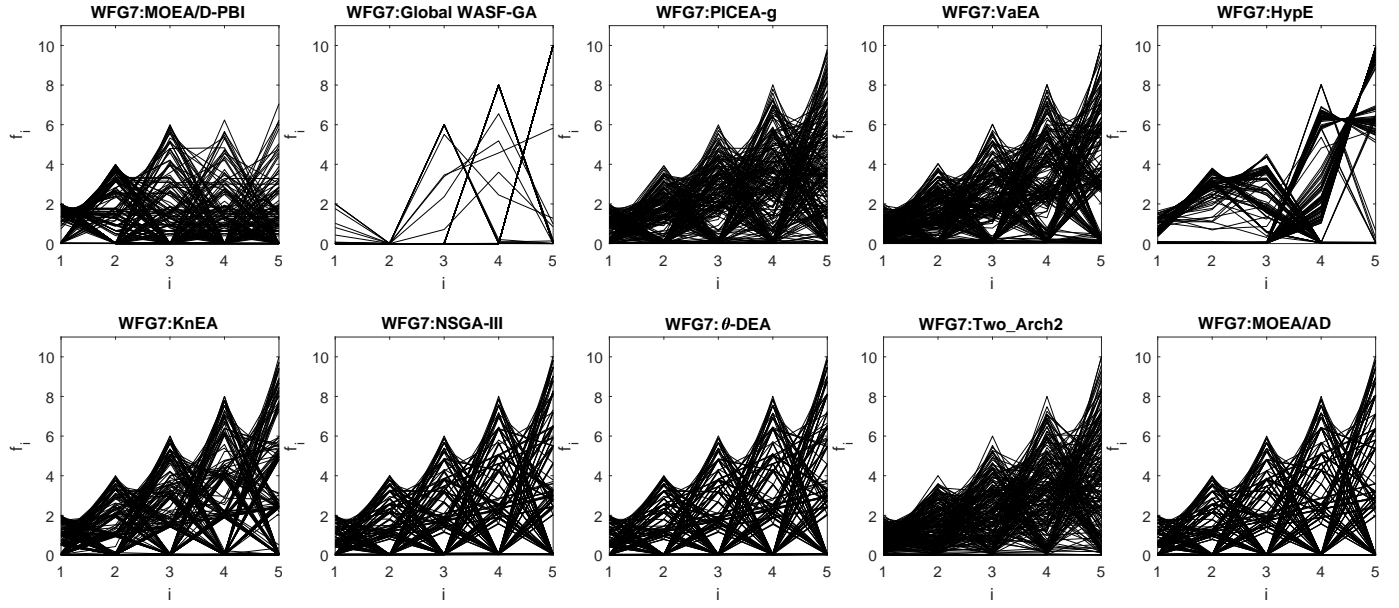


Fig. 48: Final solution sets on 5-objective WFG7 test problem obtained by 10 algorithms in the run of median HV metric values with $\mathbf{z}^r = (2, \dots, 2)^T$.

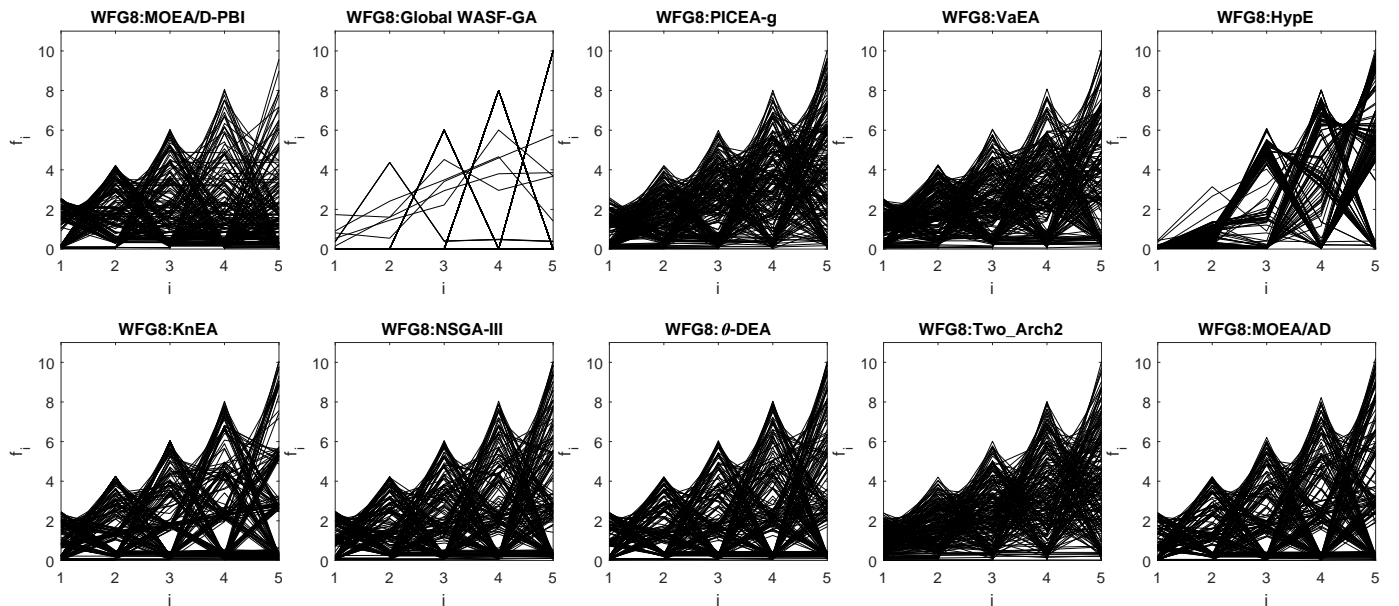


Fig. 49: Final solution sets on 5-objective WFG8 test problem obtained by 10 algorithms in the run of median HV metric values with $\mathbf{z}^r = (2, \dots, 2)^T$.

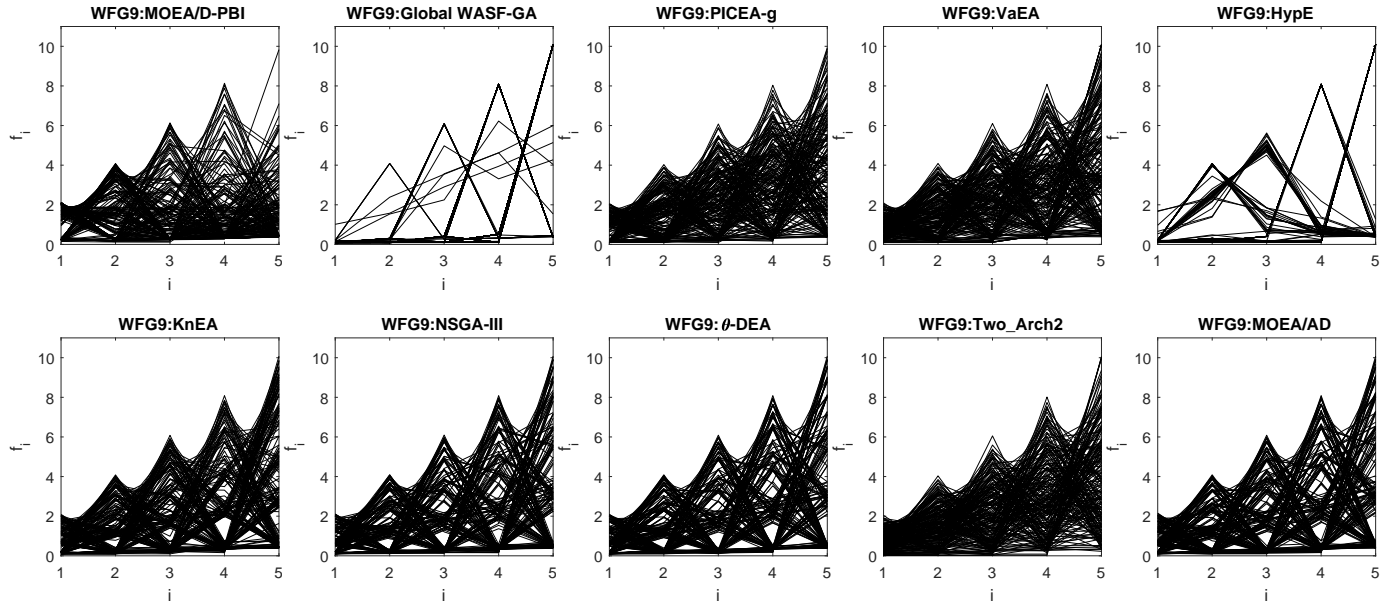


Fig. 50: Final solution sets on 5-objective WFG9 test problem obtained by 10 algorithms in the run of median HV metric values with $\mathbf{z}^r = (2, \dots, 2)^T$.

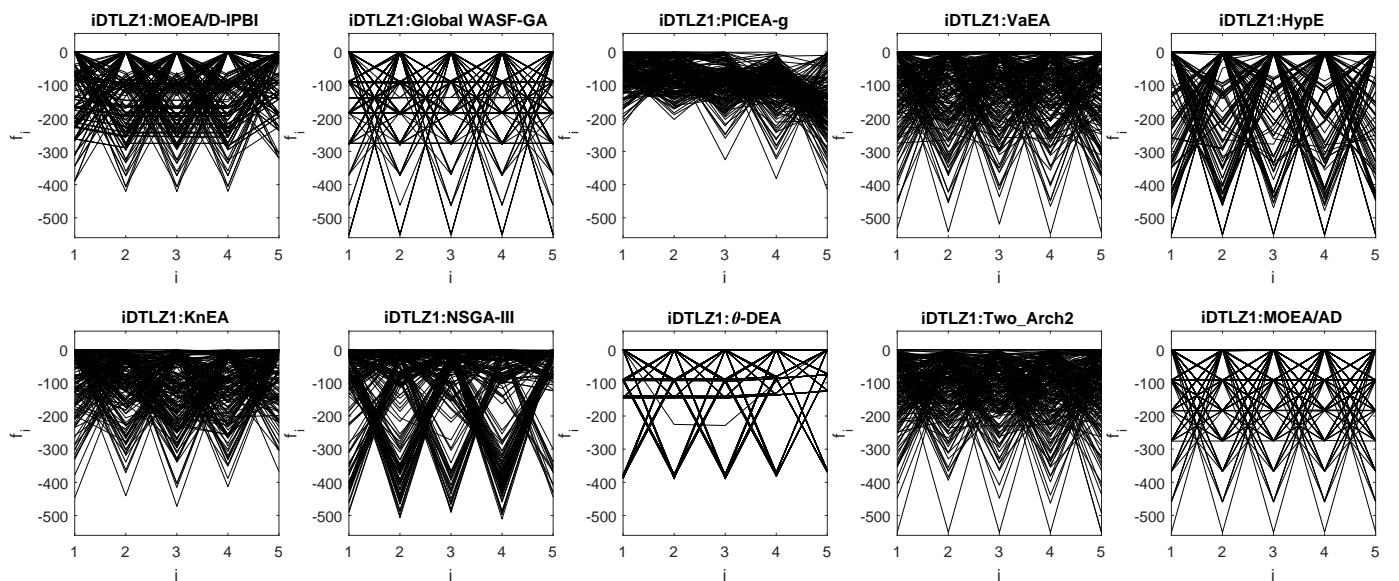


Fig. 51: Final solution sets on 5-objective DTLZ1⁻¹ test problem obtained by 10 algorithms in the run of median HV metric values with $\mathbf{z}^r = (2, \dots, 2)^T$.

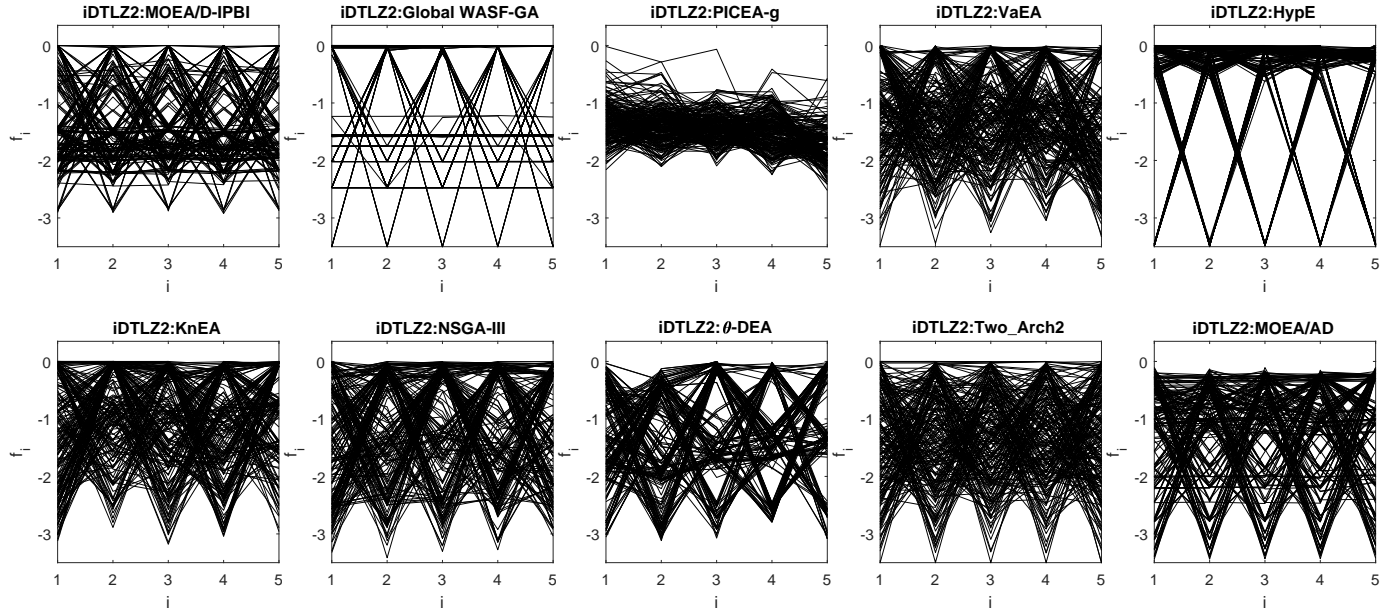


Fig. 52: Final solution sets on 5-objective DTLZ2^{-1} test problem obtained by 10 algorithms in the run of median HV metric values with $\mathbf{z}^r = (2, \dots, 2)^T$.

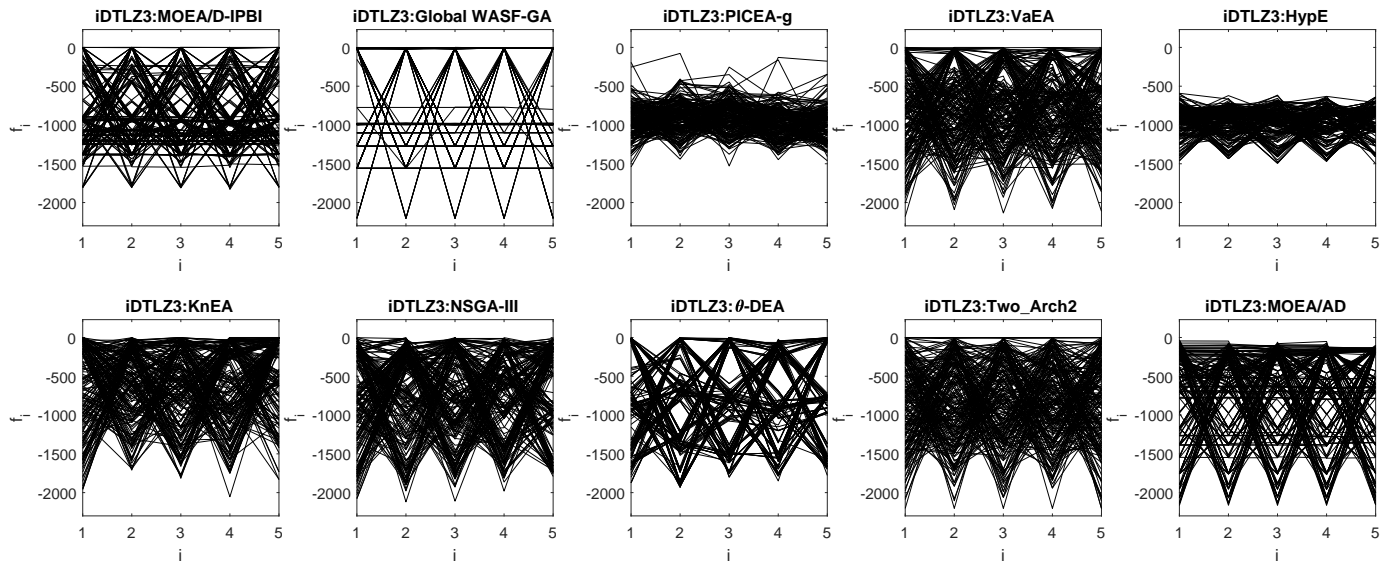


Fig. 53: Final solution sets on 5-objective DTLZ3^{-1} test problem obtained by 10 algorithms in the run of median HV metric values with $\mathbf{z}^r = (2, \dots, 2)^T$.

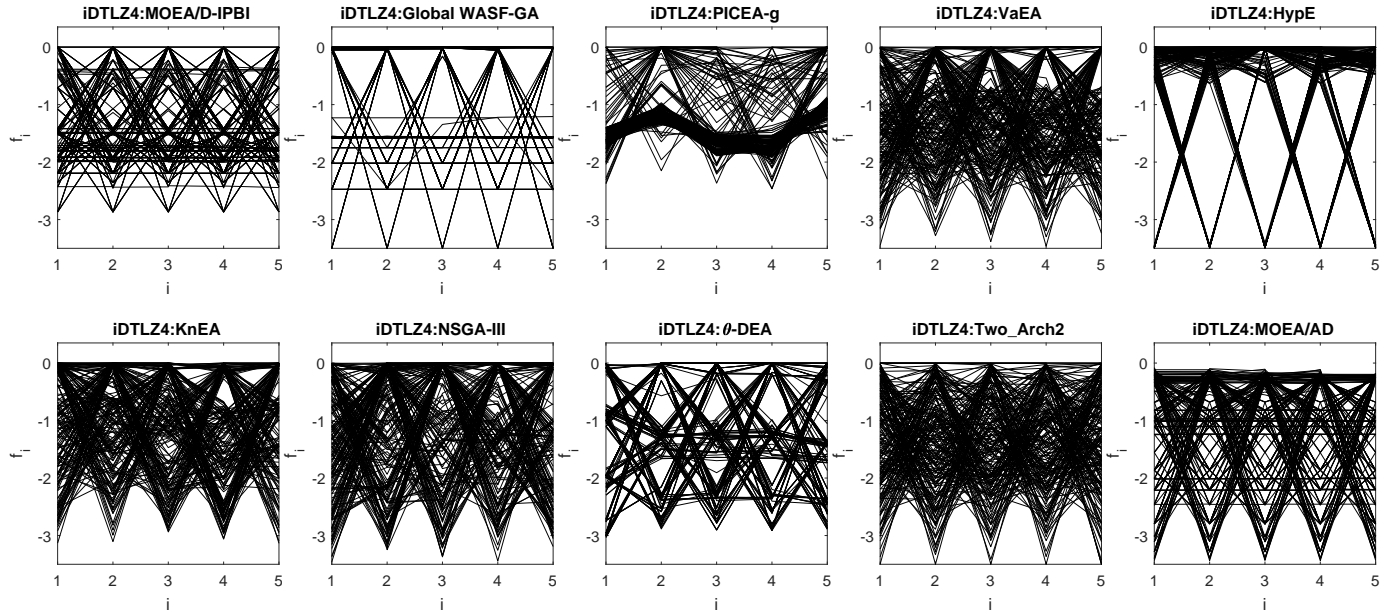


Fig. 54: Final solution sets on 5-objective $DTLZ4^{-1}$ test problem obtained by 10 algorithms in the run of median HV metric values with $\mathbf{z}^r = (2, \dots, 2)^T$.

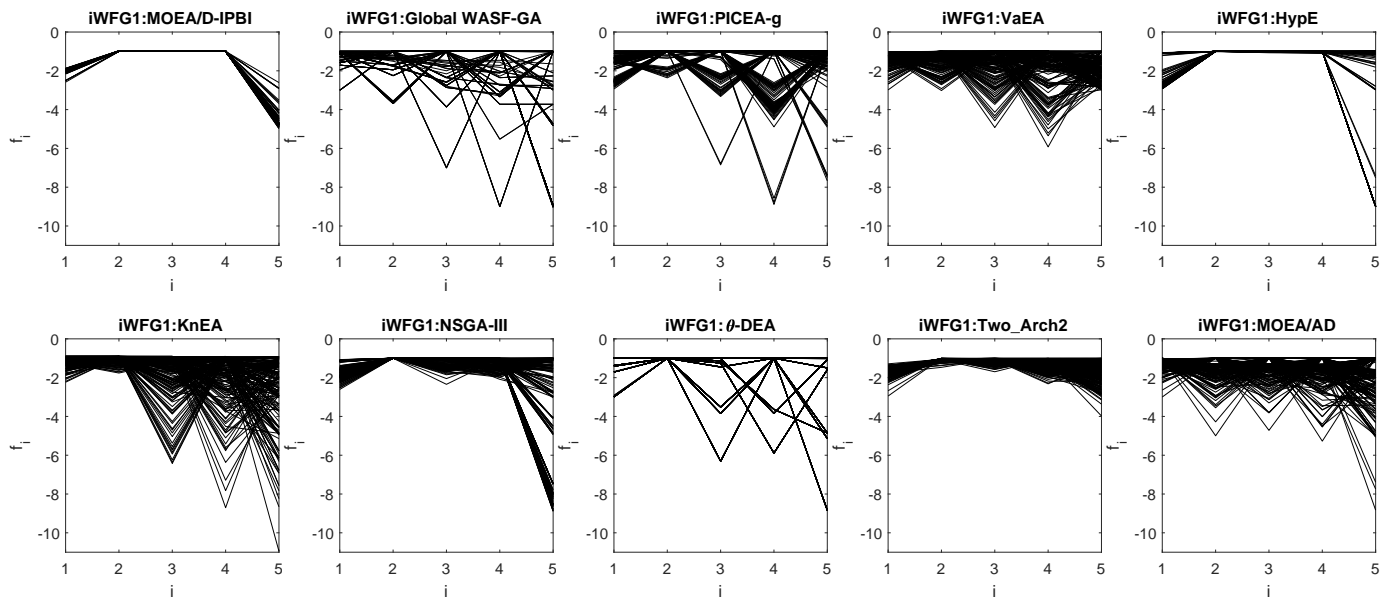


Fig. 55: Final solution sets on 5-objective $WFG1^{-1}$ test problem obtained by 10 algorithms in the run of median HV metric values with $\mathbf{z}^r = (2, \dots, 2)^T$.

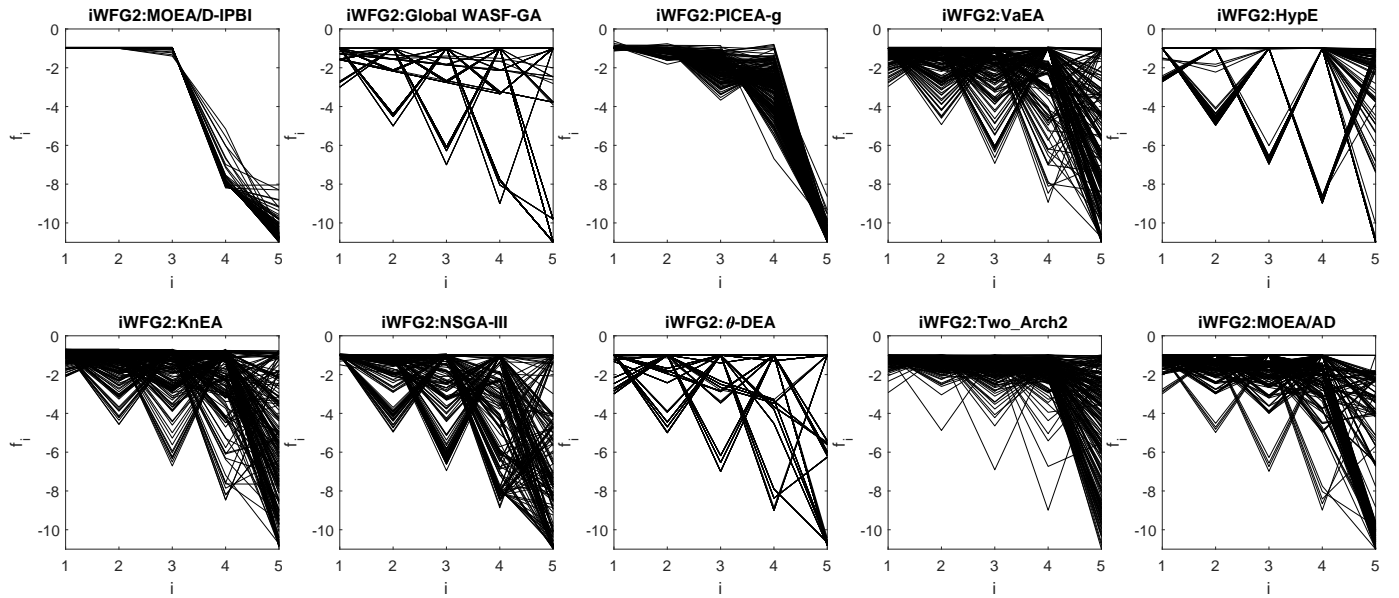


Fig. 56: Final solution sets on 5-objective WFG2 $^{-1}$ test problem obtained by 10 algorithms in the run of median HV metric values with $\mathbf{z}^r = (2, \dots, 2)^T$.

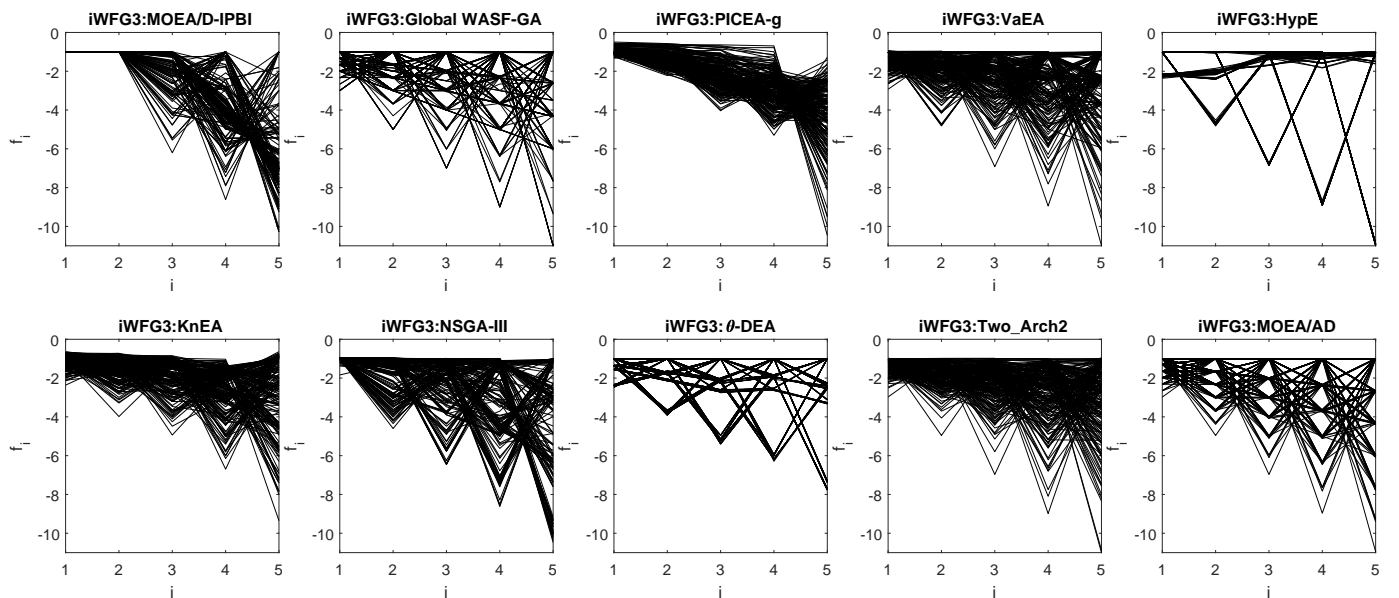


Fig. 57: Final solution sets on 5-objective WFG3 $^{-1}$ test problem obtained by 10 algorithms in the run of median HV metric values with $\mathbf{z}^r = (2, \dots, 2)^T$.

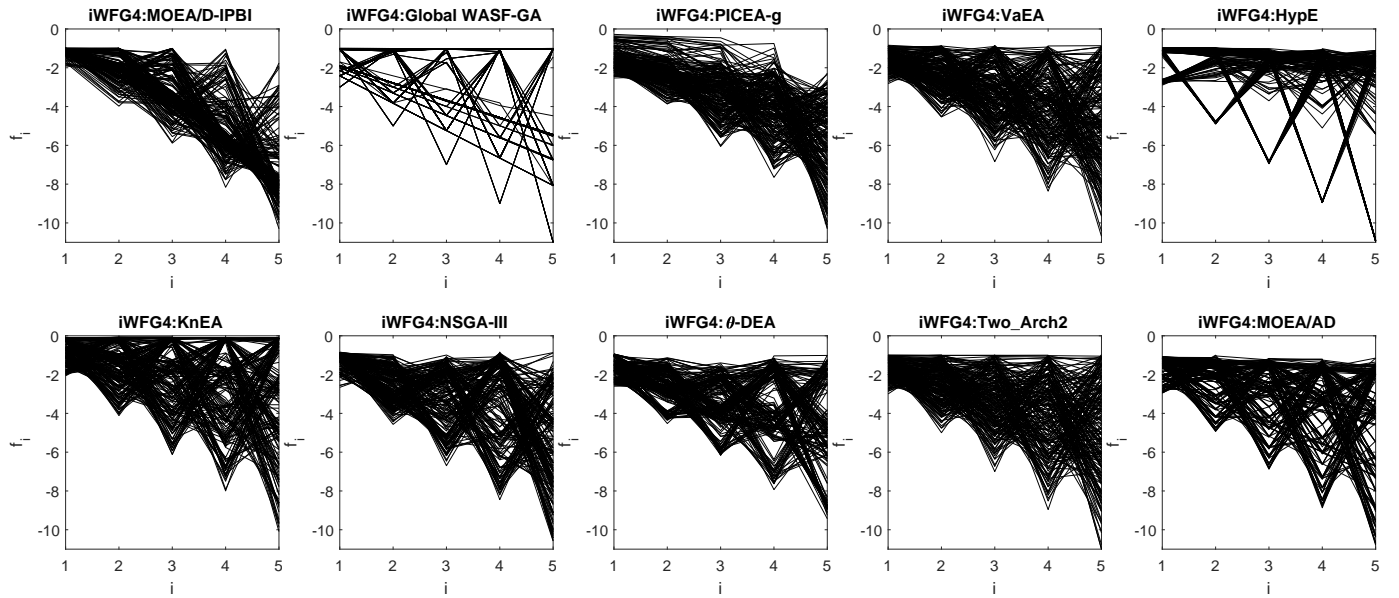


Fig. 58: Final solution sets on 5-objective WFG4⁻¹ test problem obtained by 10 algorithms in the run of median HV metric values with $\mathbf{z}^r = (2, \dots, 2)^T$.

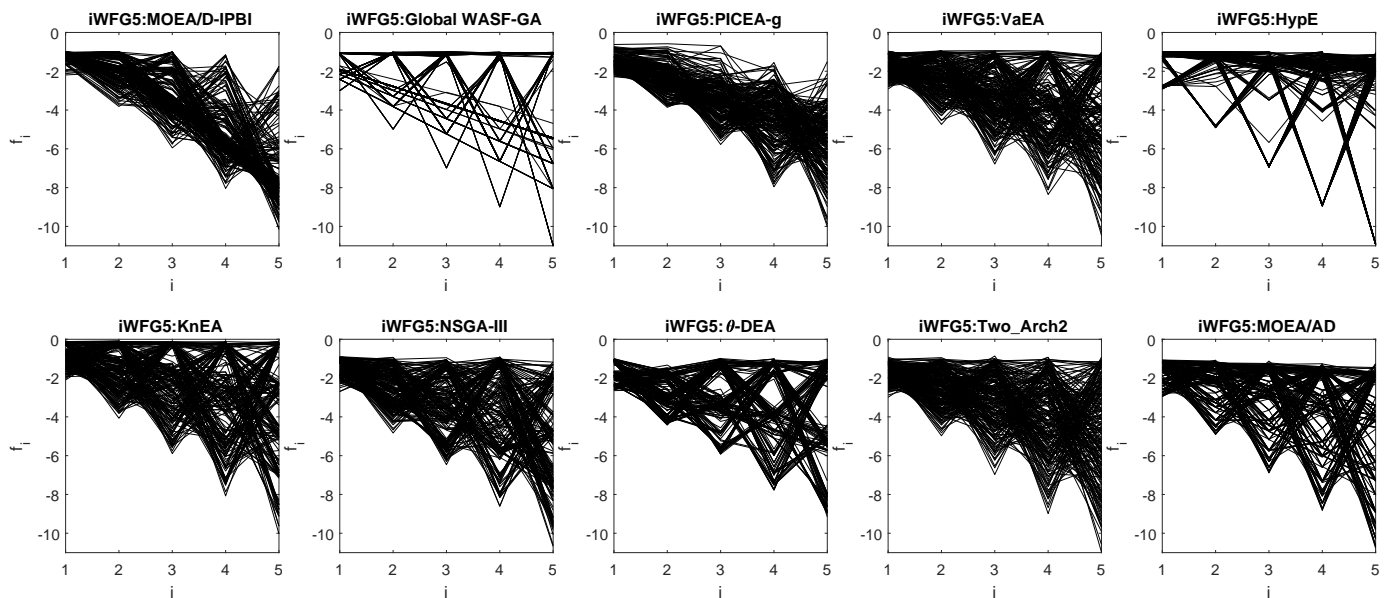


Fig. 59: Final solution sets on 5-objective WFG5⁻¹ test problem obtained by 10 algorithms in the run of median HV metric values with $\mathbf{z}^r = (2, \dots, 2)^T$.

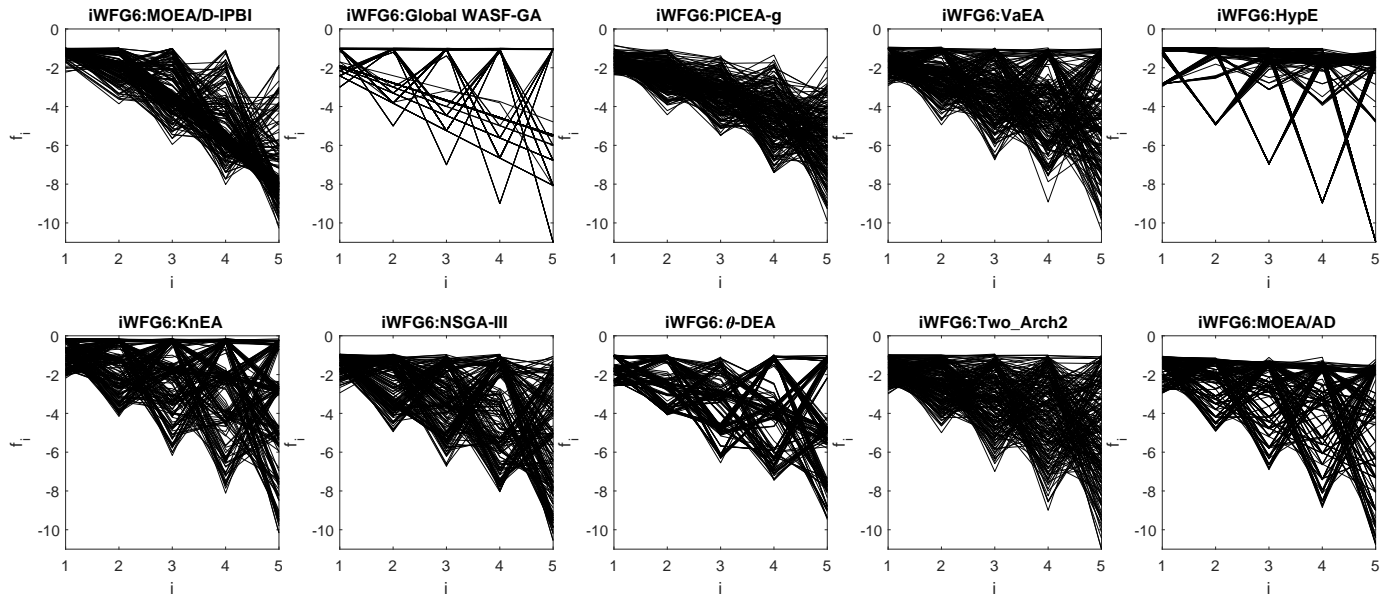


Fig. 60: Final solution sets on 5-objective WFG6^{-1} test problem obtained by 10 algorithms in the run of median HV metric values with $\mathbf{z}^r = (2, \dots, 2)^T$.

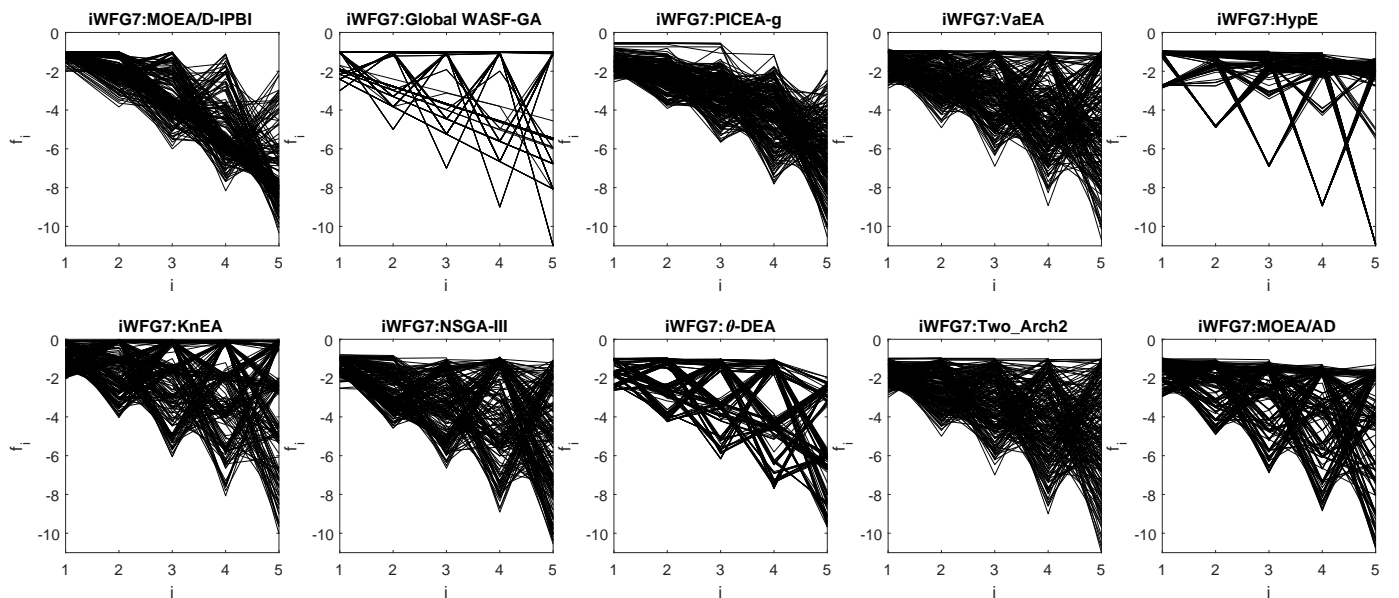


Fig. 61: Final solution sets on 5-objective WFG7^{-1} test problem obtained by 10 algorithms in the run of median HV metric values with $\mathbf{z}^r = (2, \dots, 2)^T$.

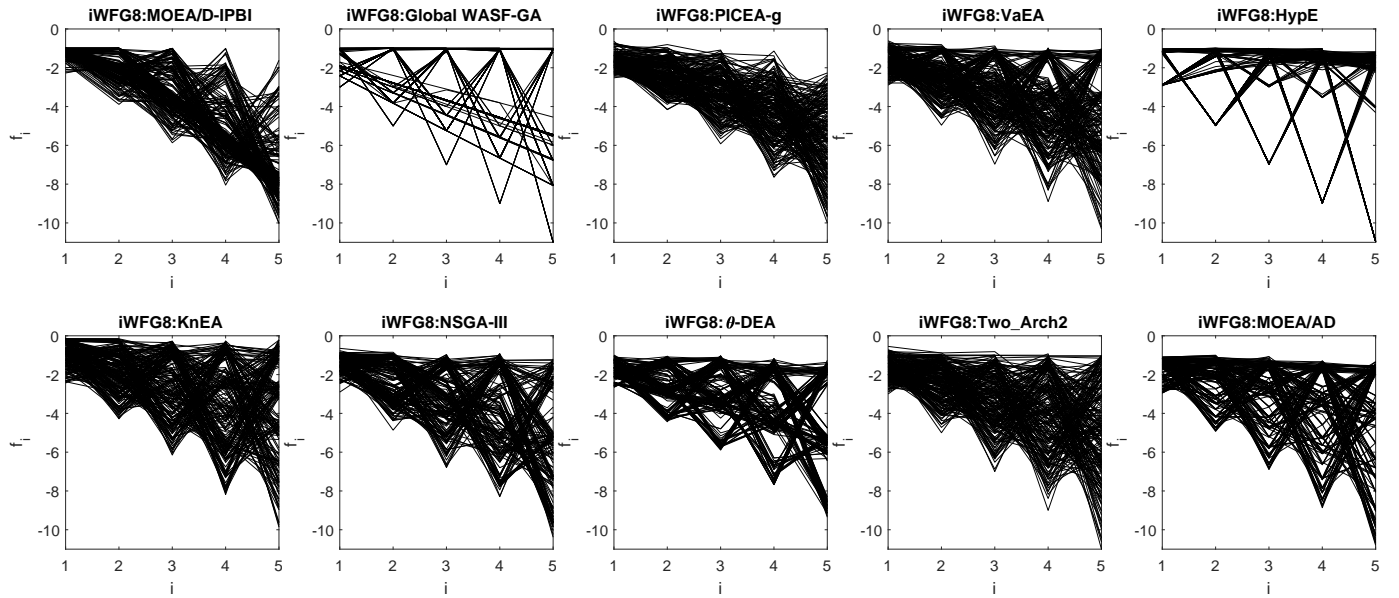


Fig. 62: Final solution sets on 5-objective WFG8^{-1} test problem obtained by 10 algorithms in the run of median HV metric values with $\mathbf{z}^r = (2, \dots, 2)^T$.

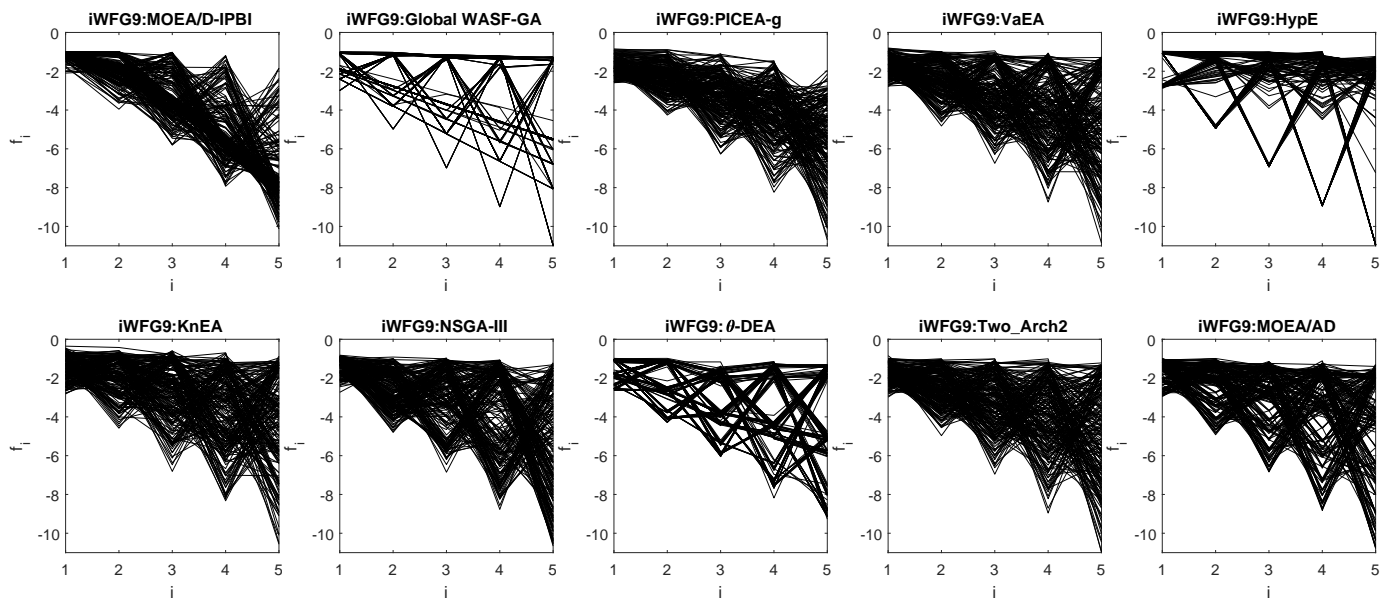


Fig. 63: Final solution sets on 5-objective WFG9^{-1} test problem obtained by 10 algorithms in the run of median HV metric values with $\mathbf{z}^r = (2, \dots, 2)^T$.

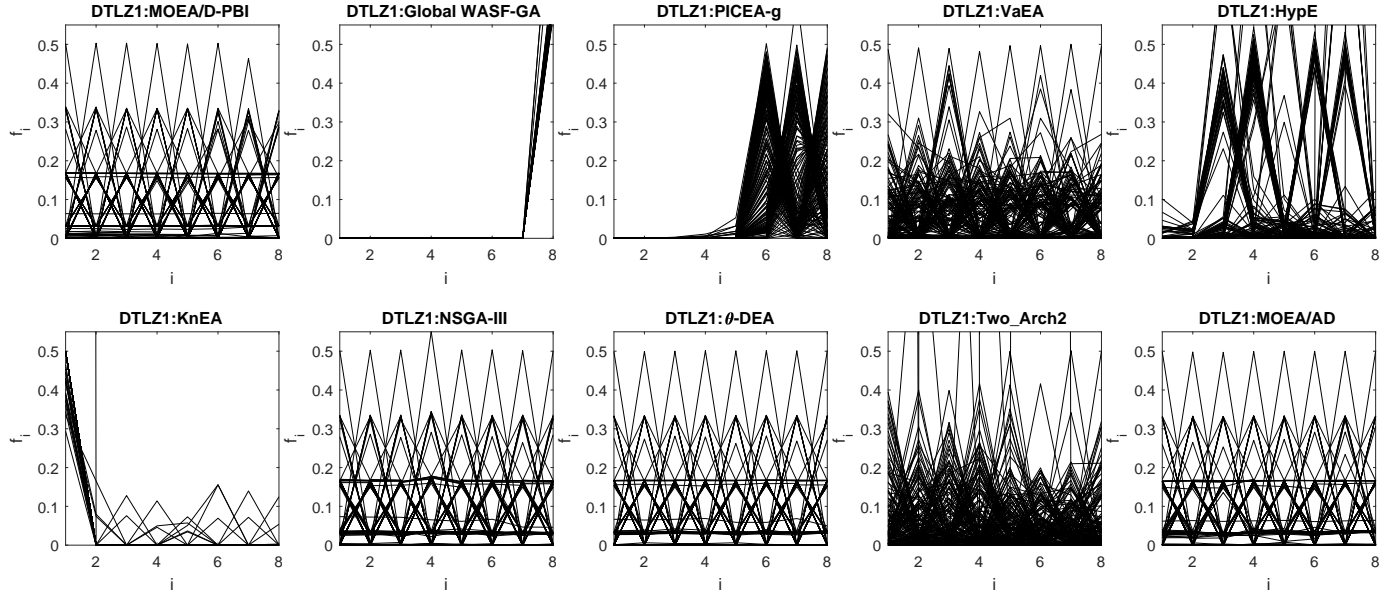


Fig. 64: Final solution sets on 8-objective DTLZ1 test problem obtained by 10 algorithms in the run of median HV metric values with $\mathbf{z}^r = (2, \dots, 2)^T$.

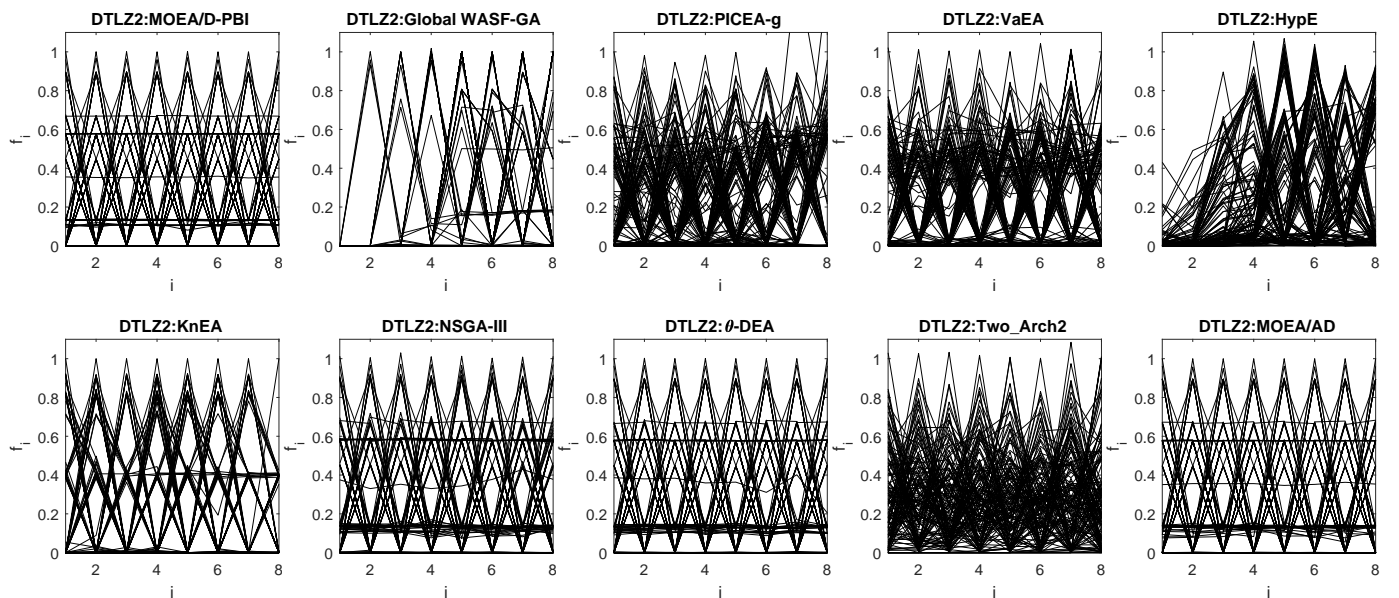


Fig. 65: Final solution sets on 8-objective DTLZ2 test problem obtained by 10 algorithms in the run of median HV metric values with $\mathbf{z}^r = (2, \dots, 2)^T$.

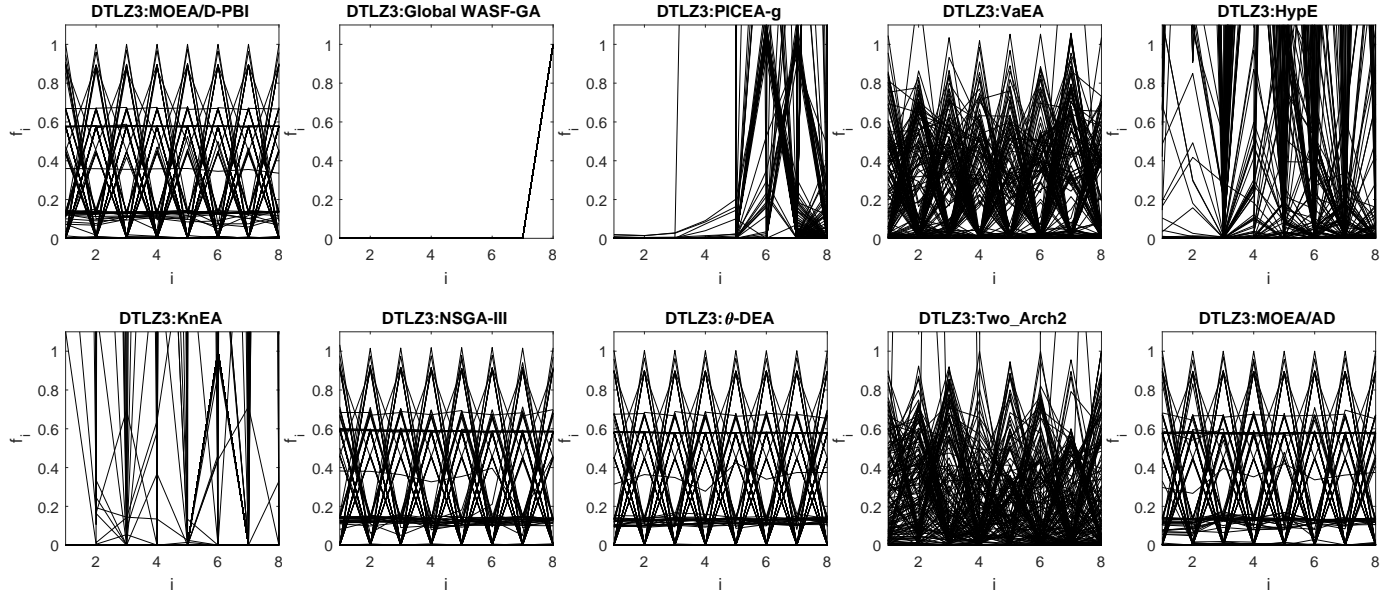


Fig. 66: Final solution sets on 8-objective DTLZ3 test problem obtained by 10 algorithms in the run of median HV metric values with $\mathbf{z}^r = (2, \dots, 2)^T$.

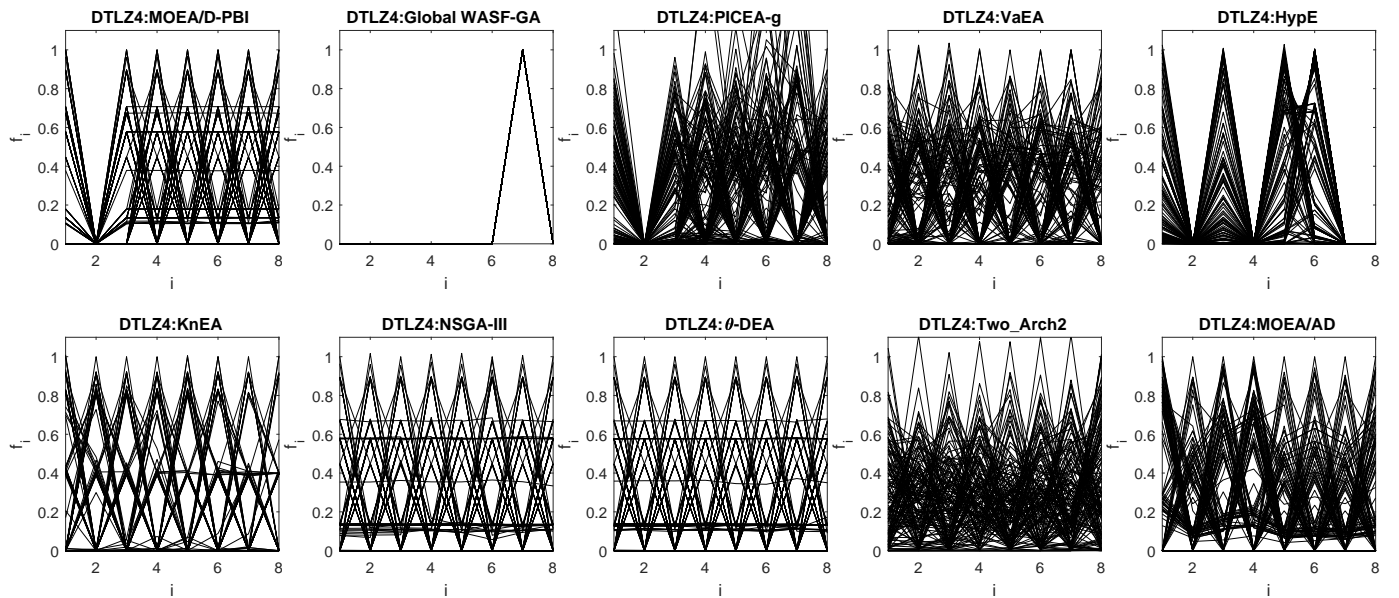


Fig. 67: Final solution sets on 8-objective DTLZ4 test problem obtained by 10 algorithms in the run of median HV metric values with $\mathbf{z}^r = (2, \dots, 2)^T$.

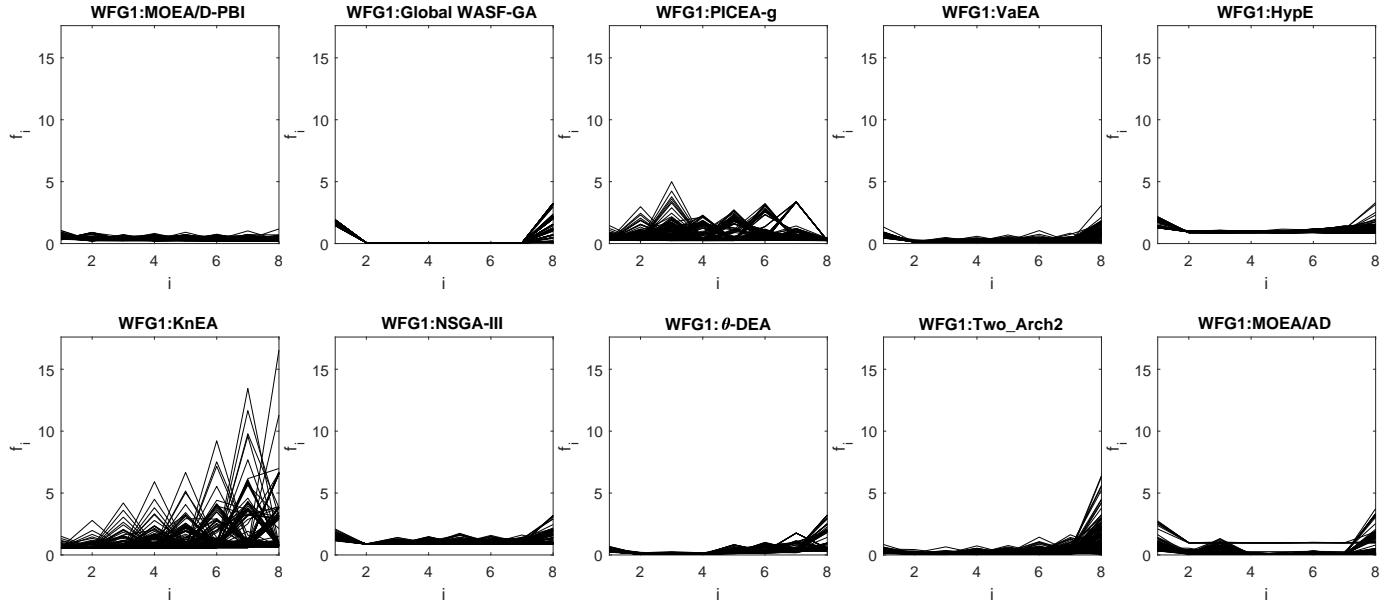


Fig. 68: Final solution sets on 8-objective WFG1 test problem obtained by 10 algorithms in the run of median HV metric values with $\mathbf{z}^r = (2, \dots, 2)^T$.

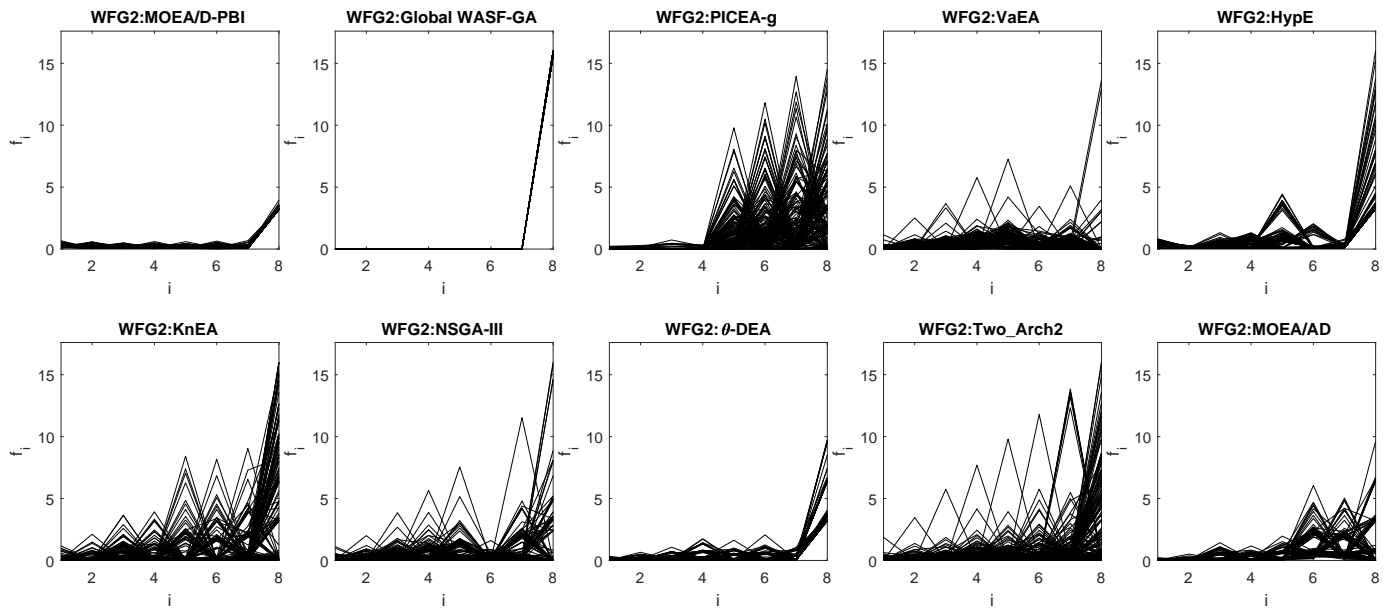


Fig. 69: Final solution sets on 8-objective WFG2 test problem obtained by 10 algorithms in the run of median HV metric values with $\mathbf{z}^r = (2, \dots, 2)^T$.

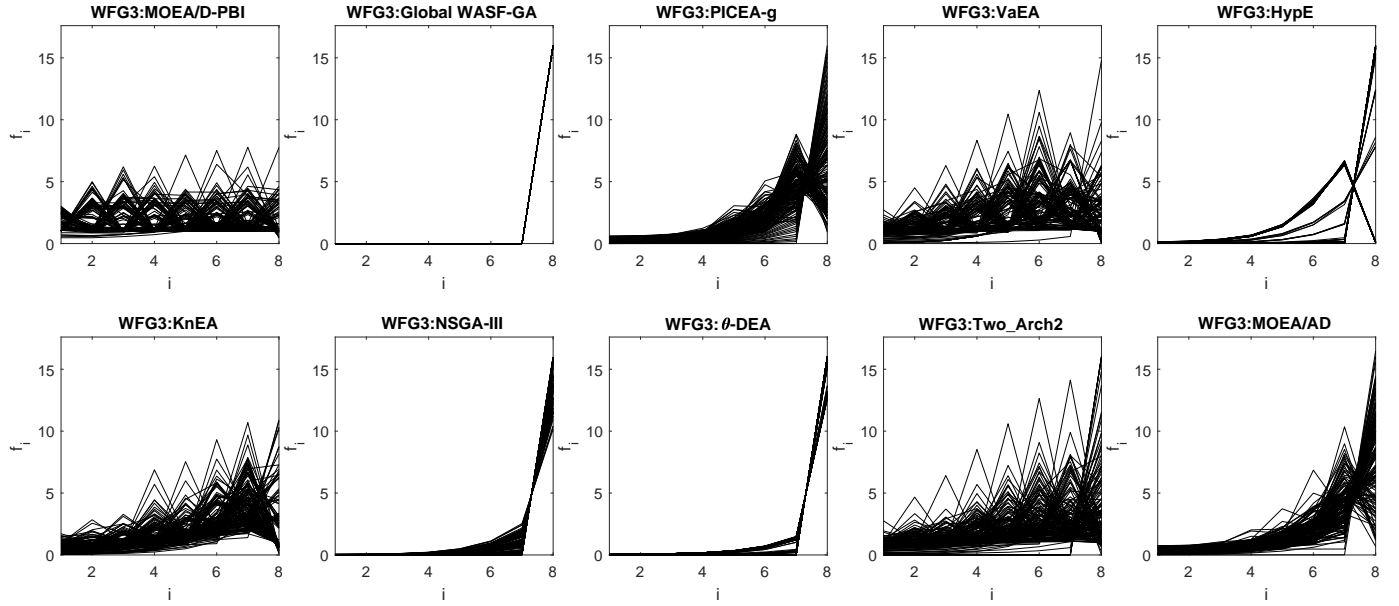


Fig. 70: Final solution sets on 8-objective WFG3 test problem obtained by 10 algorithms in the run of median HV metric values with $\mathbf{z}^r = (2, \dots, 2)^T$.

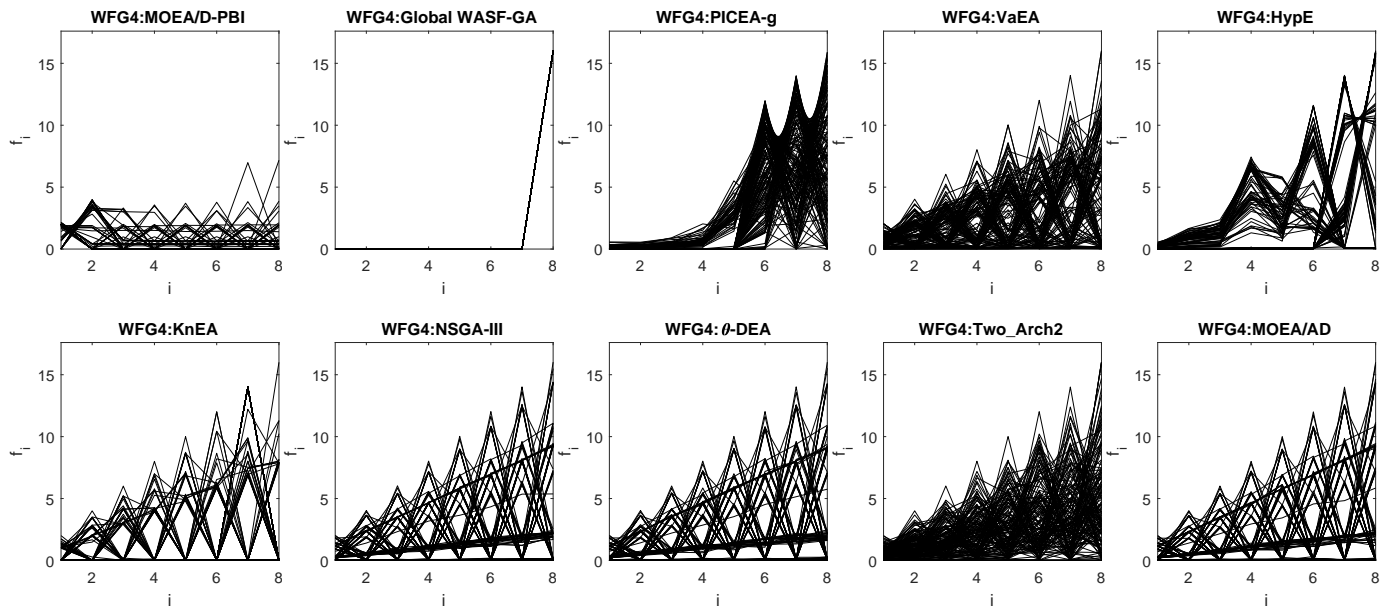


Fig. 71: Final solution sets on 8-objective WFG4 test problem obtained by 10 algorithms in the run of median HV metric values with $\mathbf{z}^r = (2, \dots, 2)^T$.

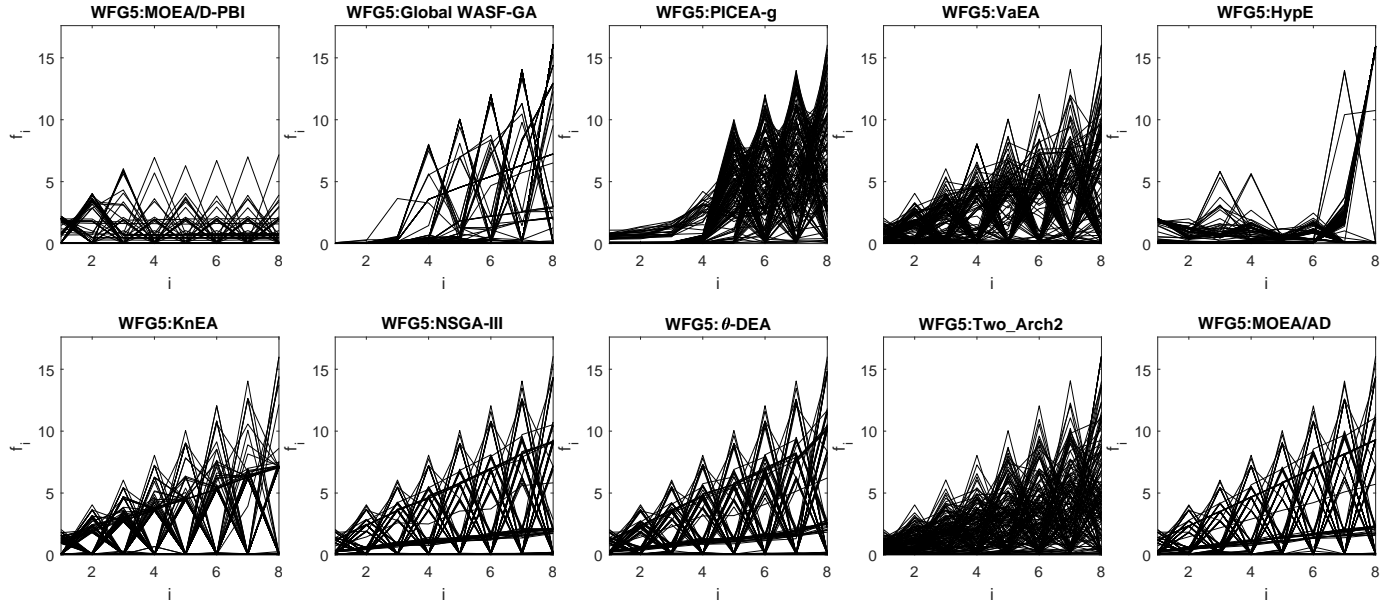


Fig. 72: Final solution sets on 8-objective WFG5 test problem obtained by 10 algorithms in the run of median HV metric values with $\mathbf{z}^r = (2, \dots, 2)^T$.

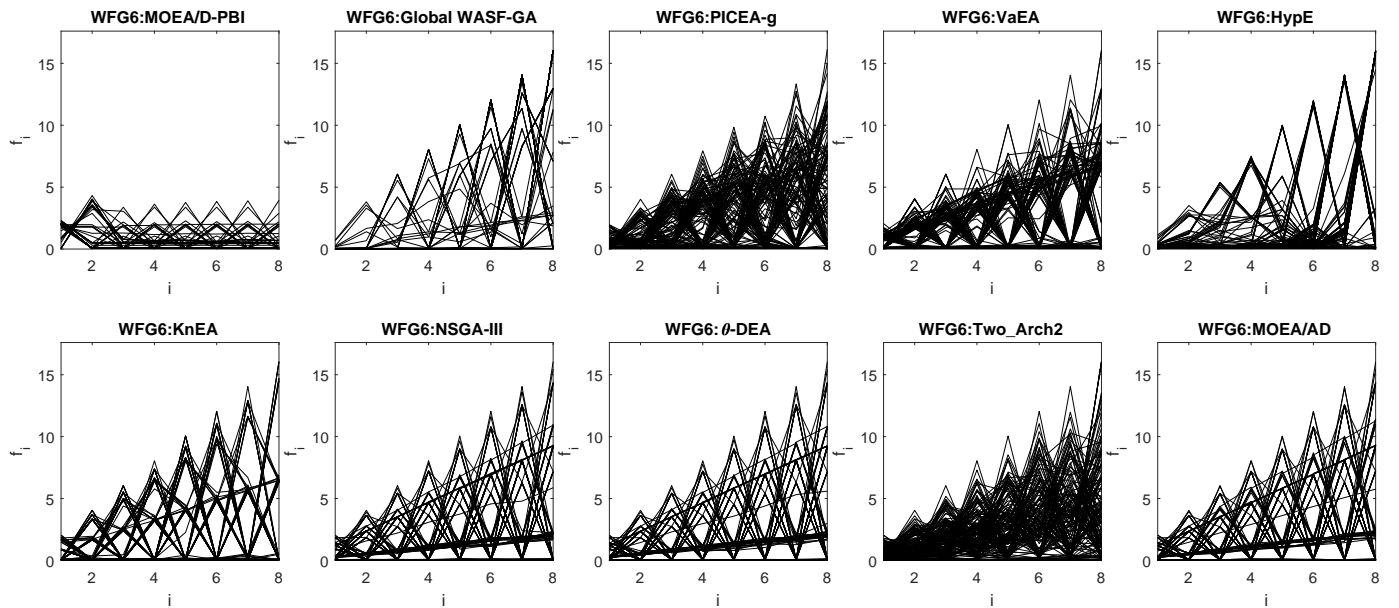


Fig. 73: Final solution sets on 8-objective WFG6 test problem obtained by 10 algorithms in the run of median HV metric values with $\mathbf{z}^r = (2, \dots, 2)^T$.

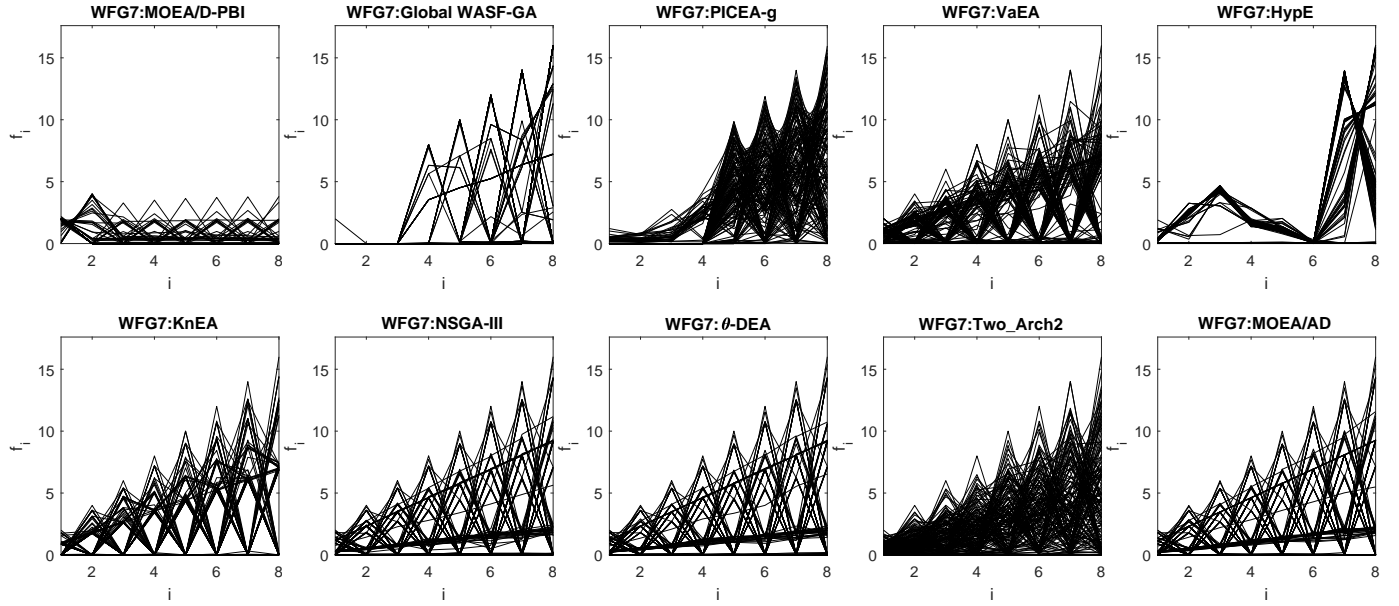


Fig. 74: Final solution sets on 8-objective WFG7 test problem obtained by 10 algorithms in the run of median HV metric values with $\mathbf{z}^r = (2, \dots, 2)^T$.

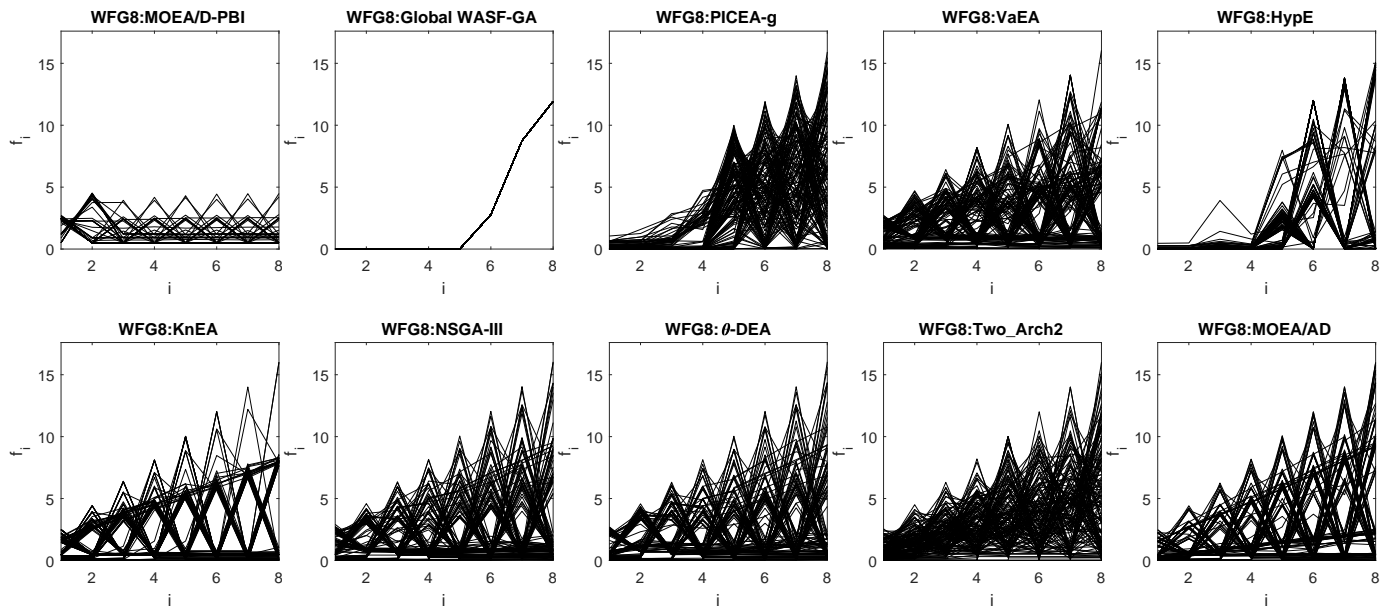


Fig. 75: Final solution sets on 8-objective WFG8 test problem obtained by 10 algorithms in the run of median HV metric values with $\mathbf{z}^r = (2, \dots, 2)^T$.

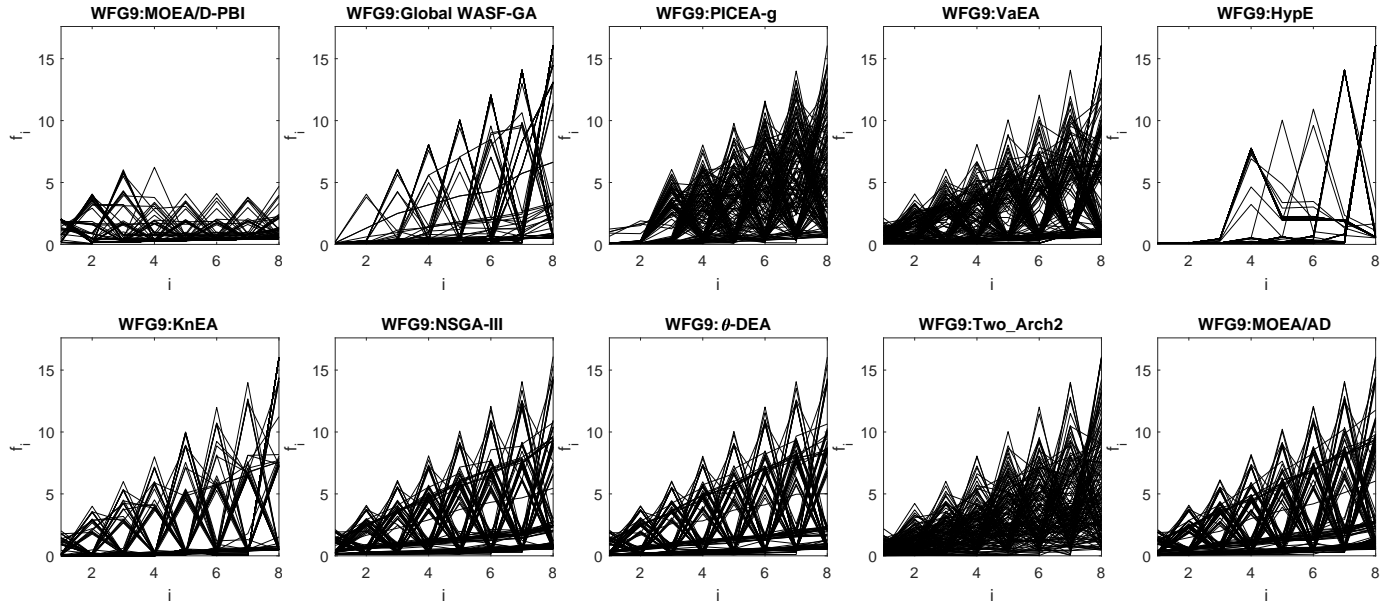


Fig. 76: Final solution sets on 8-objective WFG9 test problem obtained by 10 algorithms in the run of median HV metric values with $\mathbf{z}^r = (2, \dots, 2)^T$.

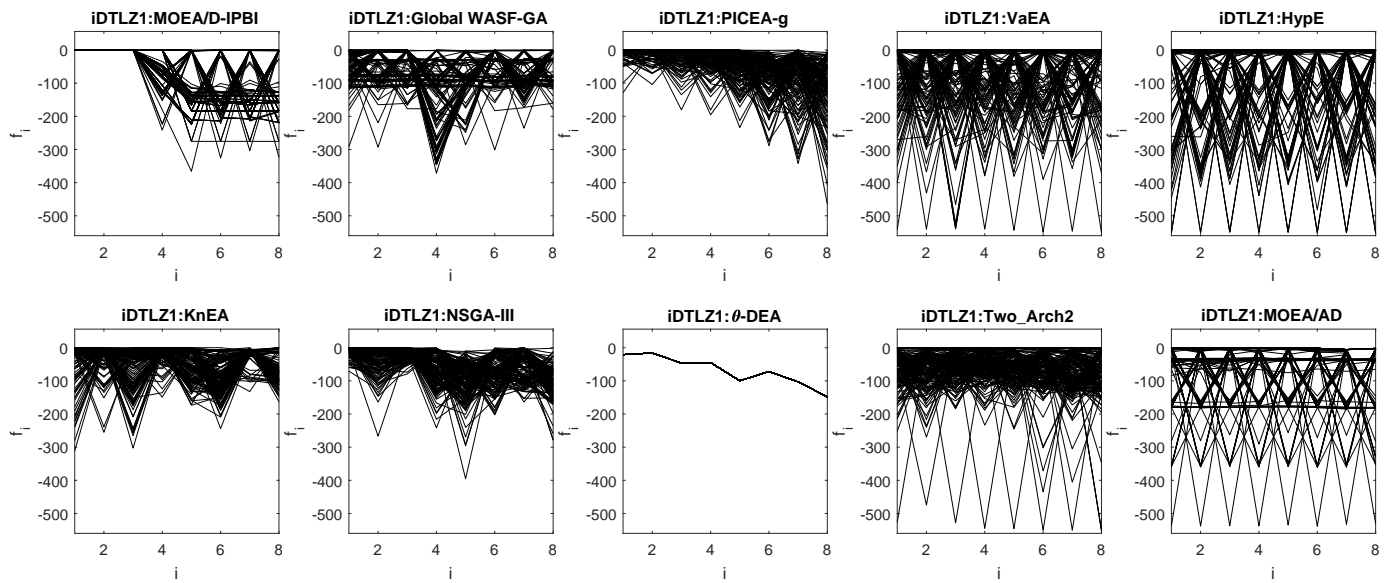


Fig. 77: Final solution sets on 8-objective DTLZ1⁻¹ test problem obtained by 10 algorithms in the run of median HV metric values with $\mathbf{z}^r = (2, \dots, 2)^T$.

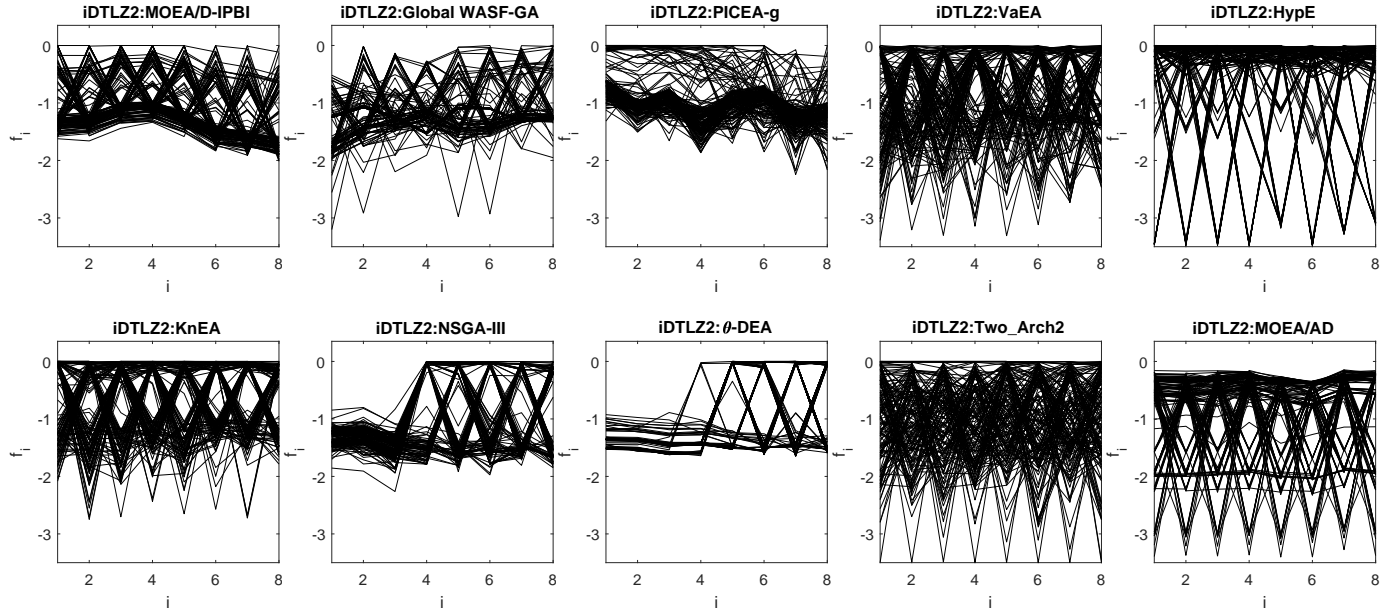


Fig. 78: Final solution sets on 8-objective DTLZ2^{-1} test problem obtained by 10 algorithms in the run of median HV metric values with $\mathbf{z}^r = (2, \dots, 2)^T$.

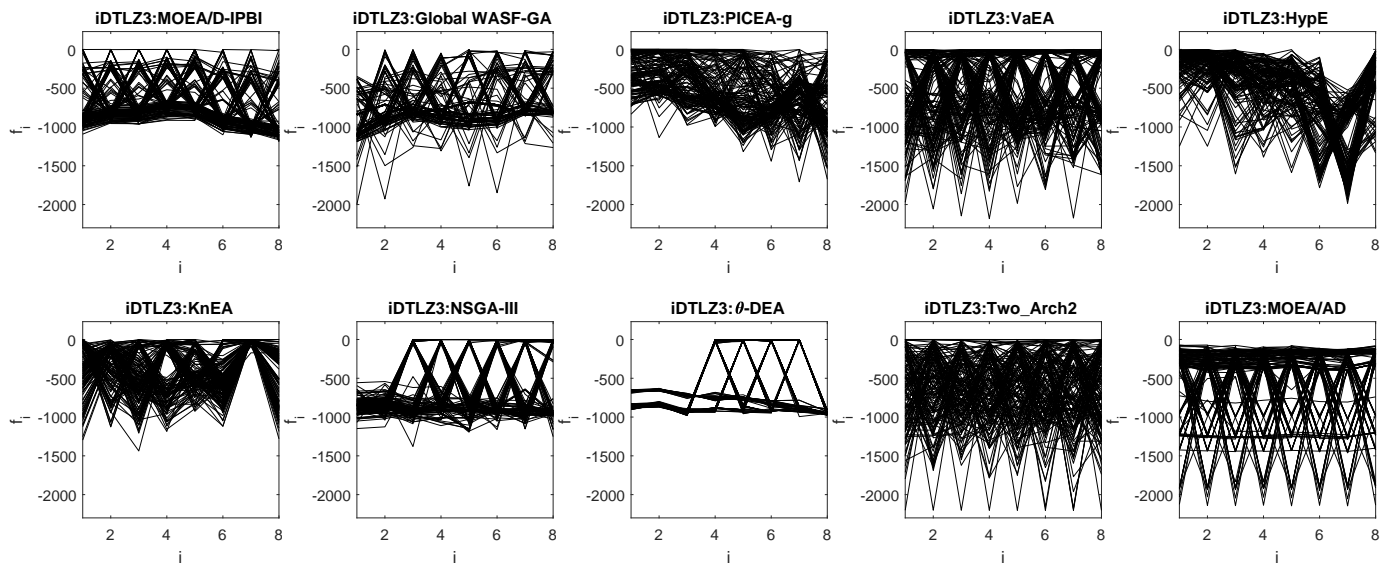


Fig. 79: Final solution sets on 8-objective DTLZ3^{-1} test problem obtained by 10 algorithms in the run of median HV metric values with $\mathbf{z}^r = (2, \dots, 2)^T$.

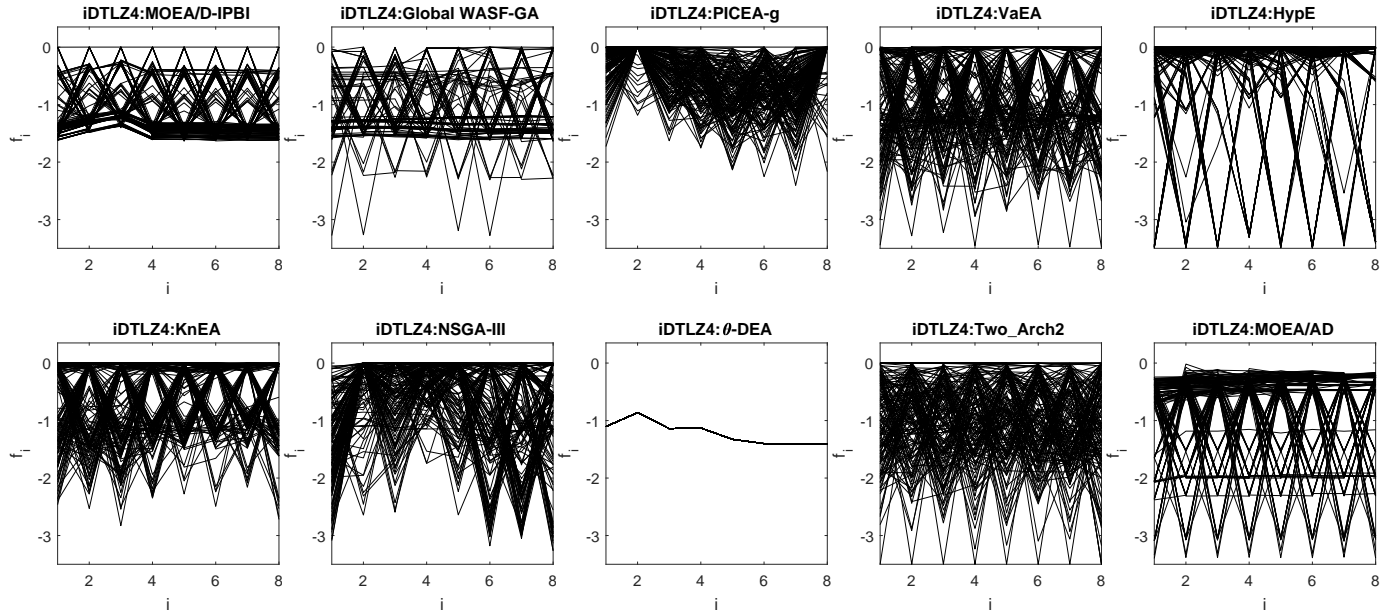


Fig. 80: Final solution sets on 8-objective DTLZ4⁻¹ test problem obtained by 10 algorithms in the run of median HV metric values with $\mathbf{z}^r = (2, \dots, 2)^T$.

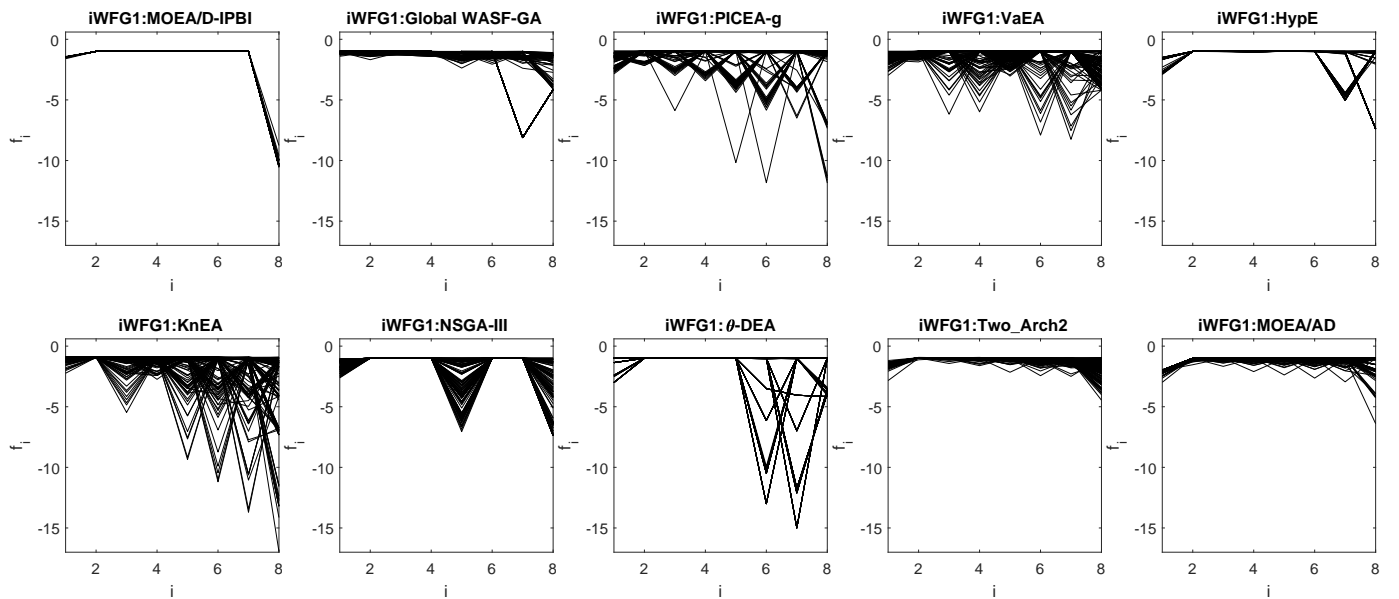


Fig. 81: Final solution sets on 8-objective WFG1⁻¹ test problem obtained by 10 algorithms in the run of median HV metric values with $\mathbf{z}^r = (2, \dots, 2)^T$.

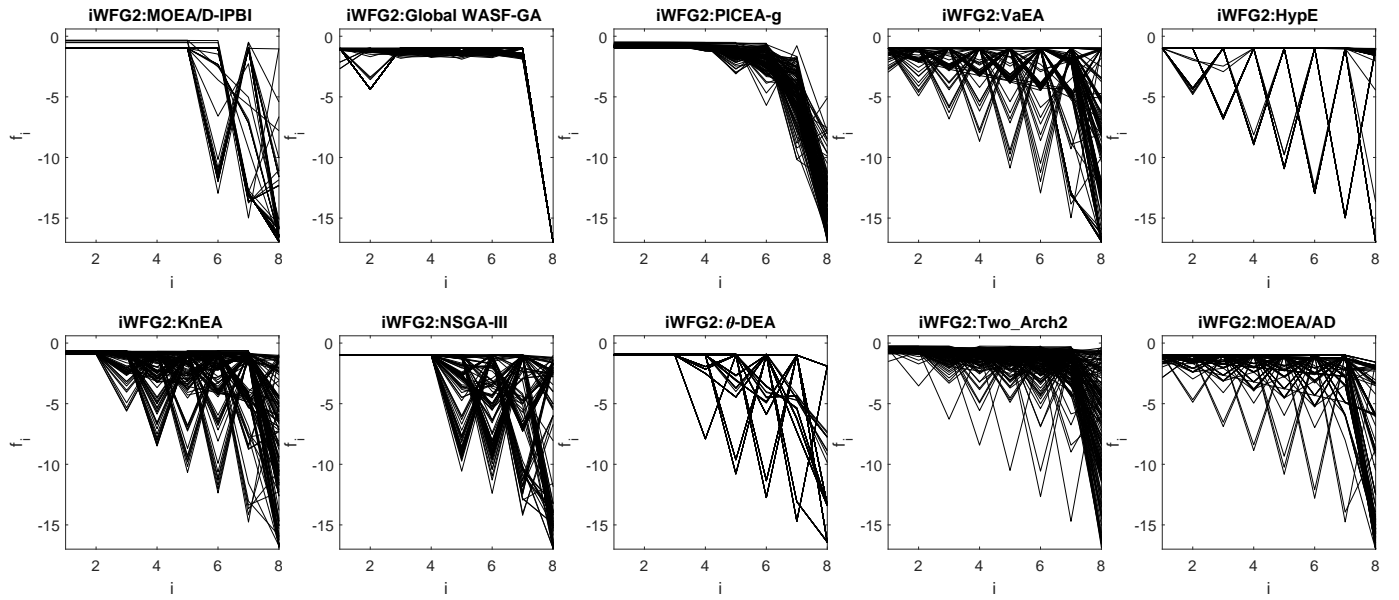


Fig. 82: Final solution sets on 8-objective WFG2⁻¹ test problem obtained by 10 algorithms in the run of median HV metric values with $\mathbf{z}^r = (2, \dots, 2)^T$.

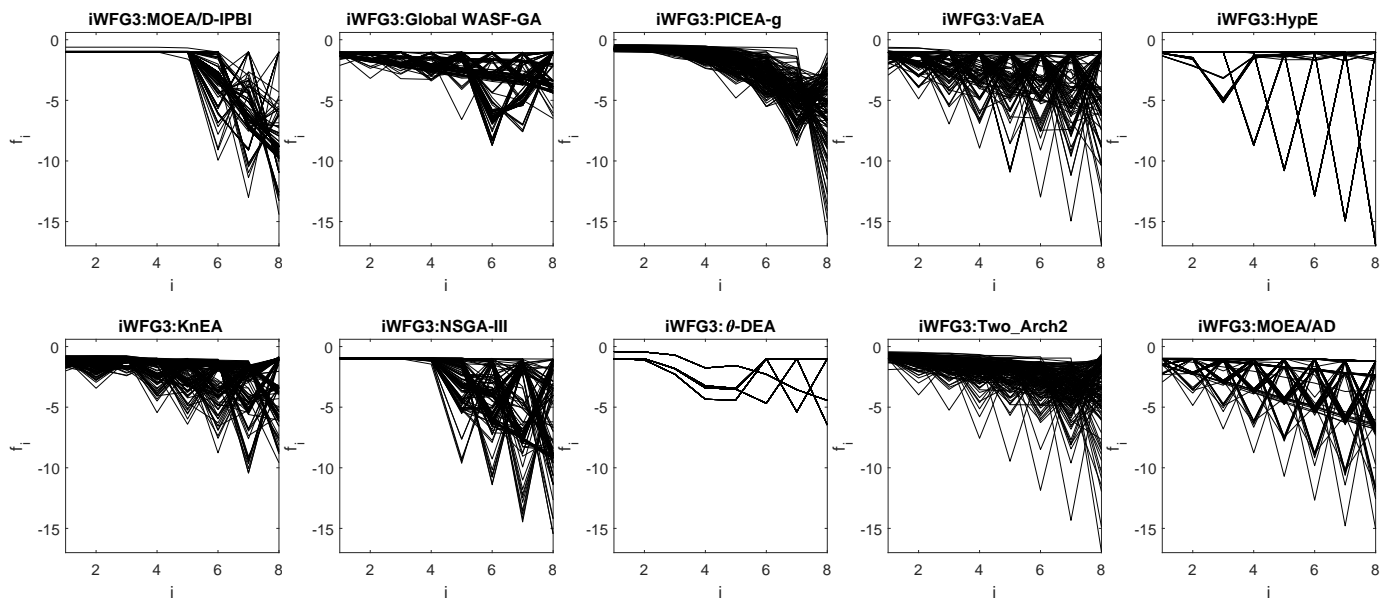


Fig. 83: Final solution sets on 8-objective WFG3⁻¹ test problem obtained by 10 algorithms in the run of median HV metric values with $\mathbf{z}^r = (2, \dots, 2)^T$.

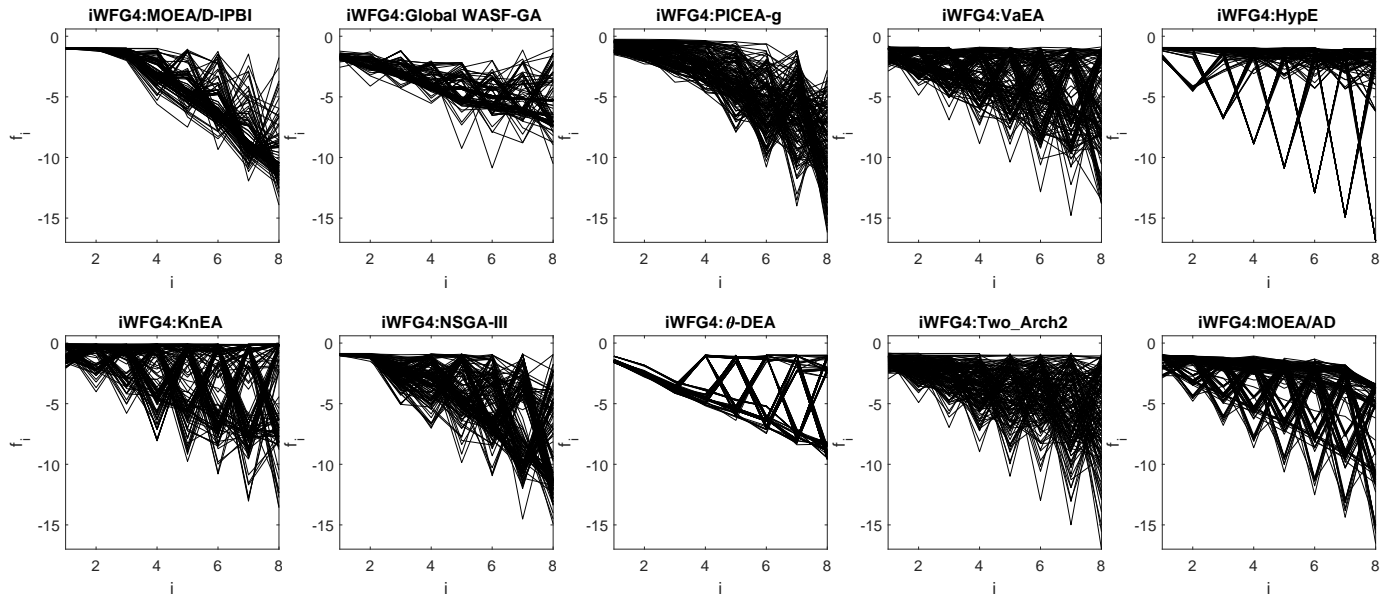


Fig. 84: Final solution sets on 8-objective WFG4 $^{-1}$ test problem obtained by 10 algorithms in the run of median HV metric values with $\mathbf{z}^r = (2, \dots, 2)^T$.

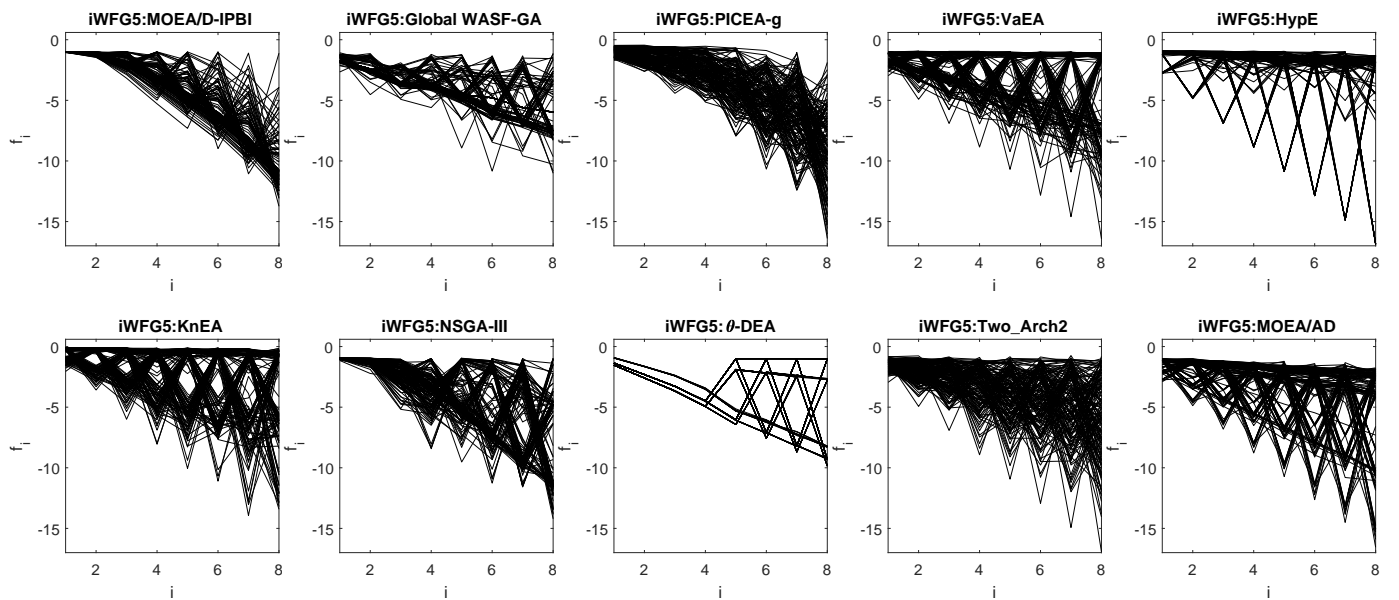


Fig. 85: Final solution sets on 8-objective WFG5 $^{-1}$ test problem obtained by 10 algorithms in the run of median HV metric values with $\mathbf{z}^r = (2, \dots, 2)^T$.

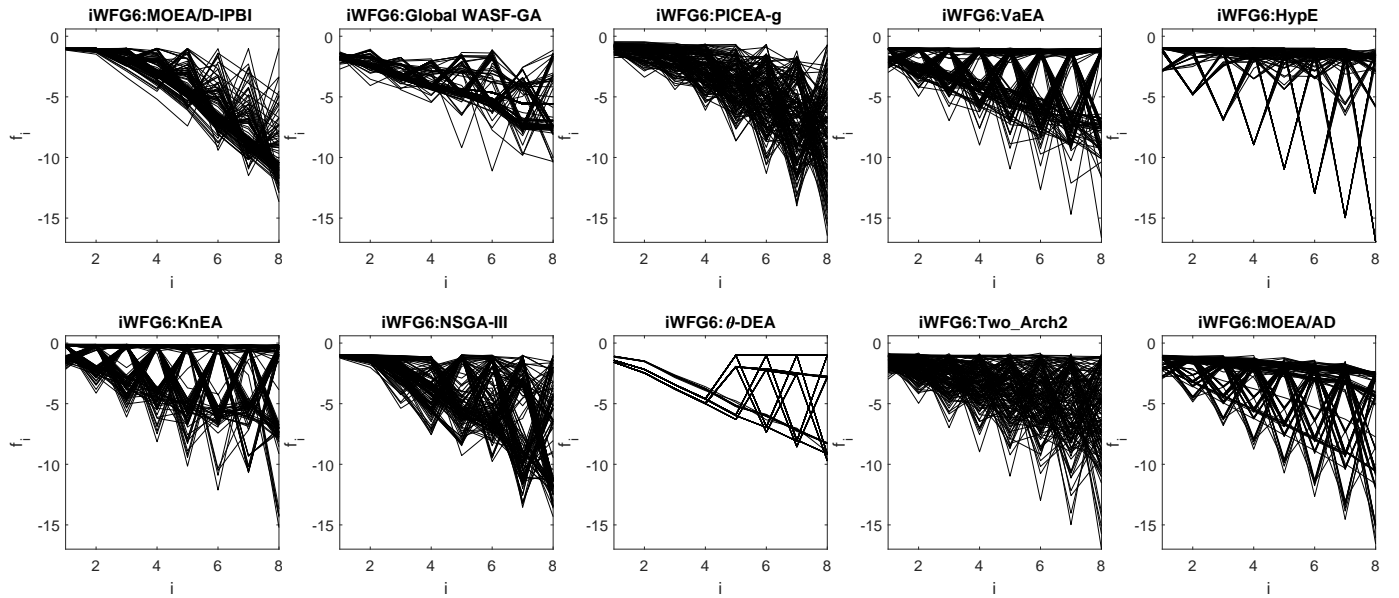


Fig. 86: Final solution sets on 8-objective WFG6⁻¹ test problem obtained by 10 algorithms in the run of median HV metric values with $\mathbf{z}^r = (2, \dots, 2)^T$.

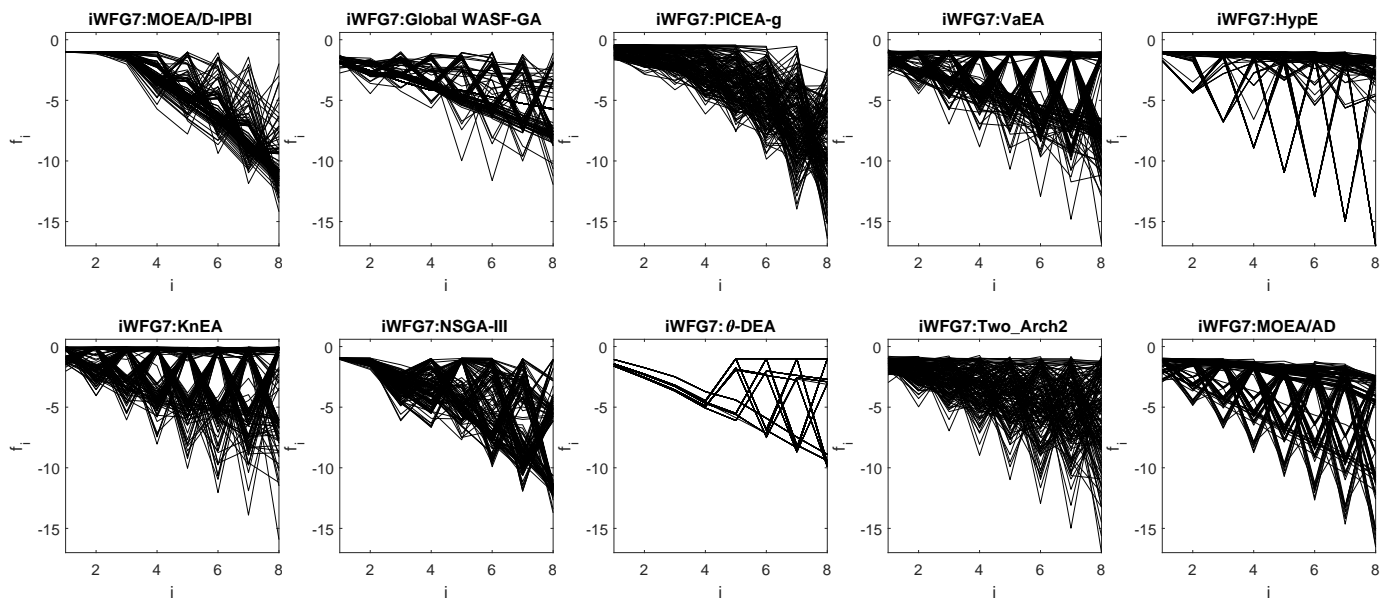


Fig. 87: Final solution sets on 8-objective WFG7⁻¹ test problem obtained by 10 algorithms in the run of median HV metric values with $\mathbf{z}^r = (2, \dots, 2)^T$.

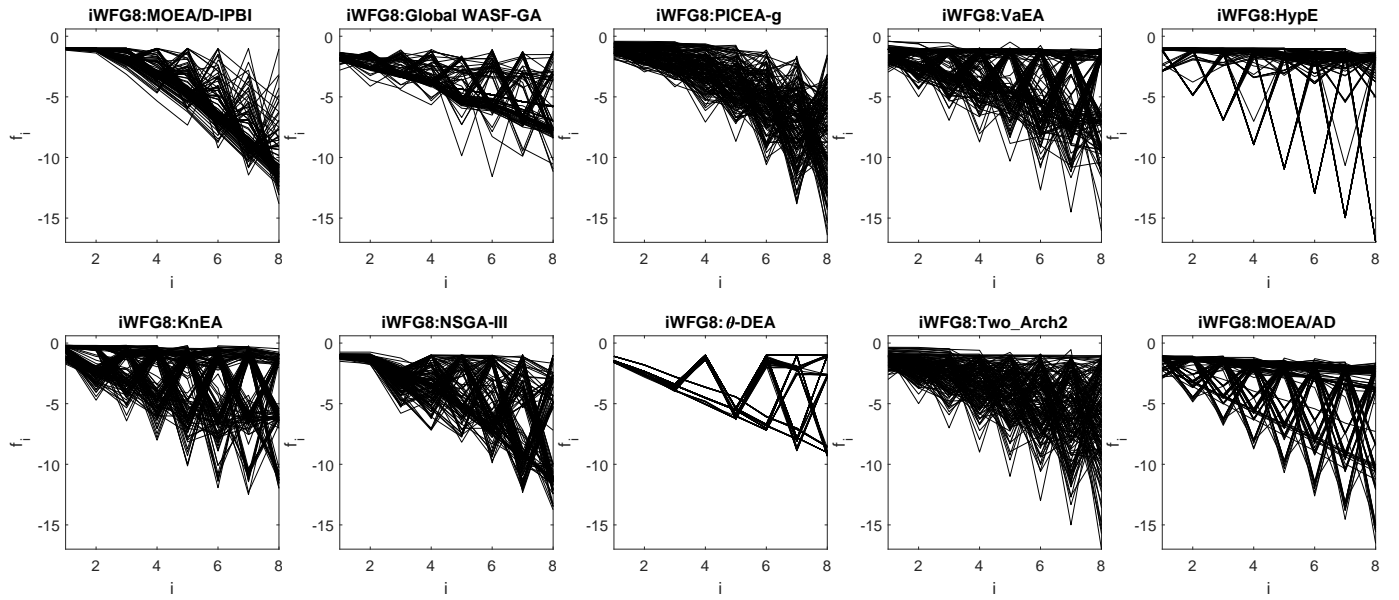


Fig. 88: Final solution sets on 8-objective WFG8⁻¹ test problem obtained by 10 algorithms in the run of median HV metric values with $\mathbf{z}^r = (2, \dots, 2)^T$.

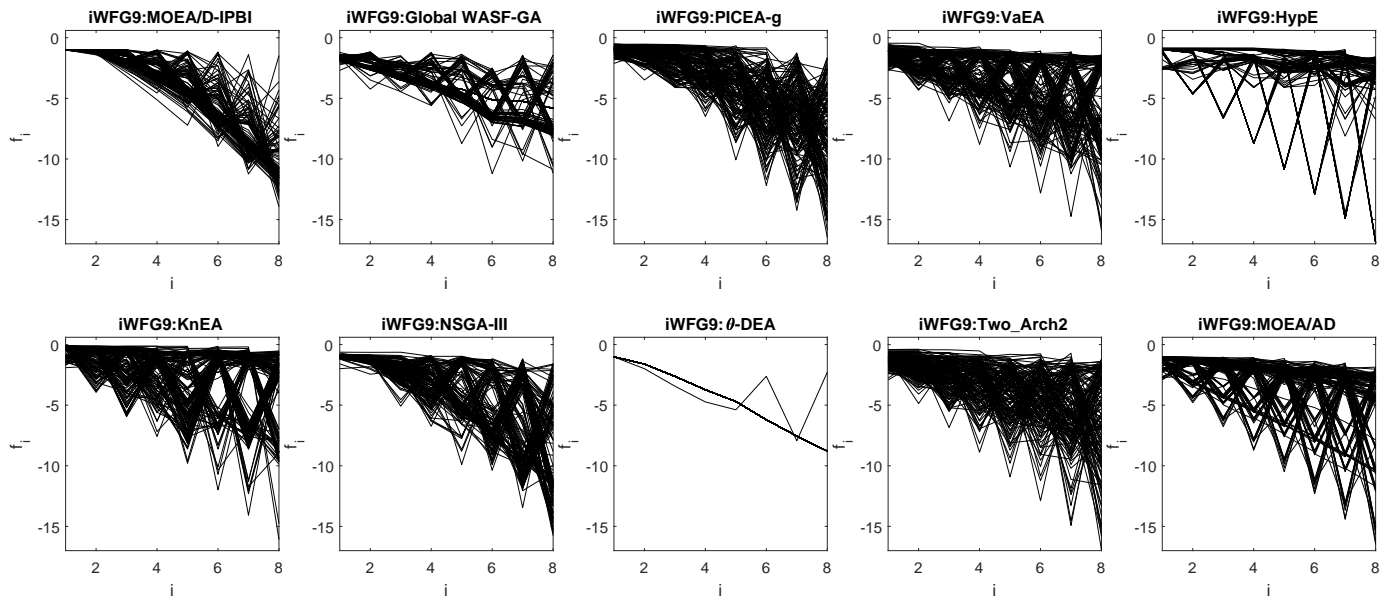


Fig. 89: Final solution sets on 8-objective WFG9⁻¹ test problem obtained by 10 algorithms in the run of median HV metric values with $\mathbf{z}^r = (2, \dots, 2)^T$.

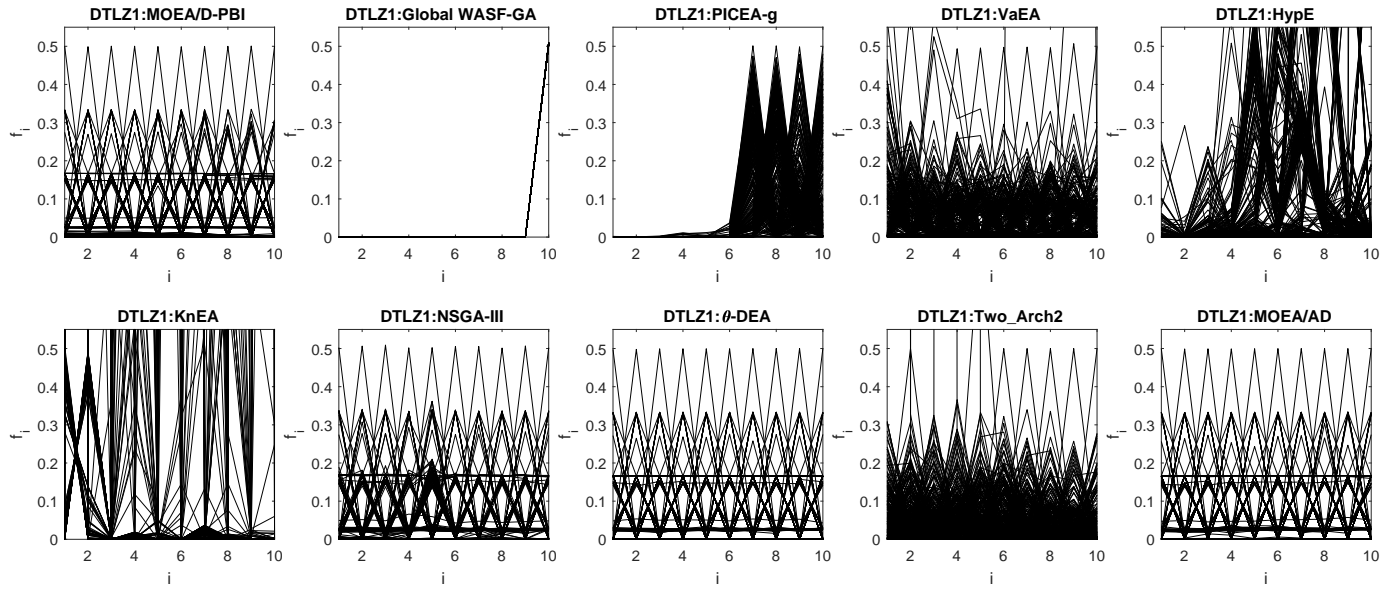


Fig. 90: Final solution sets on 10-objective DTLZ1 test problem obtained by 10 algorithms in the run of median HV metric values with $\mathbf{z}^r = (2, \dots, 2)^T$.

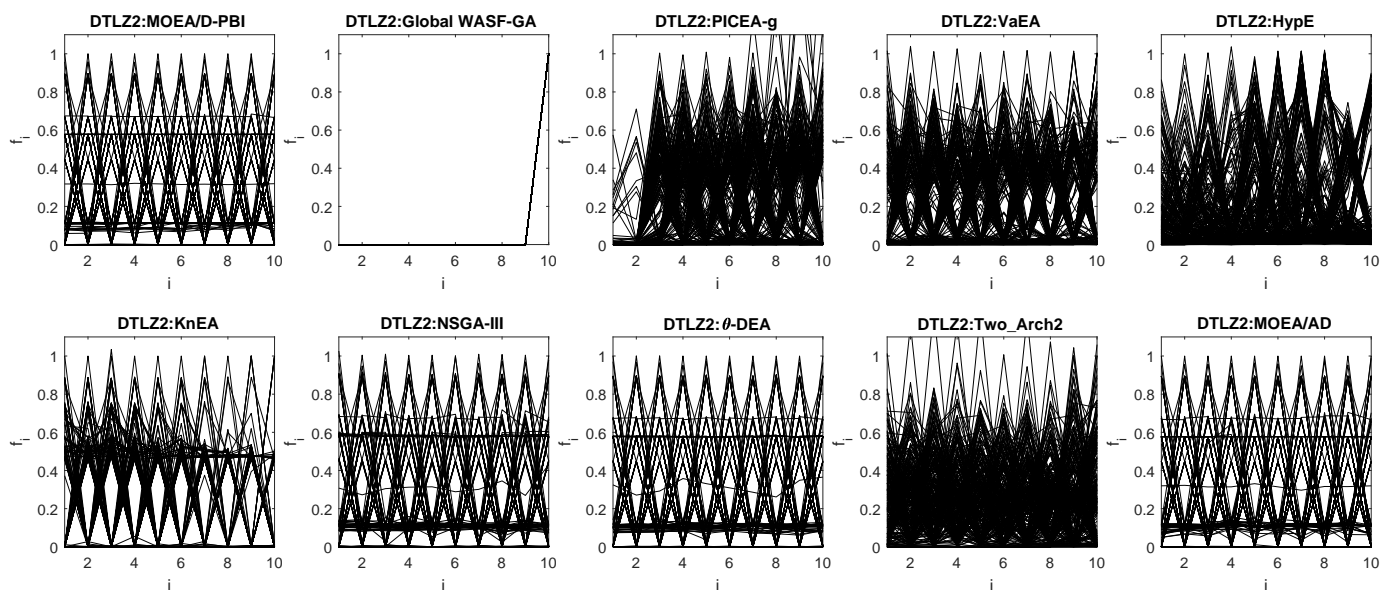


Fig. 91: Final solution sets on 10-objective DTLZ2 test problem obtained by 10 algorithms in the run of median HV metric values with $\mathbf{z}^r = (2, \dots, 2)^T$.

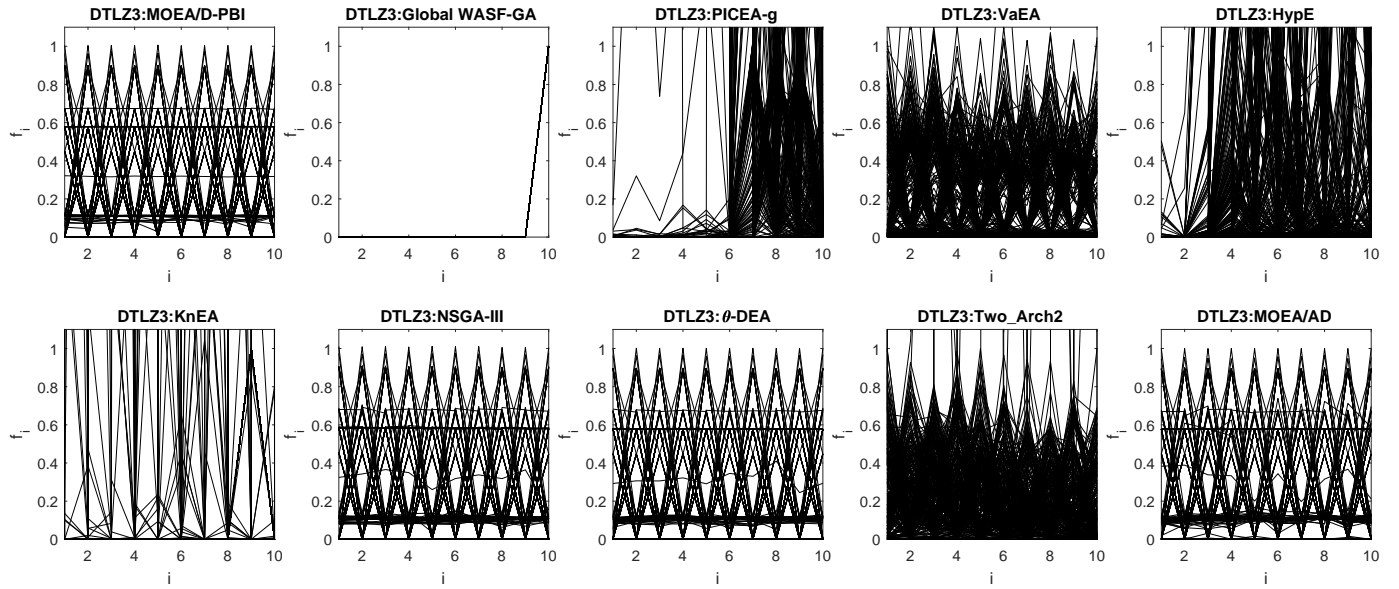


Fig. 92: Final solution sets on 10-objective DTLZ3 test problem obtained by 10 algorithms in the run of median HV metric values with $\mathbf{z}^r = (2, \dots, 2)^T$.

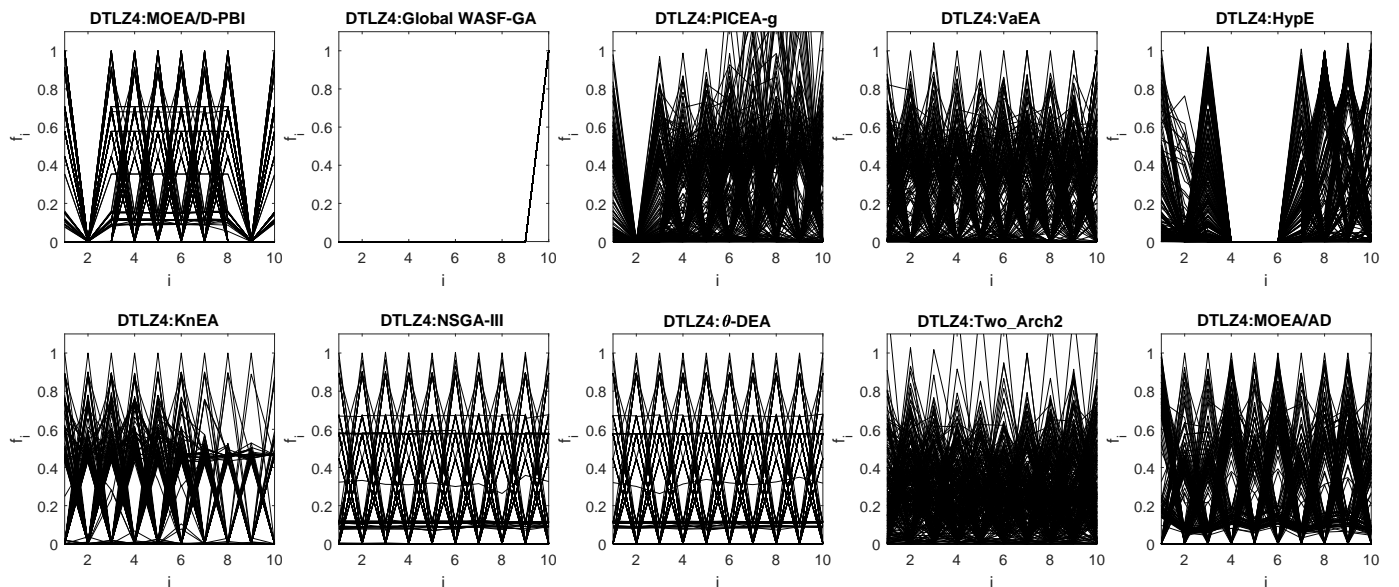


Fig. 93: Final solution sets on 10-objective DTLZ4 test problem obtained by 10 algorithms in the run of median HV metric values with $\mathbf{z}^r = (2, \dots, 2)^T$.

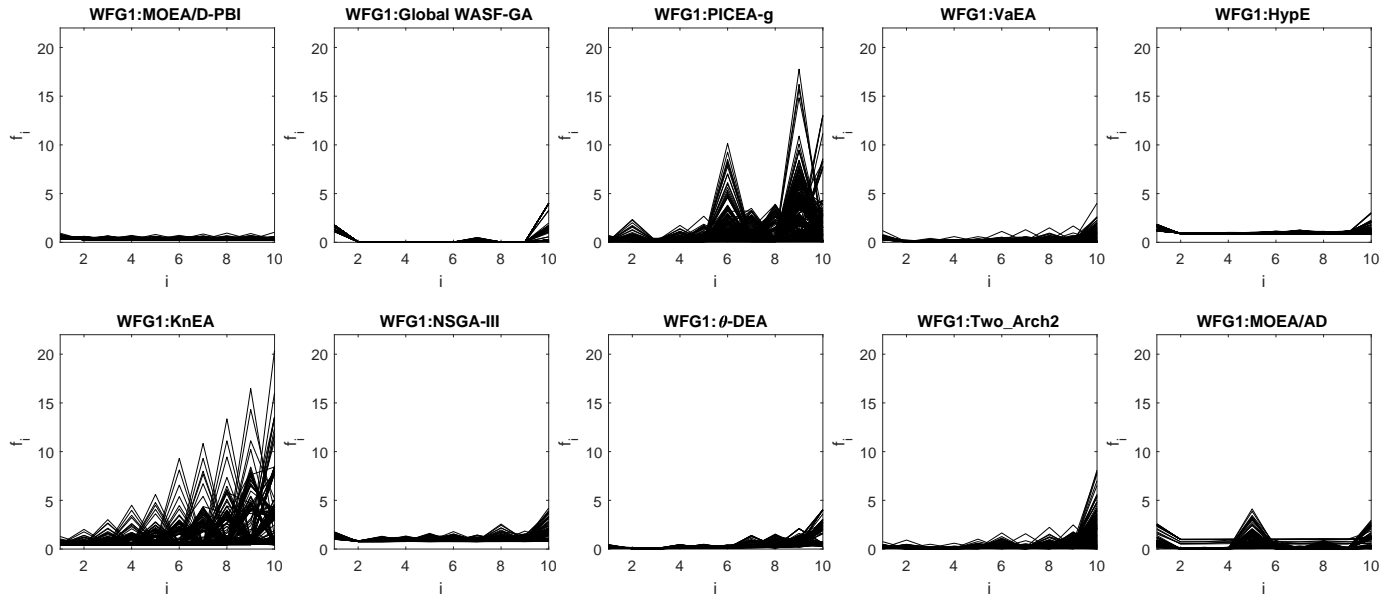


Fig. 94: Final solution sets on 10-objective WFG1 test problem obtained by 10 algorithms in the run of median HV metric values with $\mathbf{z}^r = (2, \dots, 2)^T$.

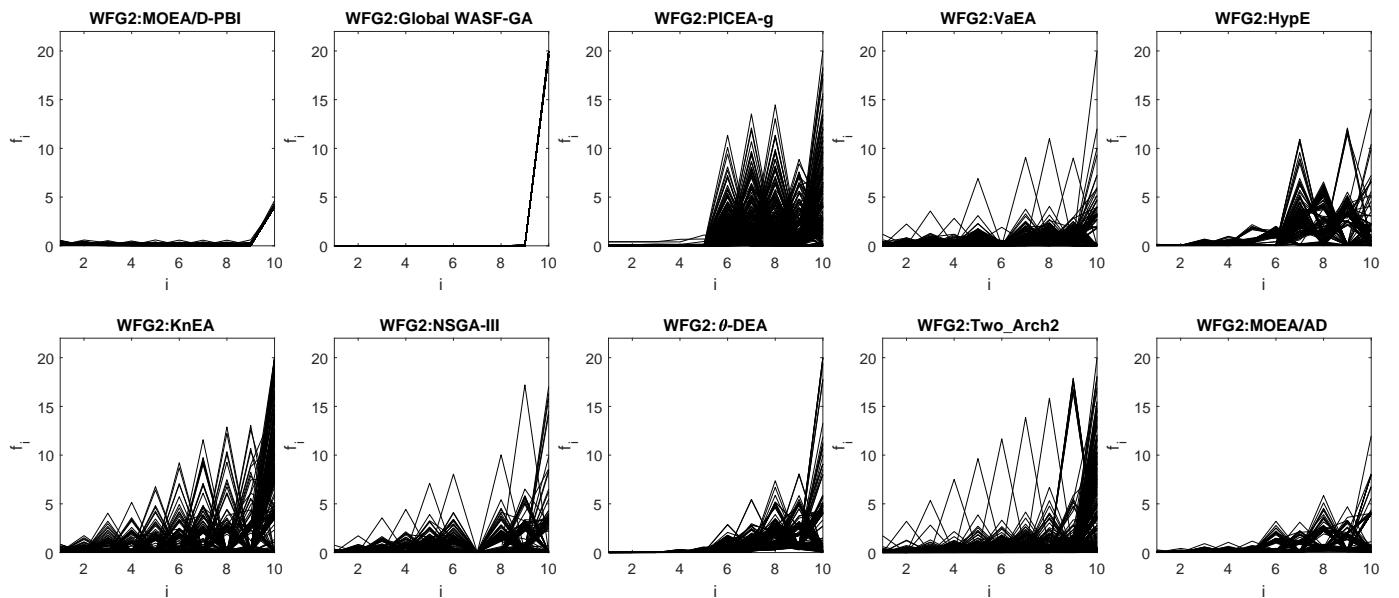


Fig. 95: Final solution sets on 10-objective WFG2 test problem obtained by 10 algorithms in the run of median HV metric values with $\mathbf{z}^r = (2, \dots, 2)^T$.

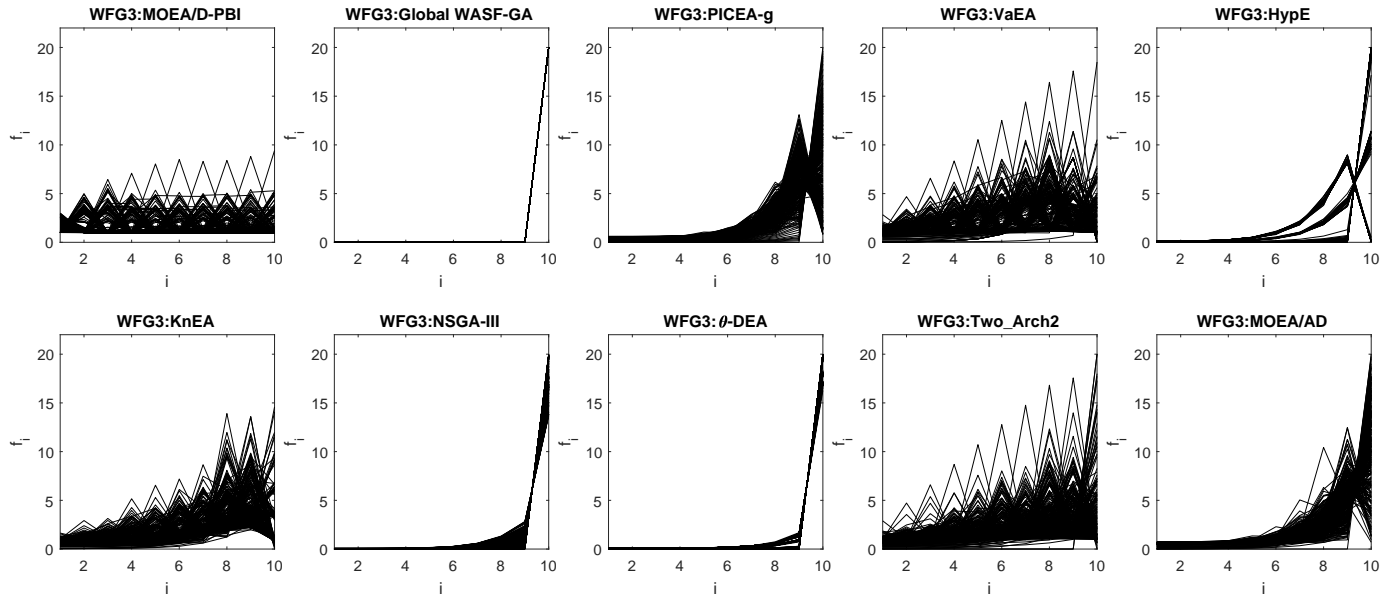


Fig. 96: Final solution sets on 10-objective WFG3 test problem obtained by 10 algorithms in the run of median HV metric values with $\mathbf{z}^r = (2, \dots, 2)^T$.

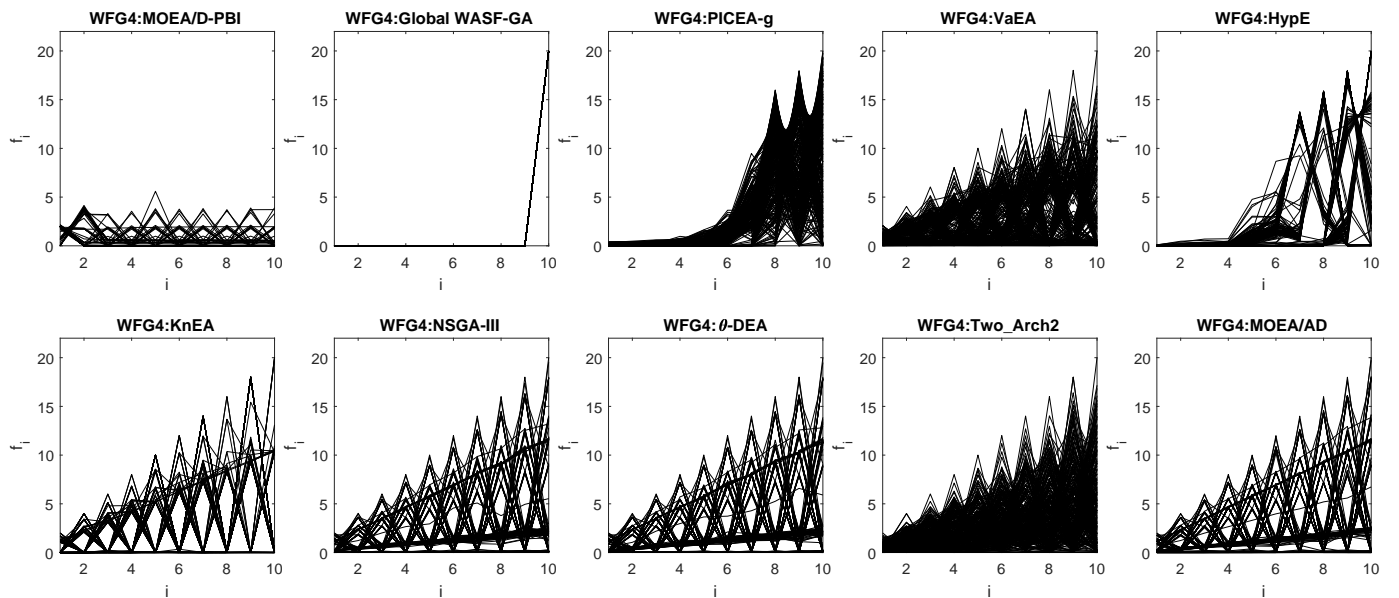


Fig. 97: Final solution sets on 10-objective WFG4 test problem obtained by 10 algorithms in the run of median HV metric values with $\mathbf{z}^r = (2, \dots, 2)^T$.

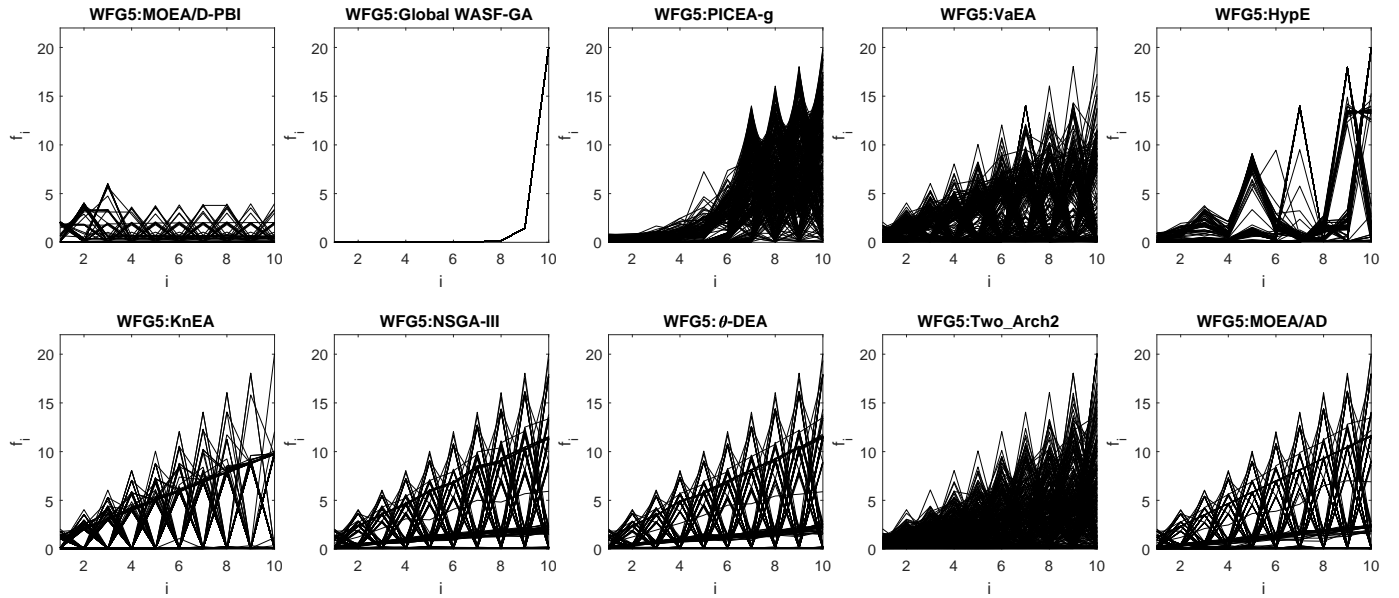


Fig. 98: Final solution sets on 10-objective WFG5 test problem obtained by 10 algorithms in the run of median HV metric values with $\mathbf{z}^r = (2, \dots, 2)^T$.

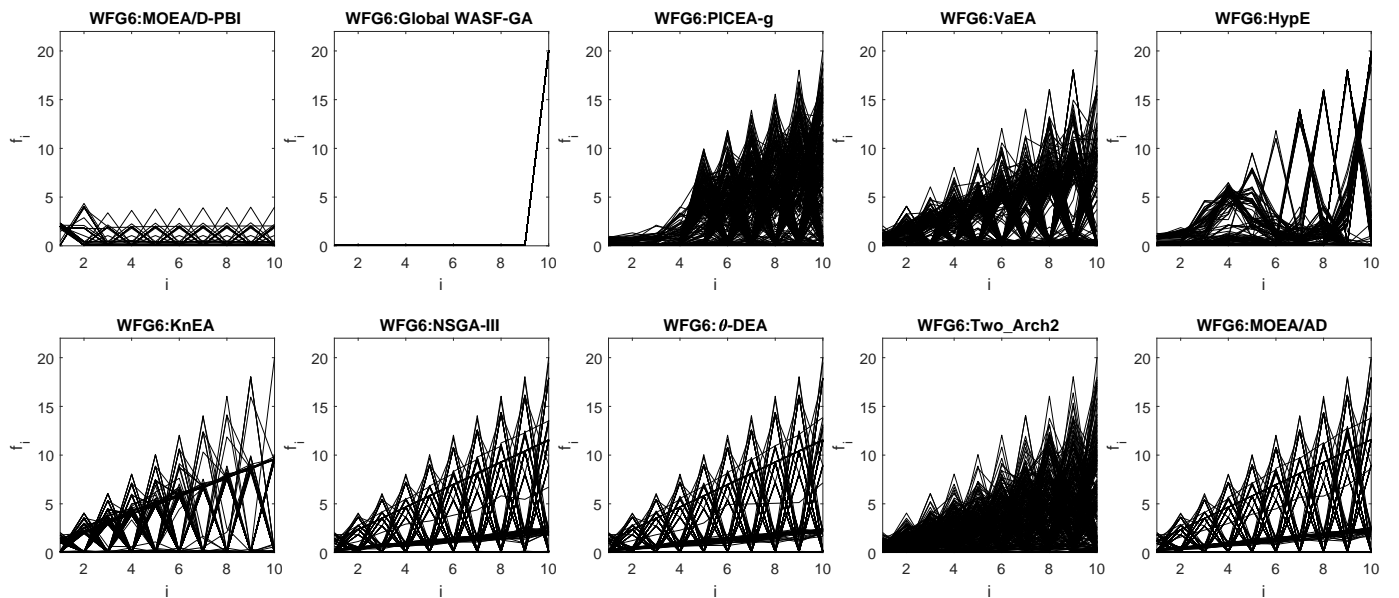


Fig. 99: Final solution sets on 10-objective WFG6 test problem obtained by 10 algorithms in the run of median HV metric values with $\mathbf{z}^r = (2, \dots, 2)^T$.

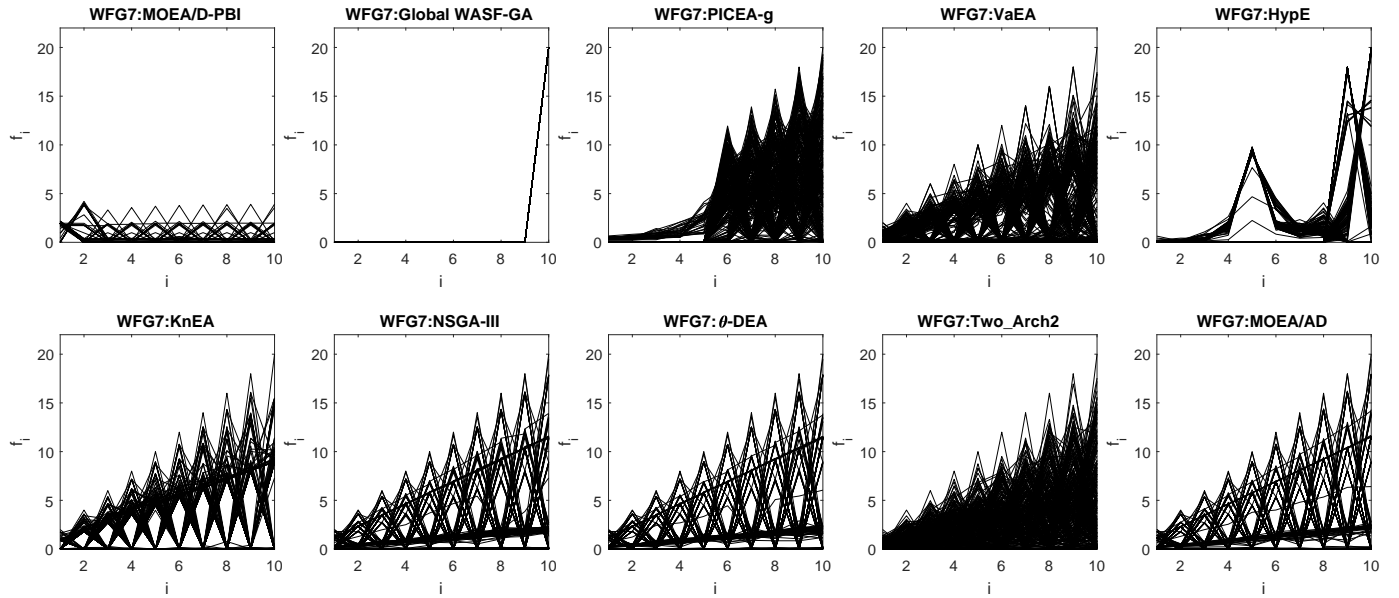


Fig. 100: Final solution sets on 10-objective WFG7 test problem obtained by 10 algorithms in the run of median HV metric values with $\mathbf{z}^r = (2, \dots, 2)^T$.

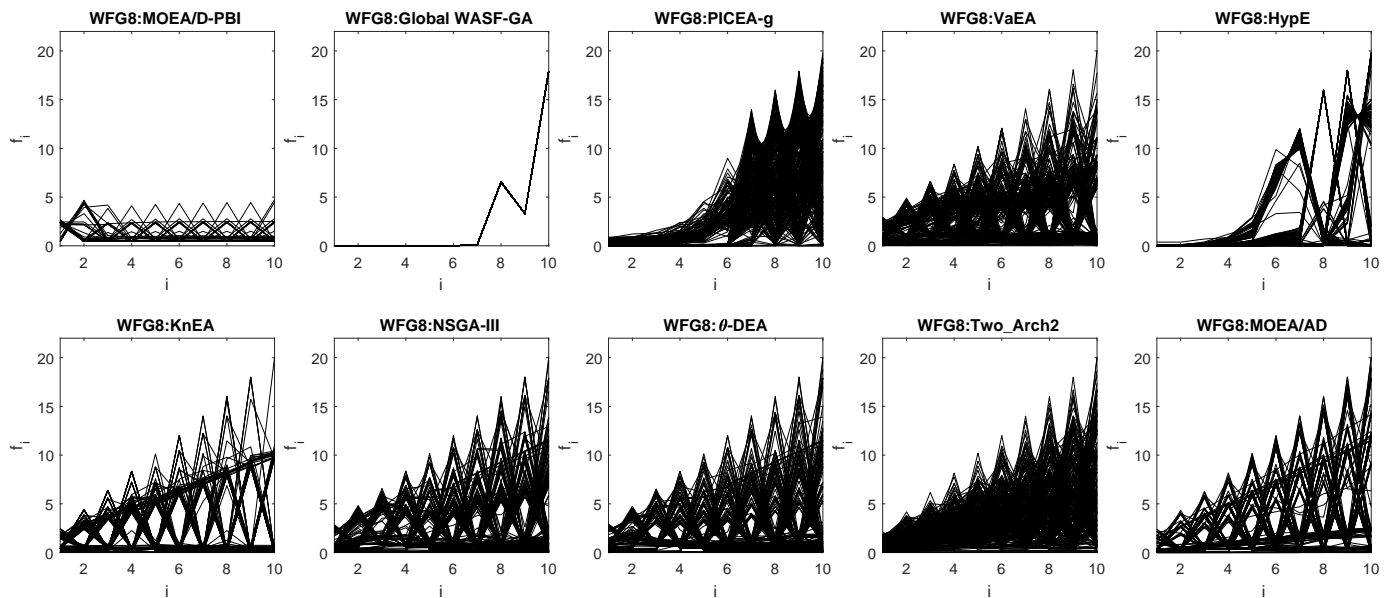


Fig. 101: Final solution sets on 10-objective WFG8 test problem obtained by 10 algorithms in the run of median HV metric values with $\mathbf{z}^r = (2, \dots, 2)^T$.

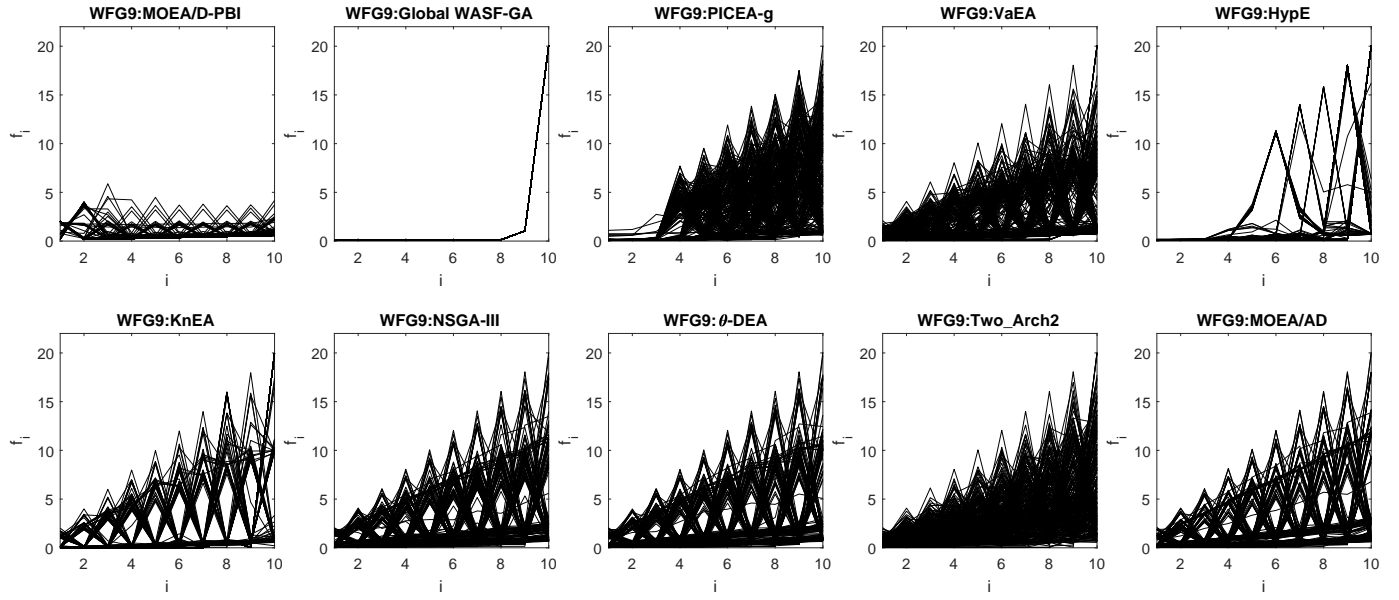


Fig. 102: Final solution sets on 10-objective WFG9 test problem obtained by 10 algorithms in the run of median HV metric values with $\mathbf{z}^r = (2, \dots, 2)^T$.

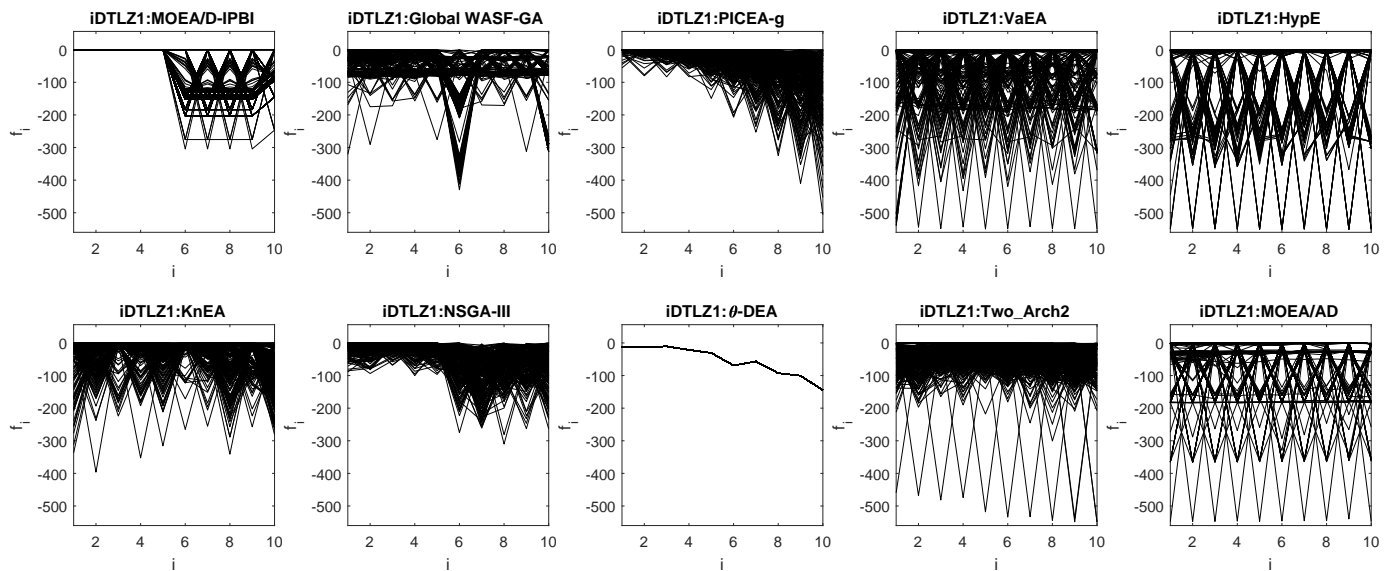


Fig. 103: Final solution sets on 10-objective DTLZ1⁻¹ test problem obtained by 10 algorithms in the run of median HV metric values with $\mathbf{z}^r = (2, \dots, 2)^T$.

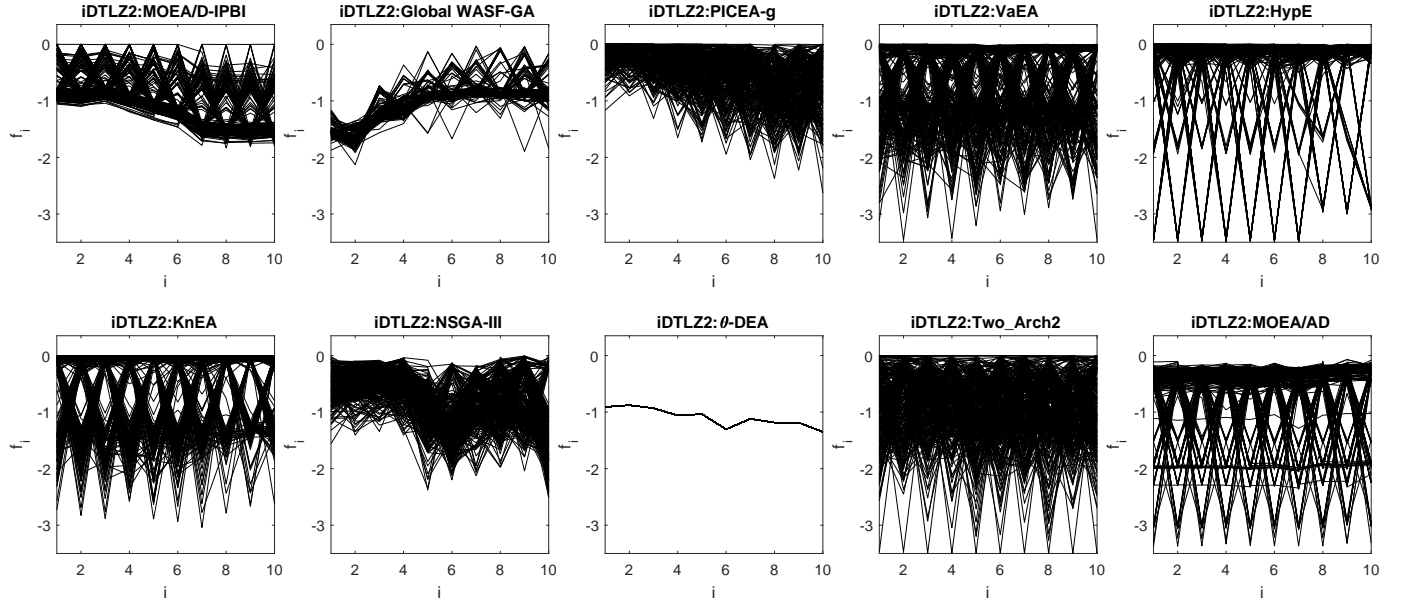


Fig. 104: Final solution sets on 10-objective DTLZ2⁻¹ test problem obtained by 10 algorithms in the run of median HV metric values with $\mathbf{z}^r = (2, \dots, 2)^T$.

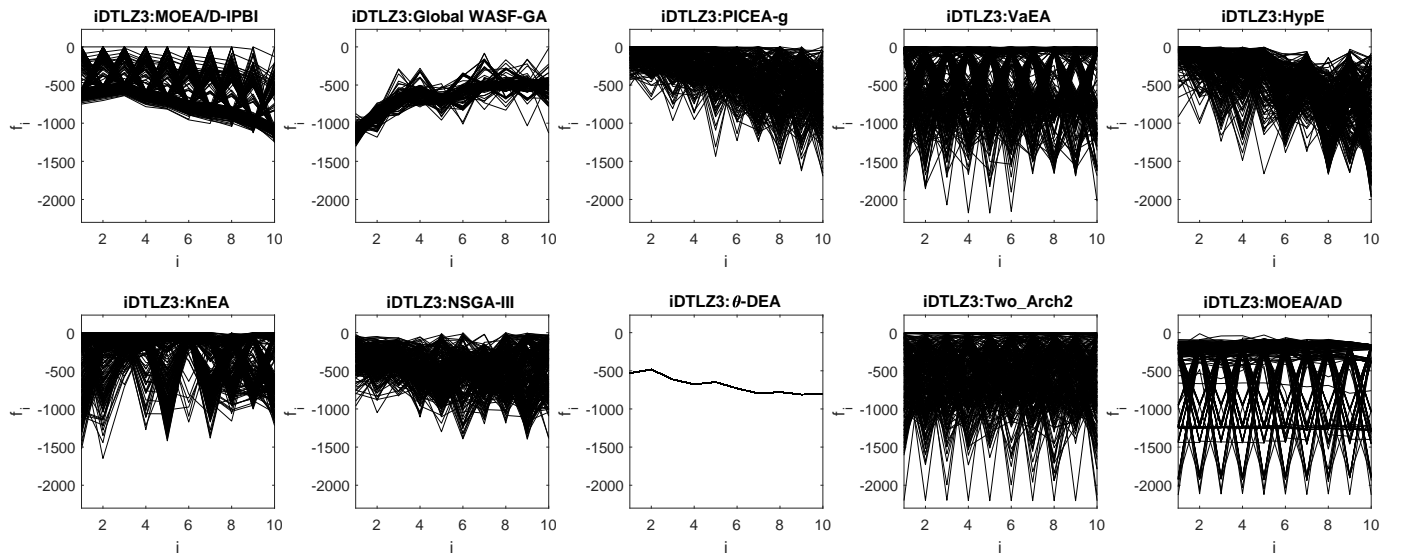


Fig. 105: Final solution sets on 10-objective DTLZ3⁻¹ test problem obtained by 10 algorithms in the run of median HV metric values with $\mathbf{z}^r = (2, \dots, 2)^T$.

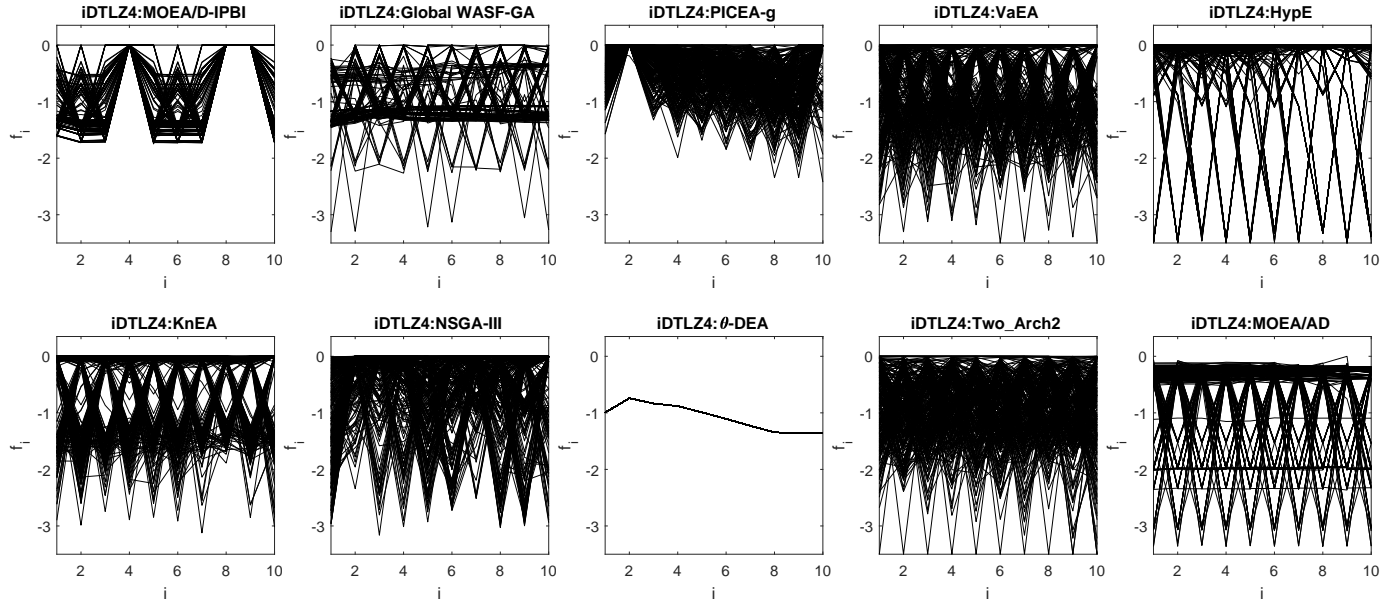


Fig. 106: Final solution sets on 10-objective DTLZ4^{-1} test problem obtained by 10 algorithms in the run of median HV metric values with $\mathbf{z}^r = (2, \dots, 2)^T$.

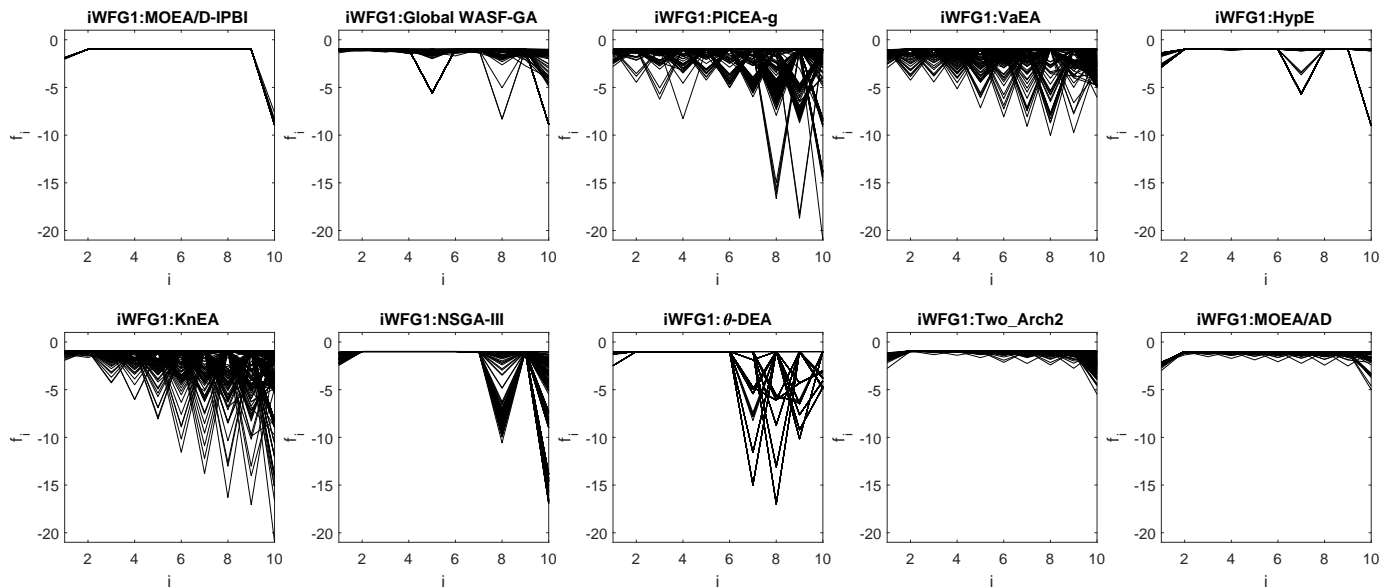


Fig. 107: Final solution sets on 10-objective WFG1^{-1} test problem obtained by 10 algorithms in the run of median HV metric values with $\mathbf{z}^r = (2, \dots, 2)^T$.

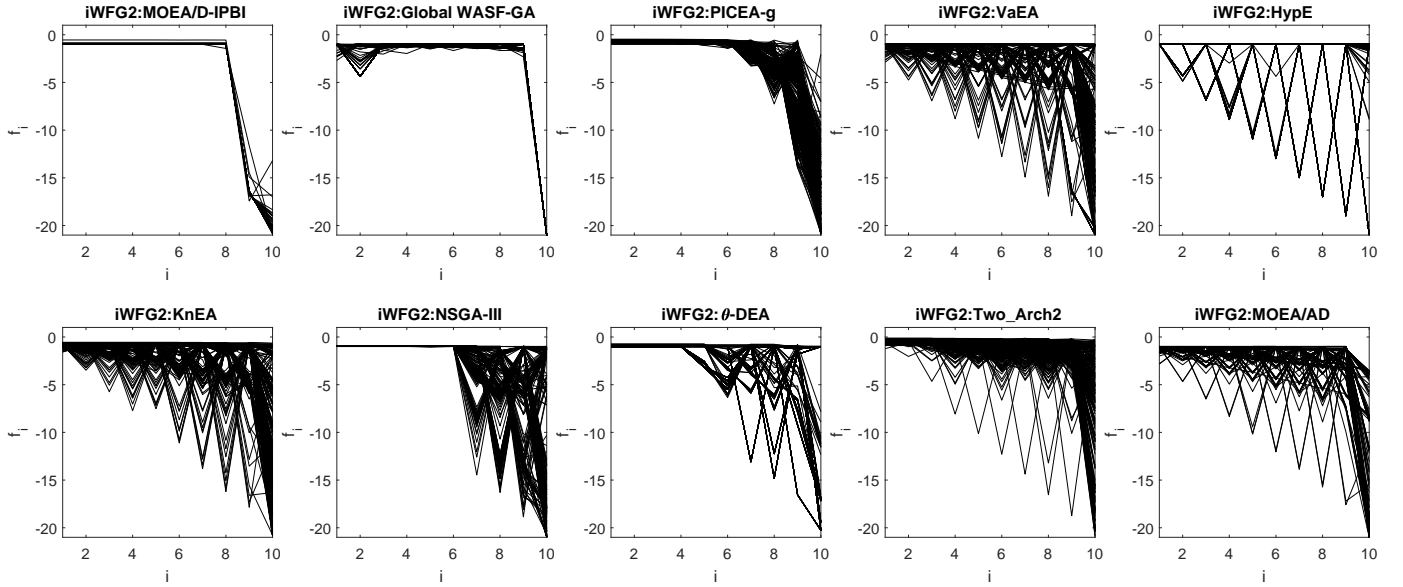


Fig. 108: Final solution sets on 10-objective WFG2⁻¹ test problem obtained by 10 algorithms in the run of median HV metric values with $\mathbf{z}^r = (2, \dots, 2)^T$.

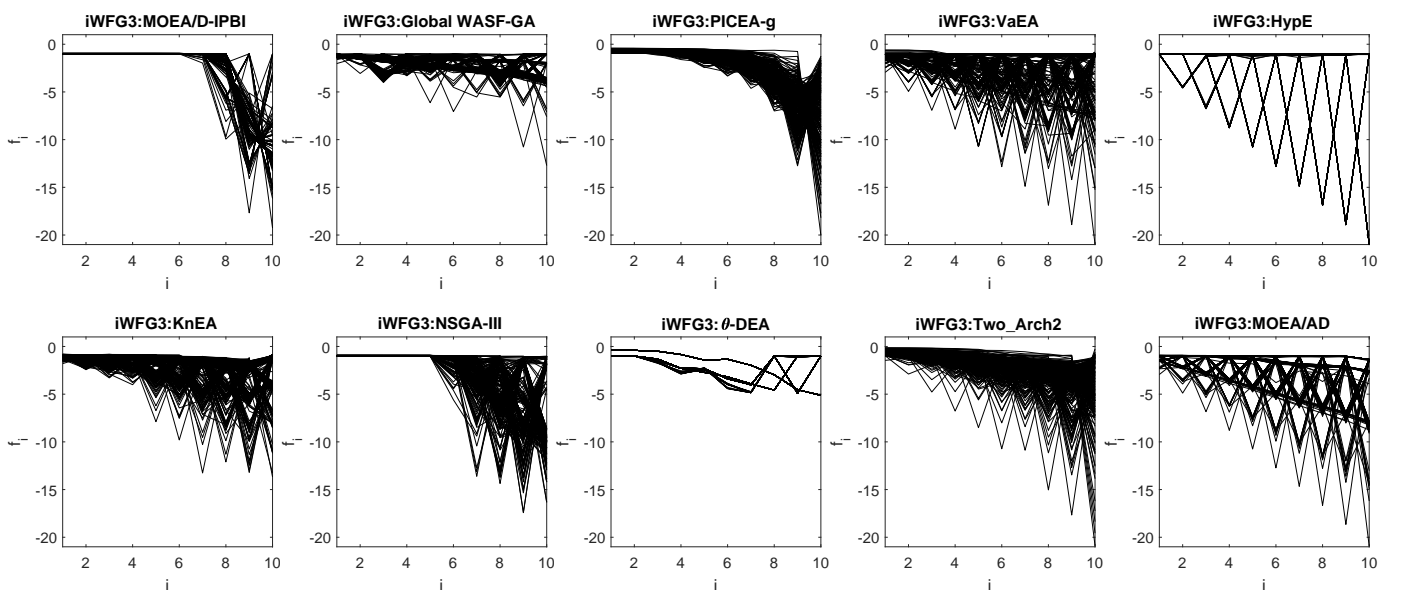


Fig. 109: Final solution sets on 10-objective WFG3⁻¹ test problem obtained by 10 algorithms in the run of median HV metric values with $\mathbf{z}^r = (2, \dots, 2)^T$.

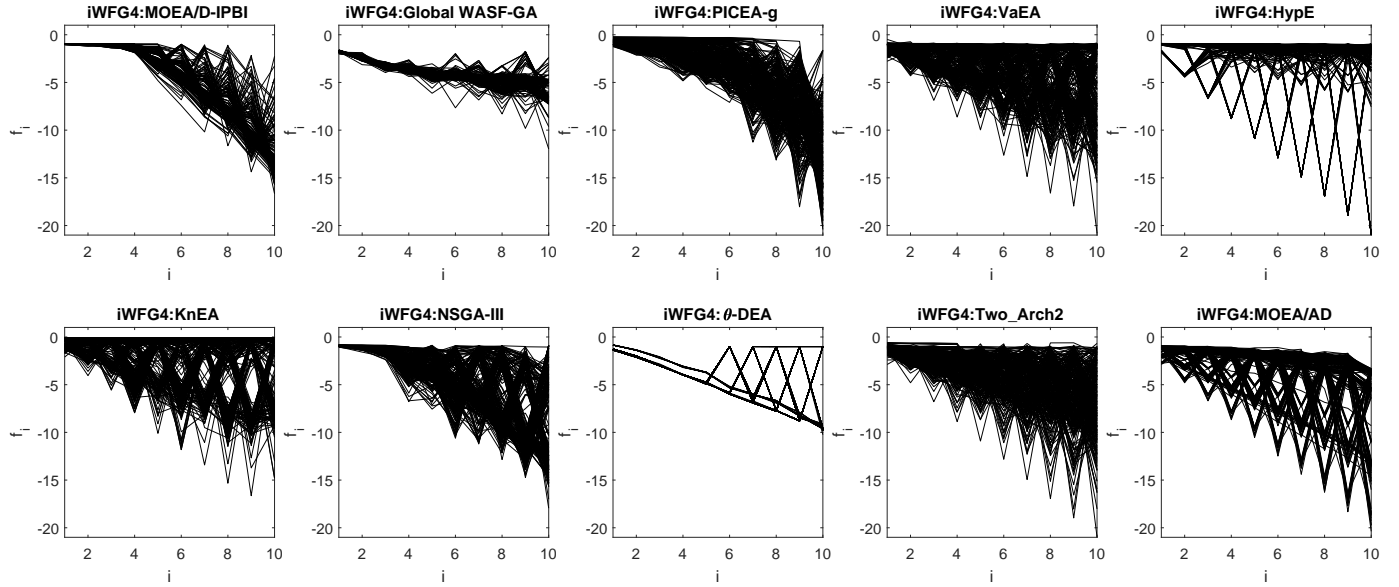


Fig. 110: Final solution sets on 10-objective WFG4⁻¹ test problem obtained by 10 algorithms in the run of median HV metric values with $\mathbf{z}^r = (2, \dots, 2)^T$.

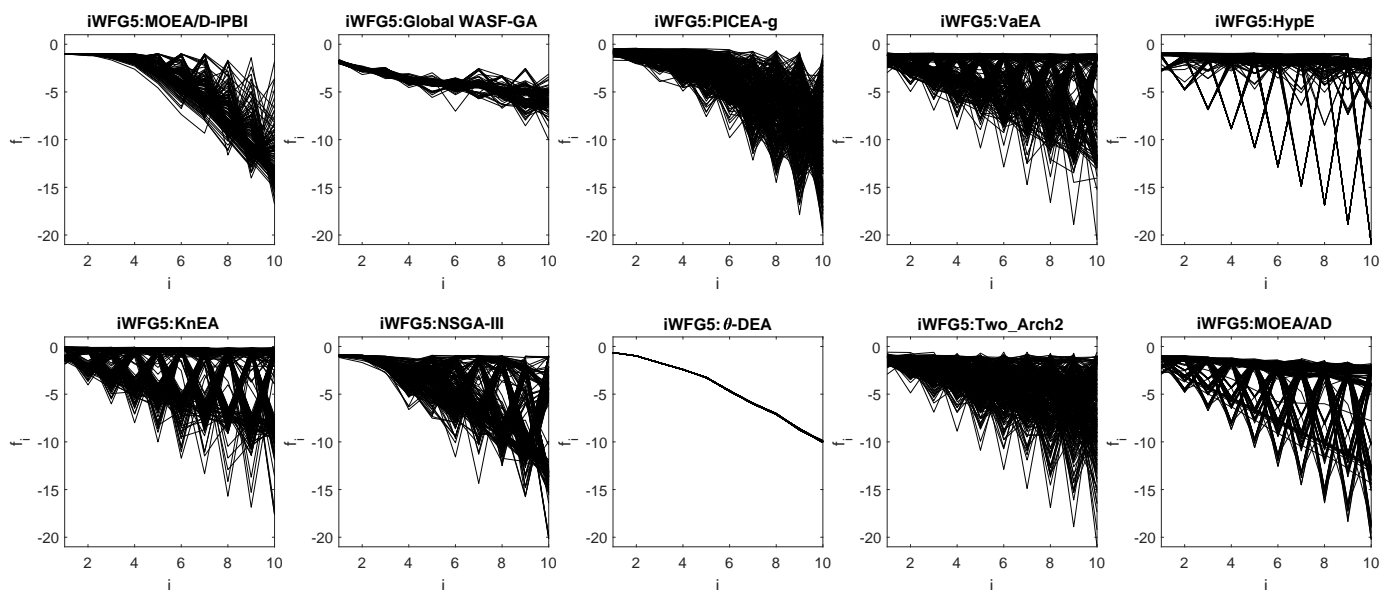


Fig. 111: Final solution sets on 10-objective WFG5⁻¹ test problem obtained by 10 algorithms in the run of median HV metric values with $\mathbf{z}^r = (2, \dots, 2)^T$.

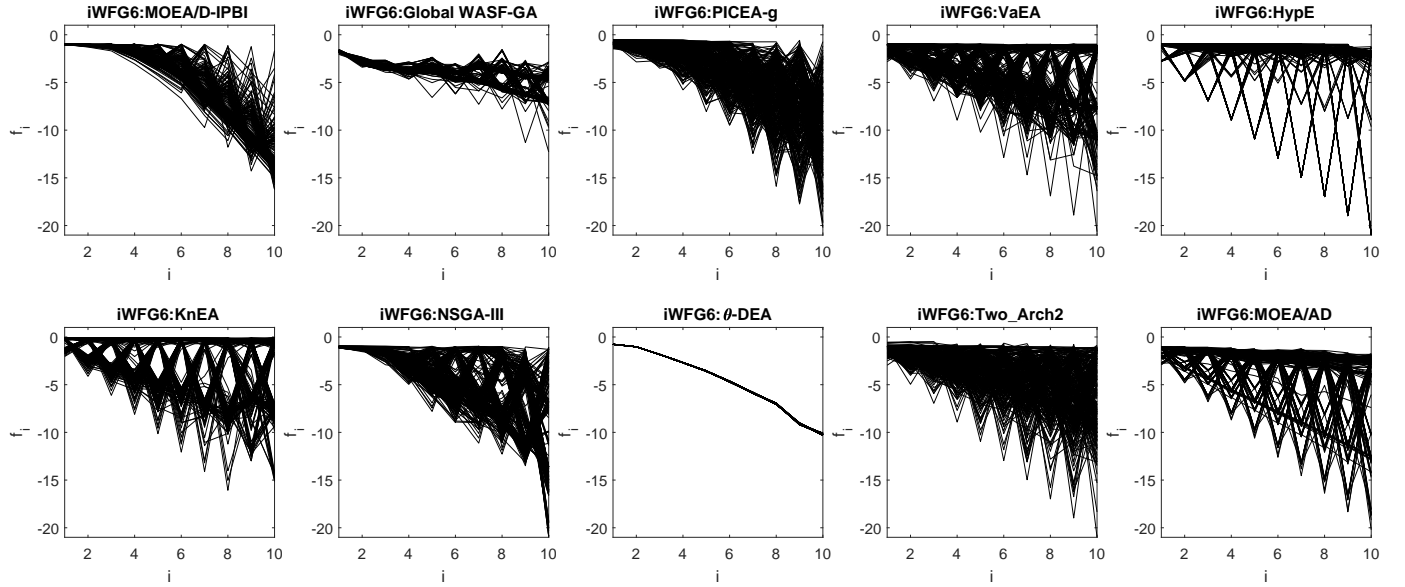


Fig. 112: Final solution sets on 10-objective WFG6⁻¹ test problem obtained by 10 algorithms in the run of median HV metric values with $\mathbf{z}^r = (2, \dots, 2)^T$.

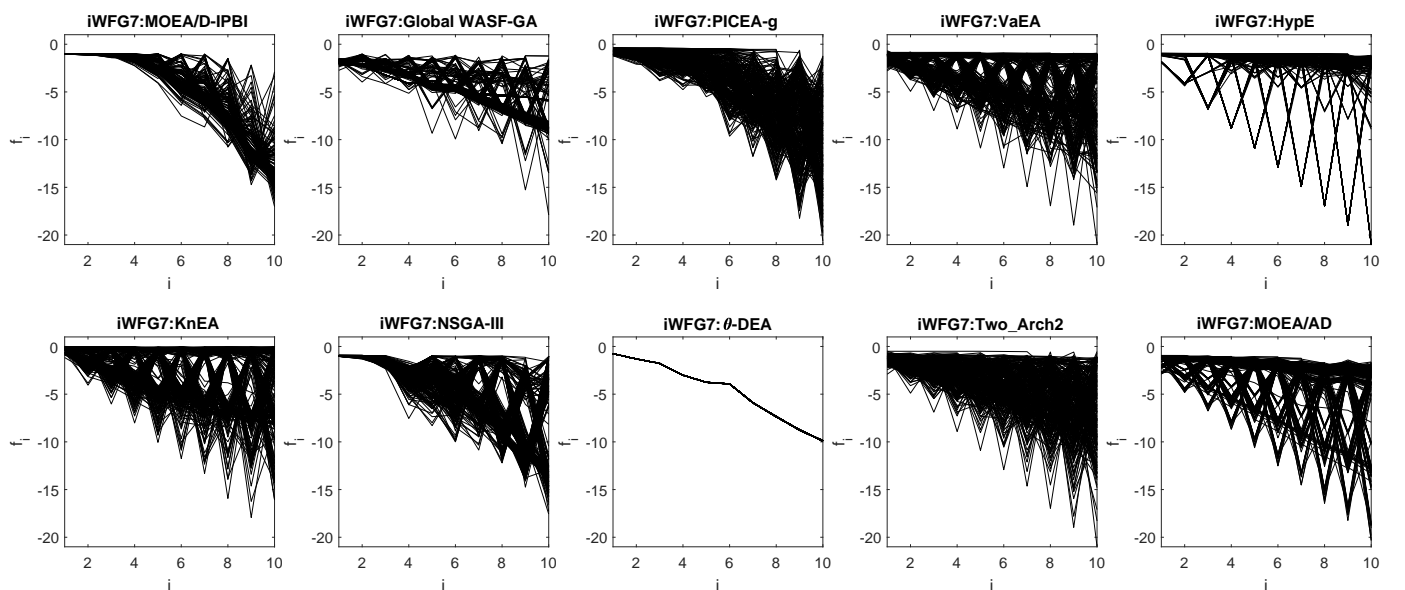


Fig. 113: Final solution sets on 10-objective WFG7⁻¹ test problem obtained by 10 algorithms in the run of median HV metric values with $\mathbf{z}^r = (2, \dots, 2)^T$.

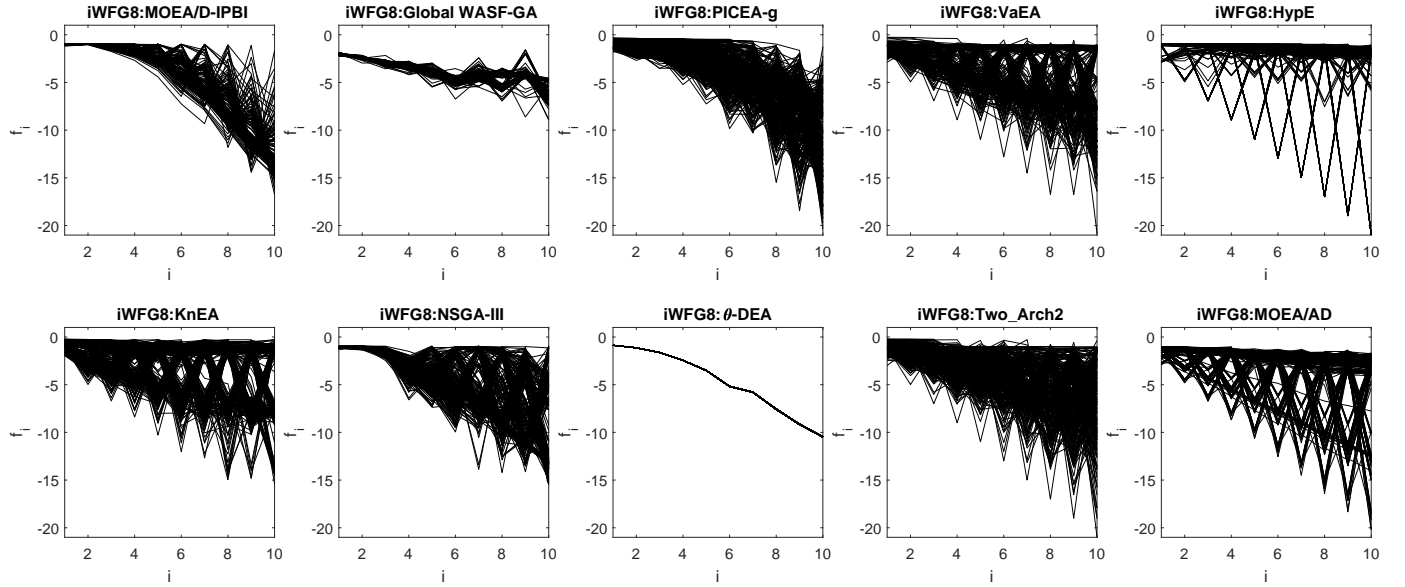


Fig. 114: Final solution sets on 10-objective WFG8⁻¹ test problem obtained by 10 algorithms in the run of median HV metric values with $\mathbf{z}^r = (2, \dots, 2)^T$.

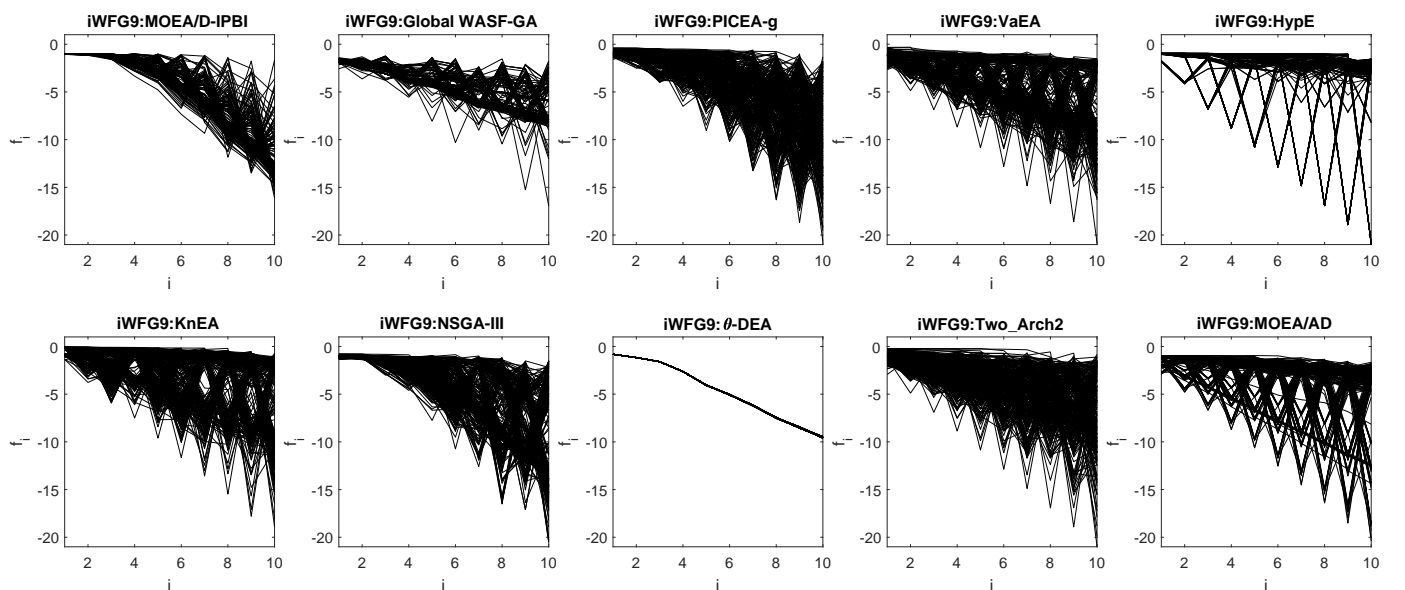


Fig. 115: Final solution sets on 10-objective WFG9⁻¹ test problem obtained by 10 algorithms in the run of median HV metric values with $\mathbf{z}^r = (2, \dots, 2)^T$.

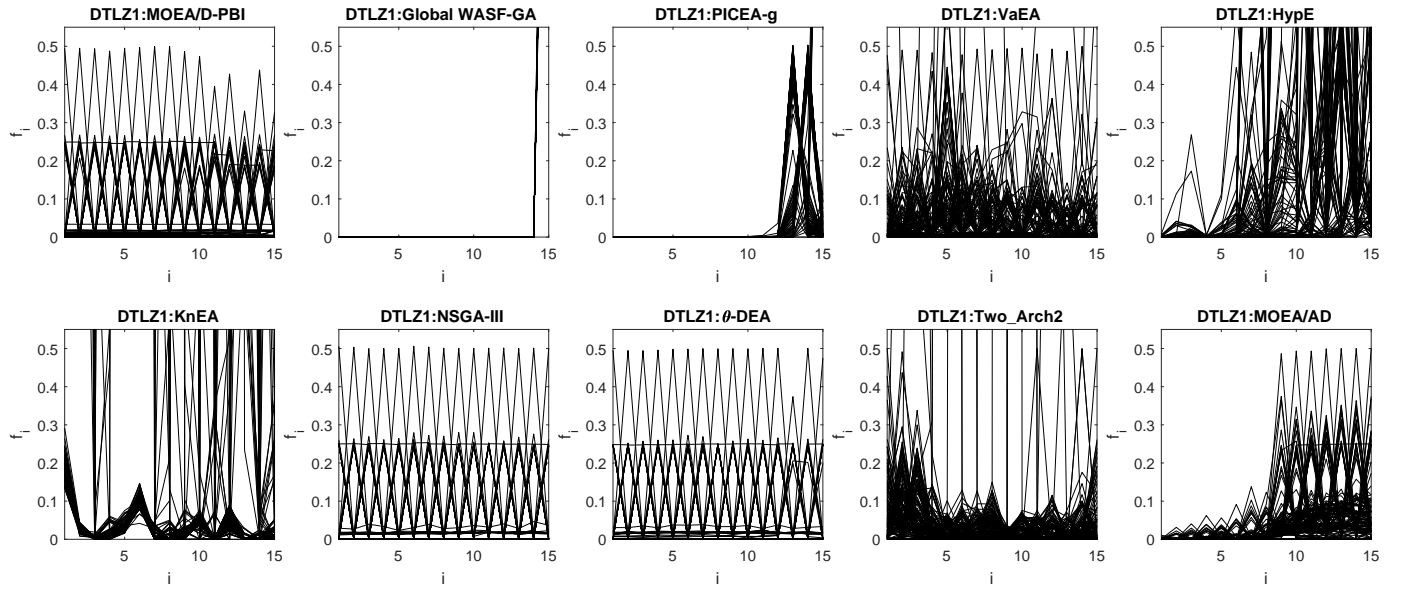


Fig. 116: Final solution sets on 15-objective DTLZ1 test problem obtained by 10 algorithms in the run of median HV metric values with $\mathbf{z}^r = (2, \dots, 2)^T$.

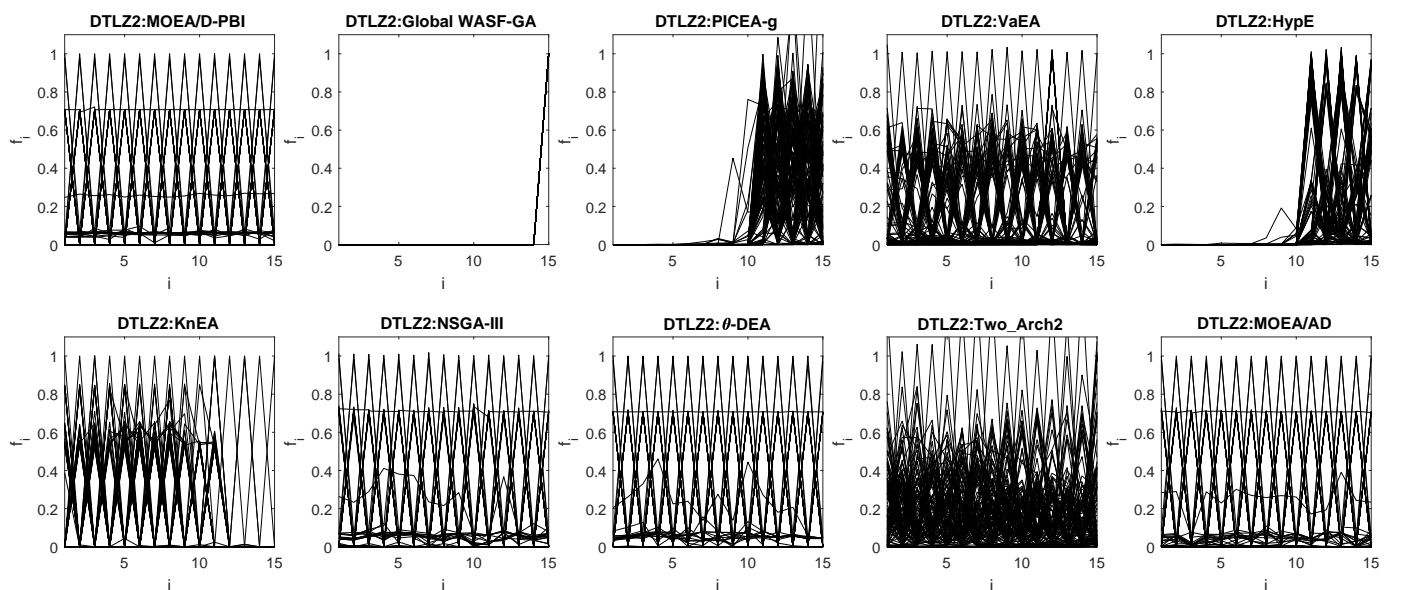


Fig. 117: Final solution sets on 15-objective DTLZ2 test problem obtained by 10 algorithms in the run of median HV metric values with $\mathbf{z}^r = (2, \dots, 2)^T$.

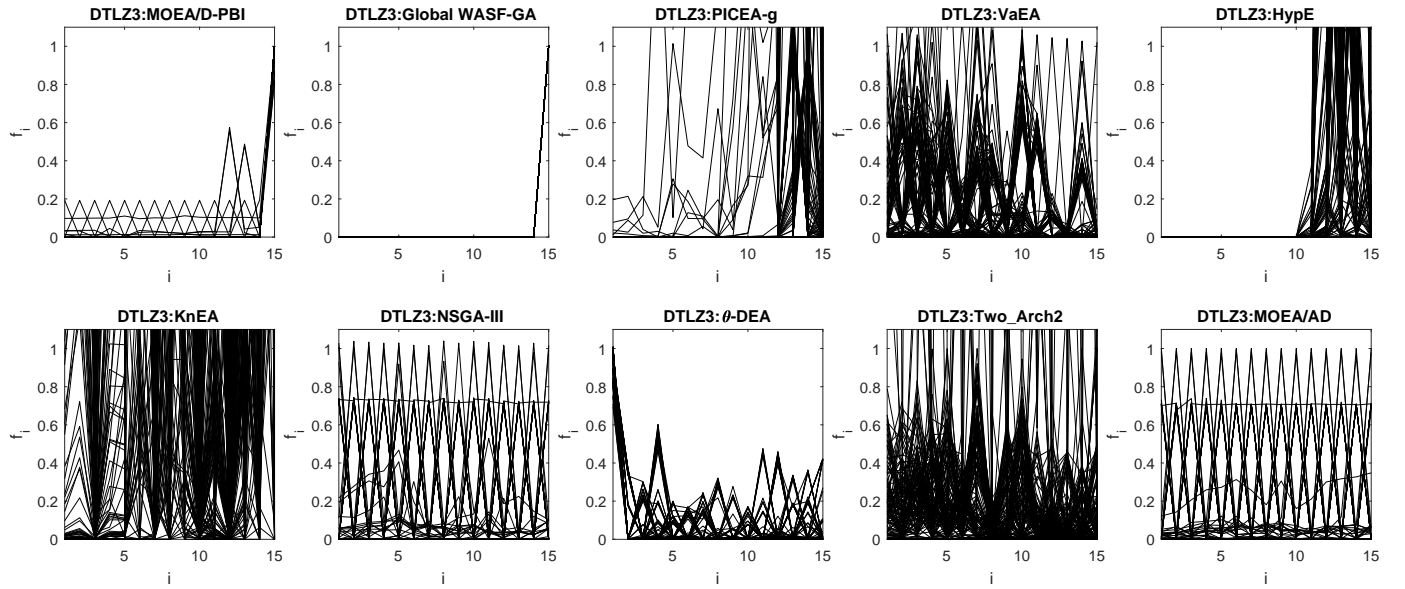


Fig. 118: Final solution sets on 15-objective DTLZ3 test problem obtained by 10 algorithms in the run of median HV metric values with $\mathbf{z}^r = (2, \dots, 2)^T$.

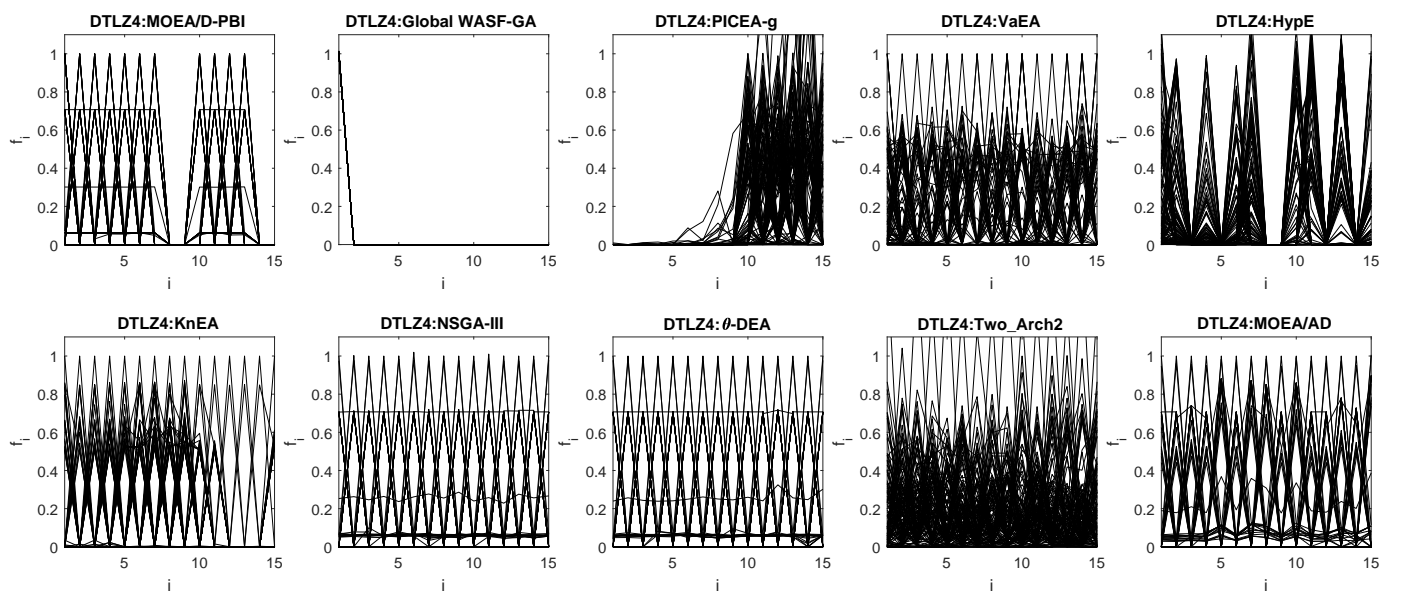


Fig. 119: Final solution sets on 15-objective DTLZ4 test problem obtained by 10 algorithms in the run of median HV metric values with $\mathbf{z}^r = (2, \dots, 2)^T$.

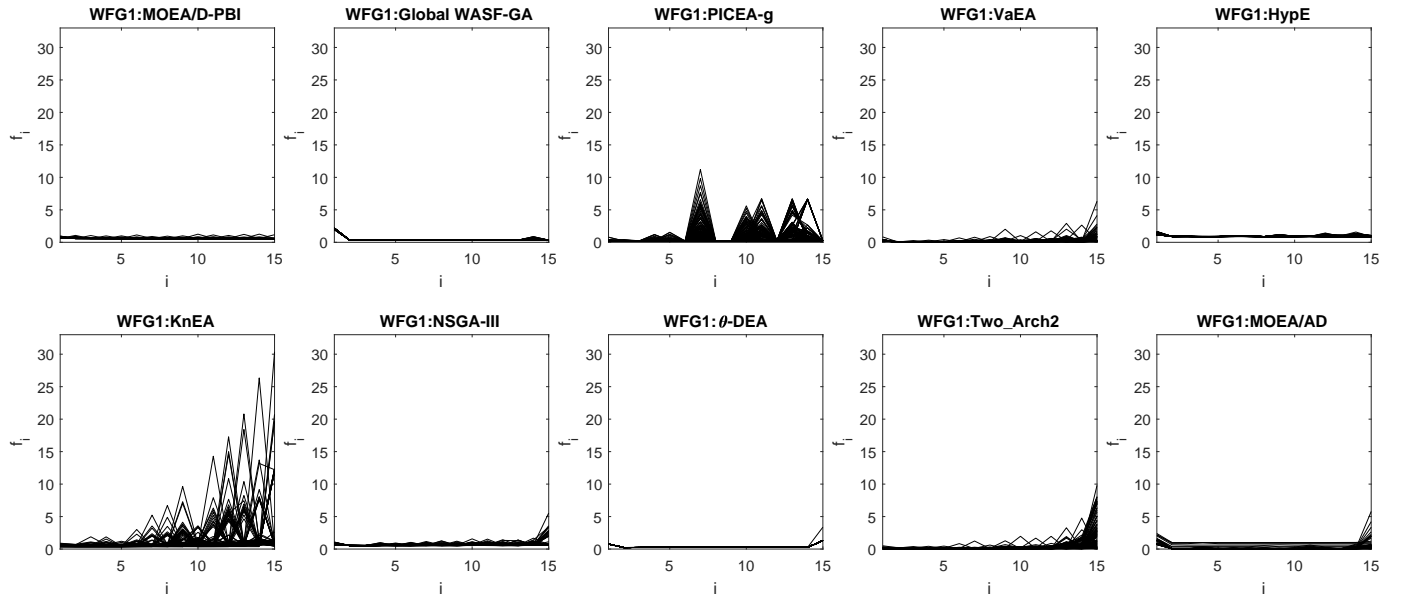


Fig. 120: Final solution sets on 15-objective WFG1 test problem obtained by 10 algorithms in the run of median HV metric values with $\mathbf{z}^r = (2, \dots, 2)^T$.

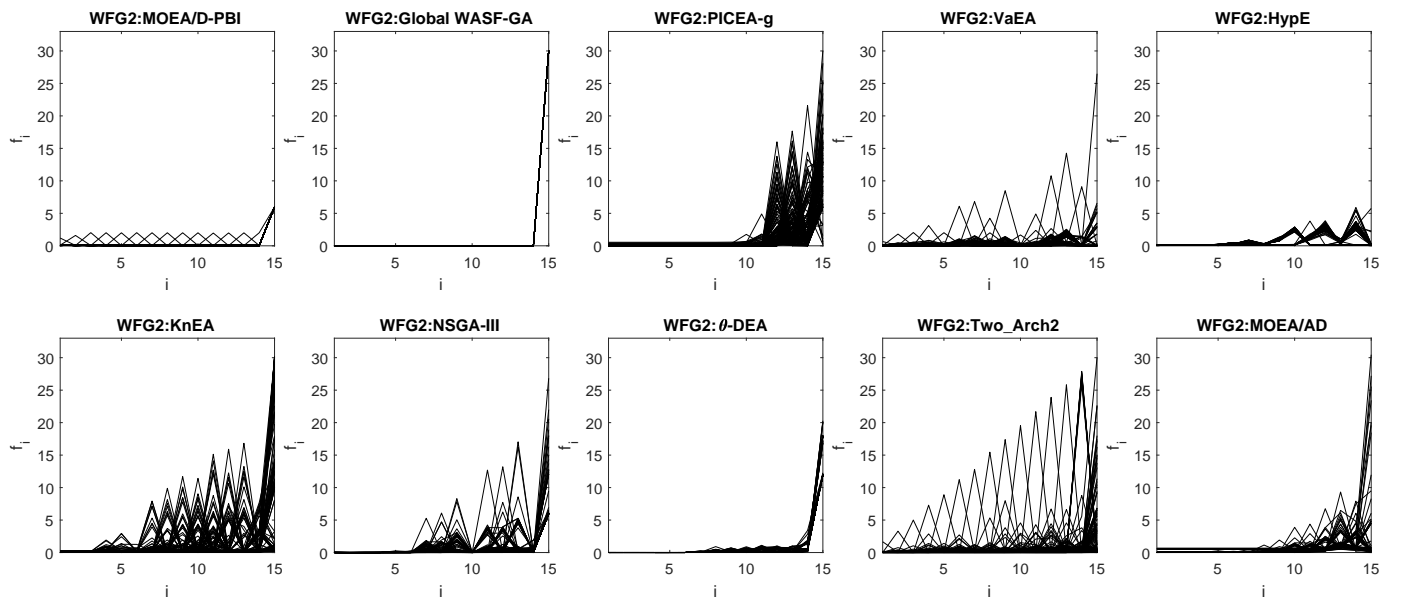


Fig. 121: Final solution sets on 15-objective WFG2 test problem obtained by 10 algorithms in the run of median HV metric values with $\mathbf{z}^r = (2, \dots, 2)^T$.

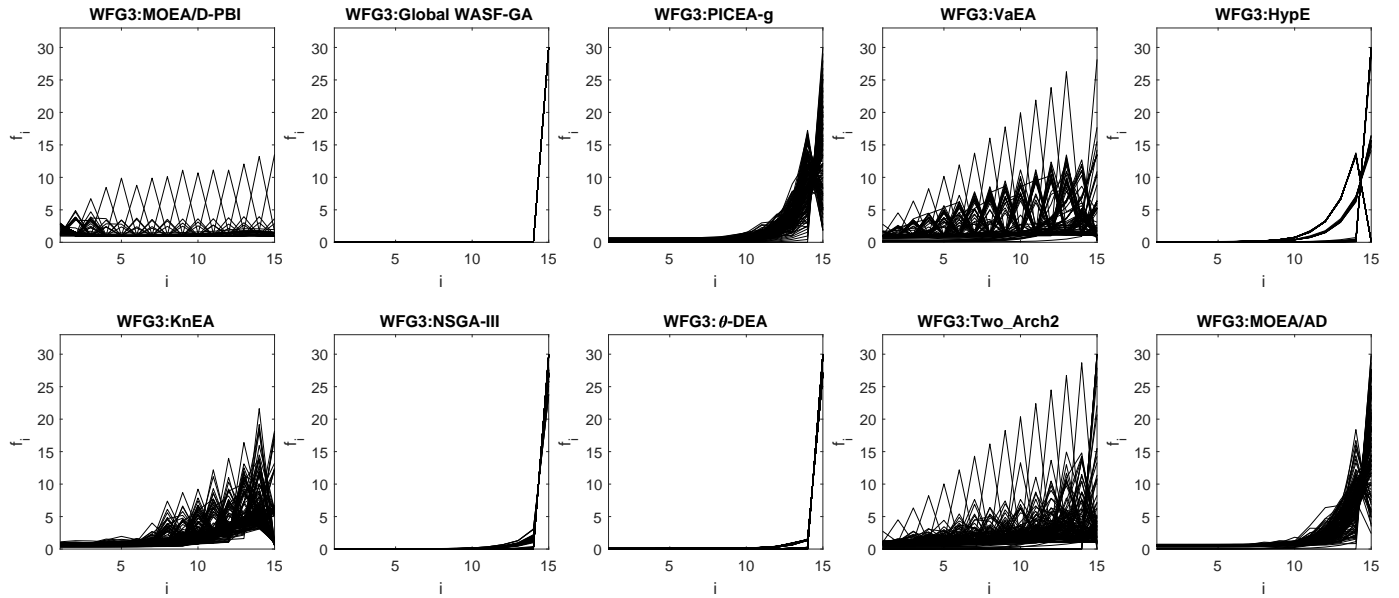


Fig. 122: Final solution sets on 15-objective WFG3 test problem obtained by 10 algorithms in the run of median HV metric values with $\mathbf{z}^r = (2, \dots, 2)^T$.

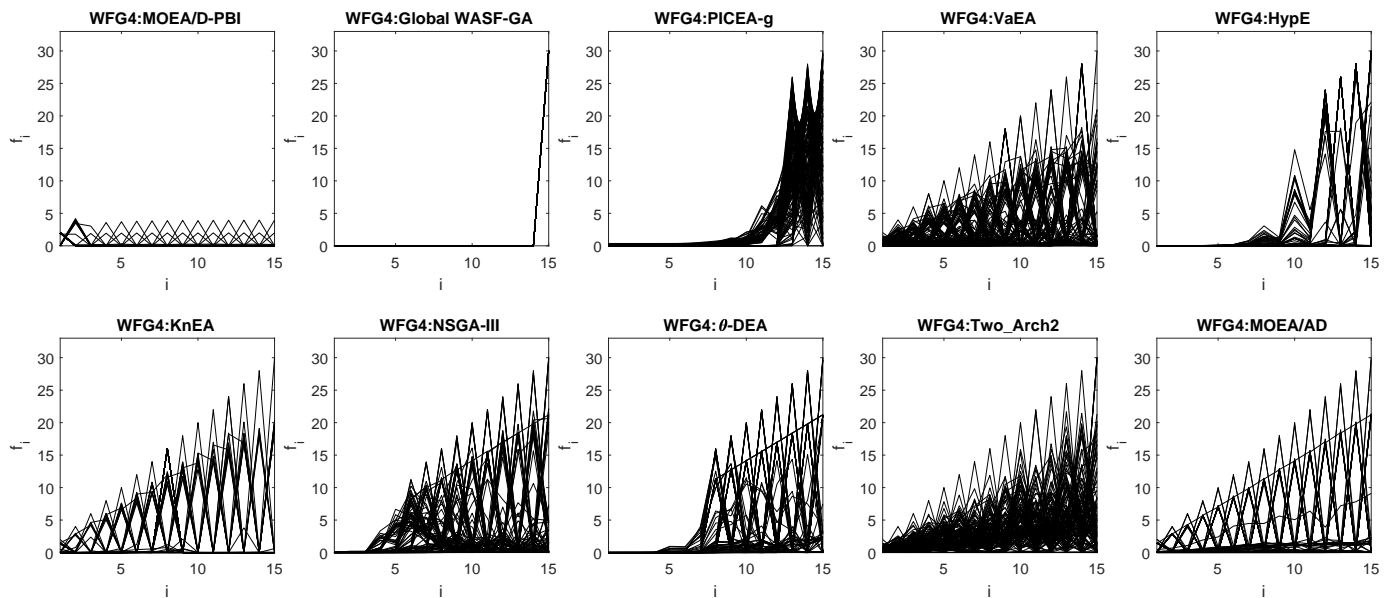


Fig. 123: Final solution sets on 15-objective WFG4 test problem obtained by 10 algorithms in the run of median HV metric values with $\mathbf{z}^r = (2, \dots, 2)^T$.

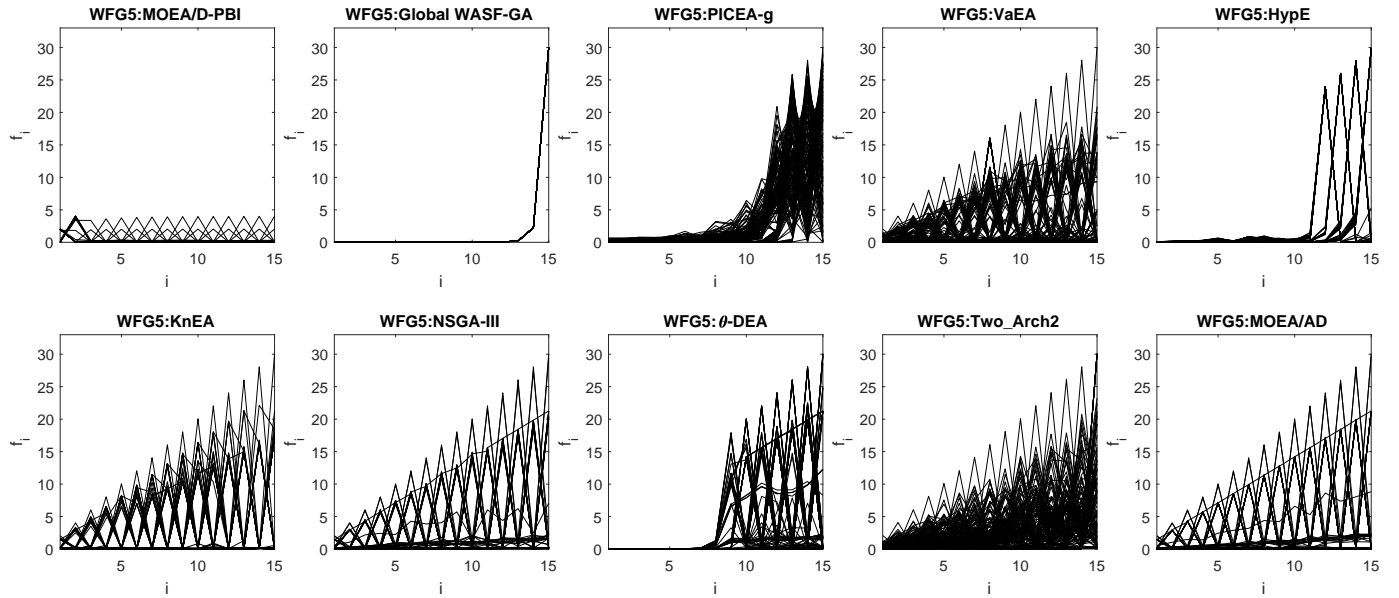


Fig. 124: Final solution sets on 15-objective WFG5 test problem obtained by 10 algorithms in the run of median HV metric values with $\mathbf{z}^r = (2, \dots, 2)^T$.

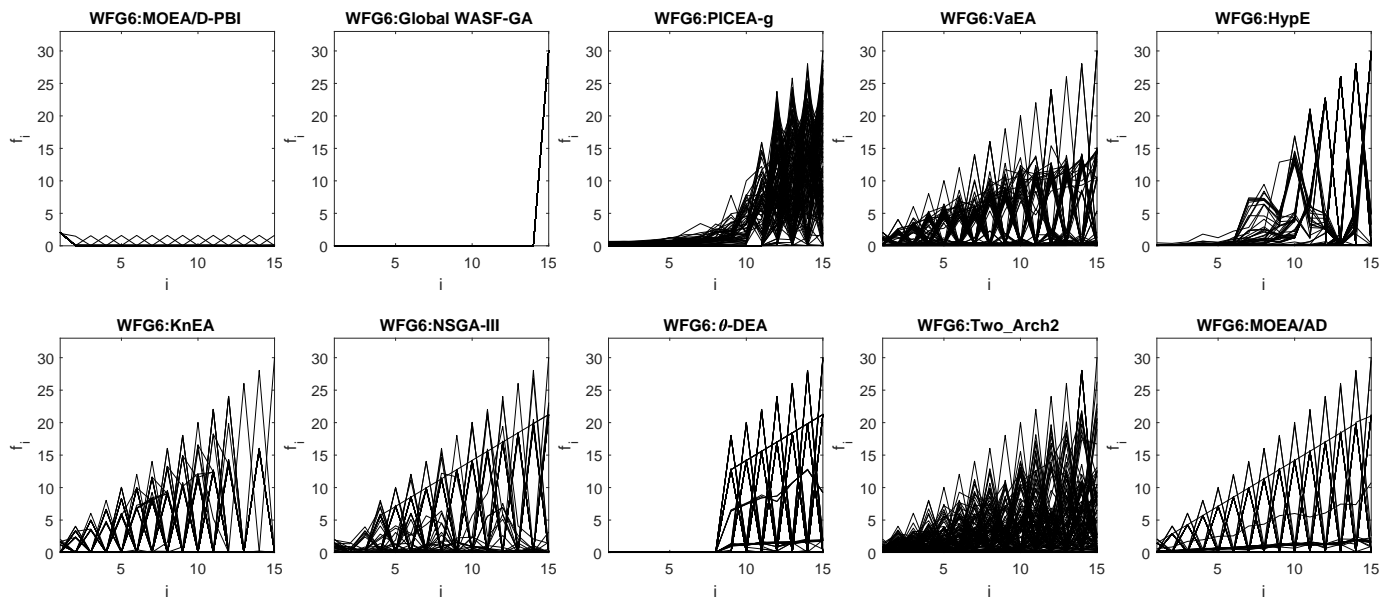


Fig. 125: Final solution sets on 15-objective WFG6 test problem obtained by 10 algorithms in the run of median HV metric values with $\mathbf{z}^r = (2, \dots, 2)^T$.

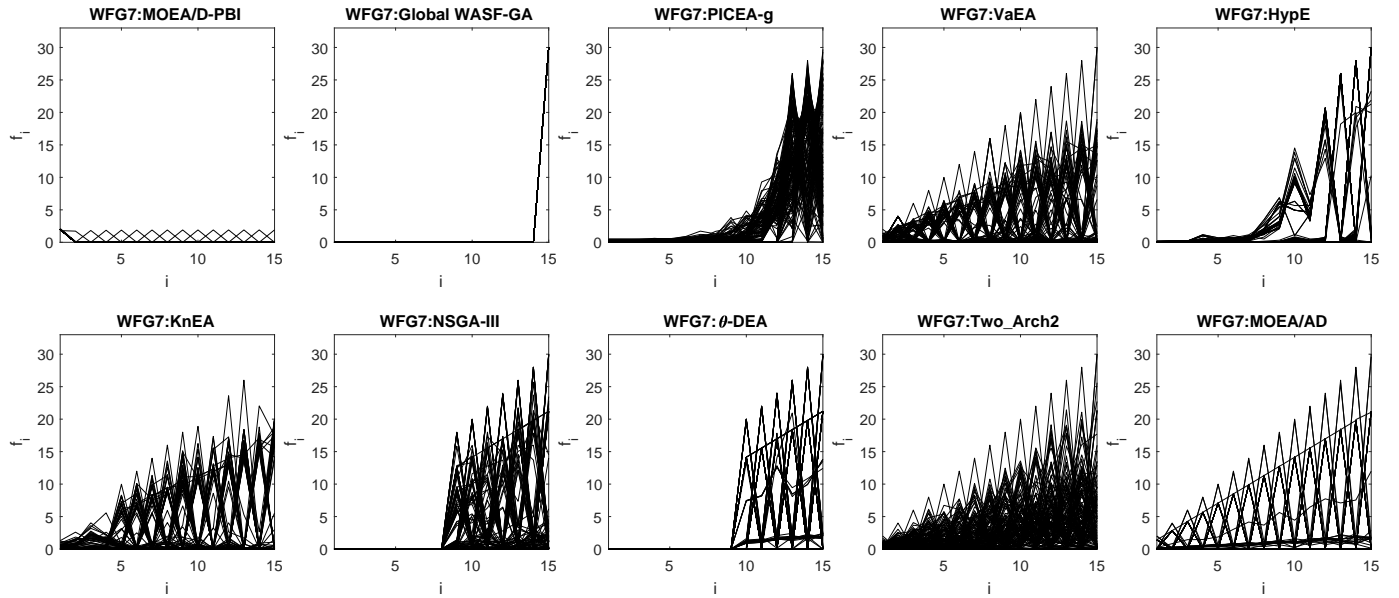


Fig. 126: Final solution sets on 15-objective WFG7 test problem obtained by 10 algorithms in the run of median HV metric values with $\mathbf{z}^r = (2, \dots, 2)^T$.

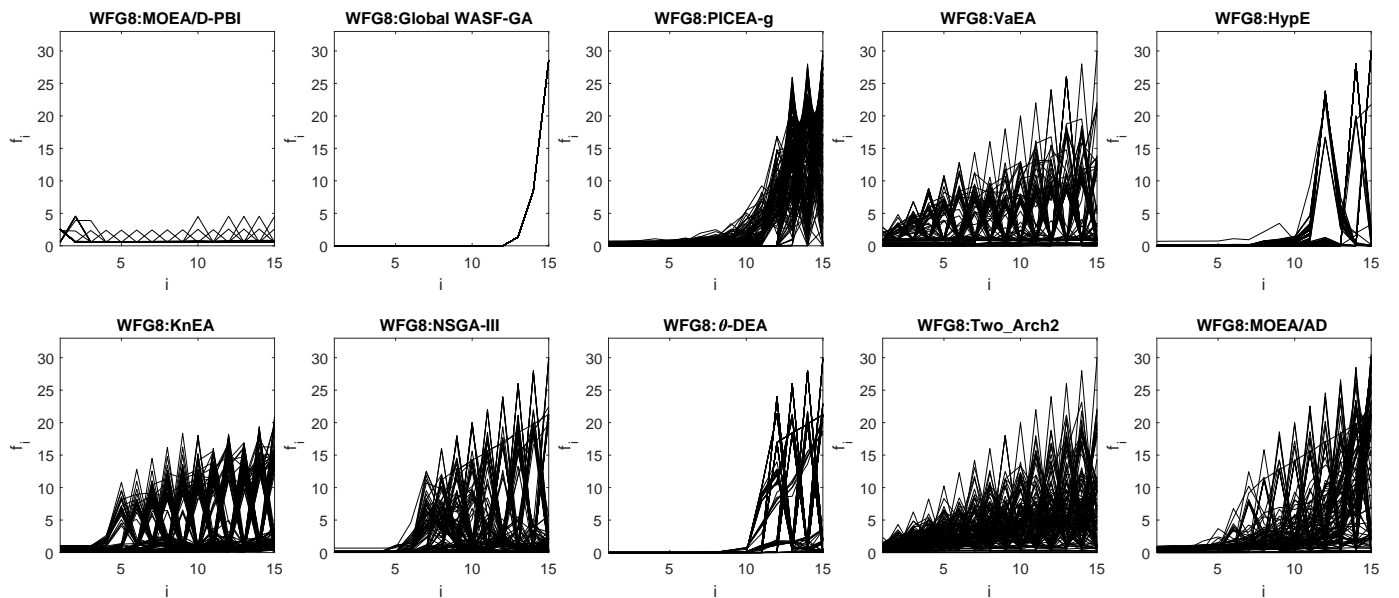


Fig. 127: Final solution sets on 15-objective WFG8 test problem obtained by 10 algorithms in the run of median HV metric values with $\mathbf{z}^r = (2, \dots, 2)^T$.

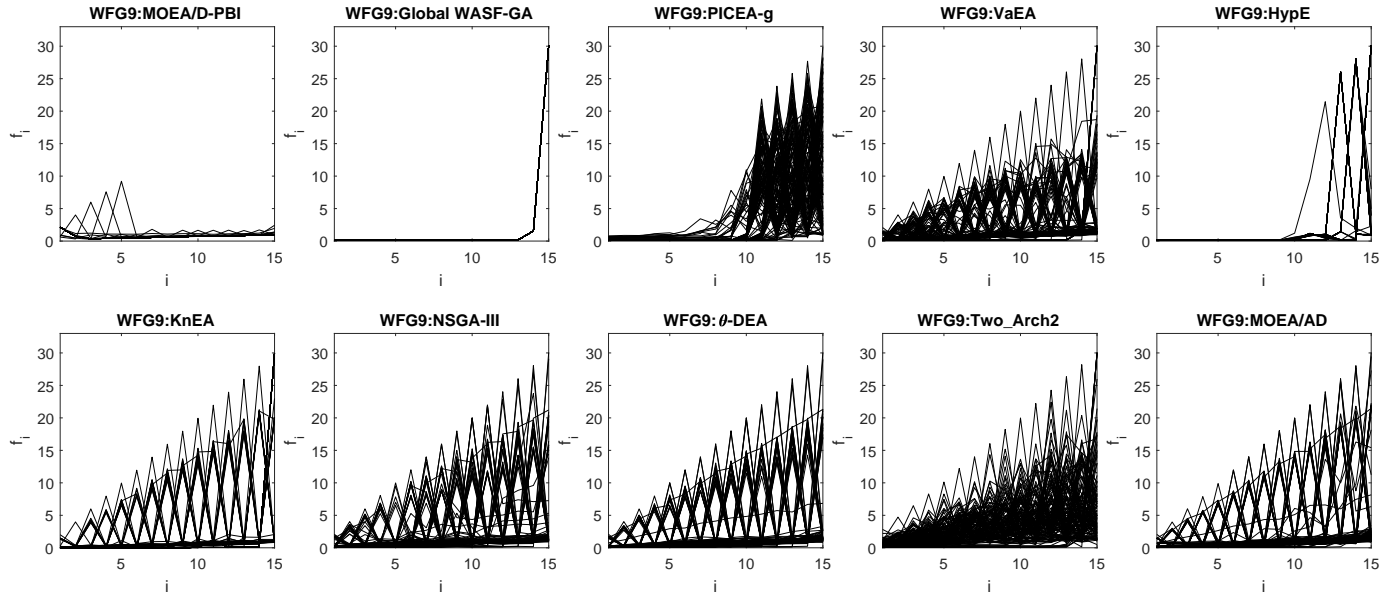


Fig. 128: Final solution sets on 15-objective WFG9 test problem obtained by 10 algorithms in the run of median HV metric values with $\mathbf{z}^r = (2, \dots, 2)^T$.

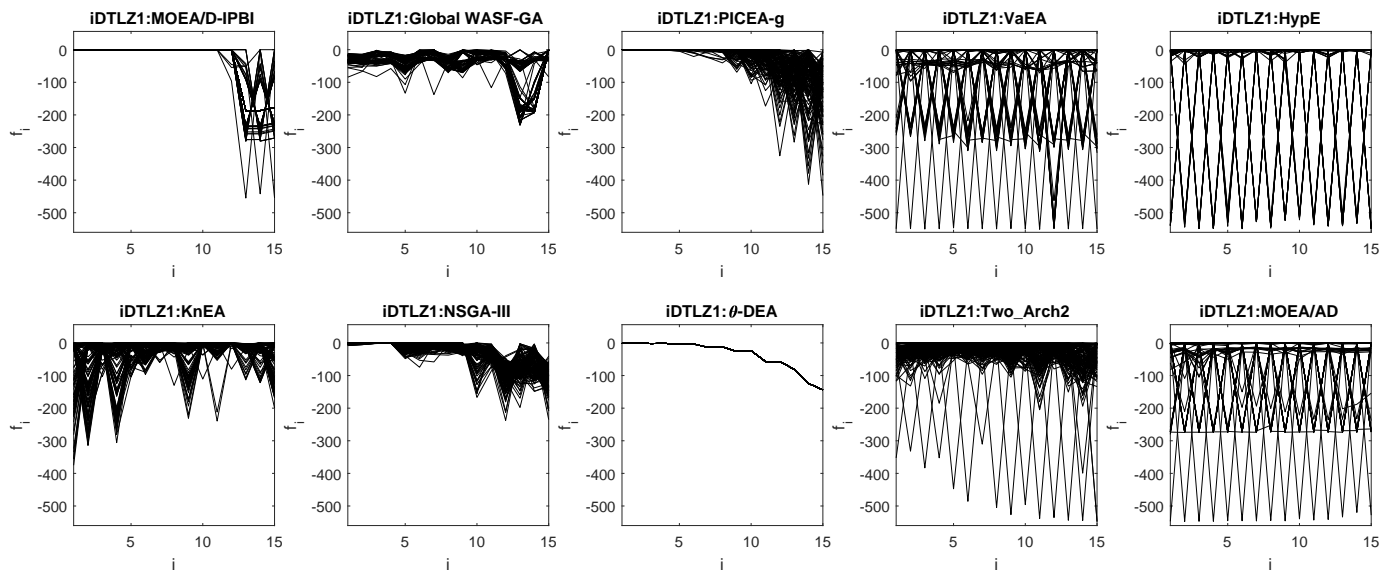


Fig. 129: Final solution sets on 15-objective DTLZ1⁻¹ test problem obtained by 10 algorithms in the run of median HV metric values with $\mathbf{z}^r = (2, \dots, 2)^T$.

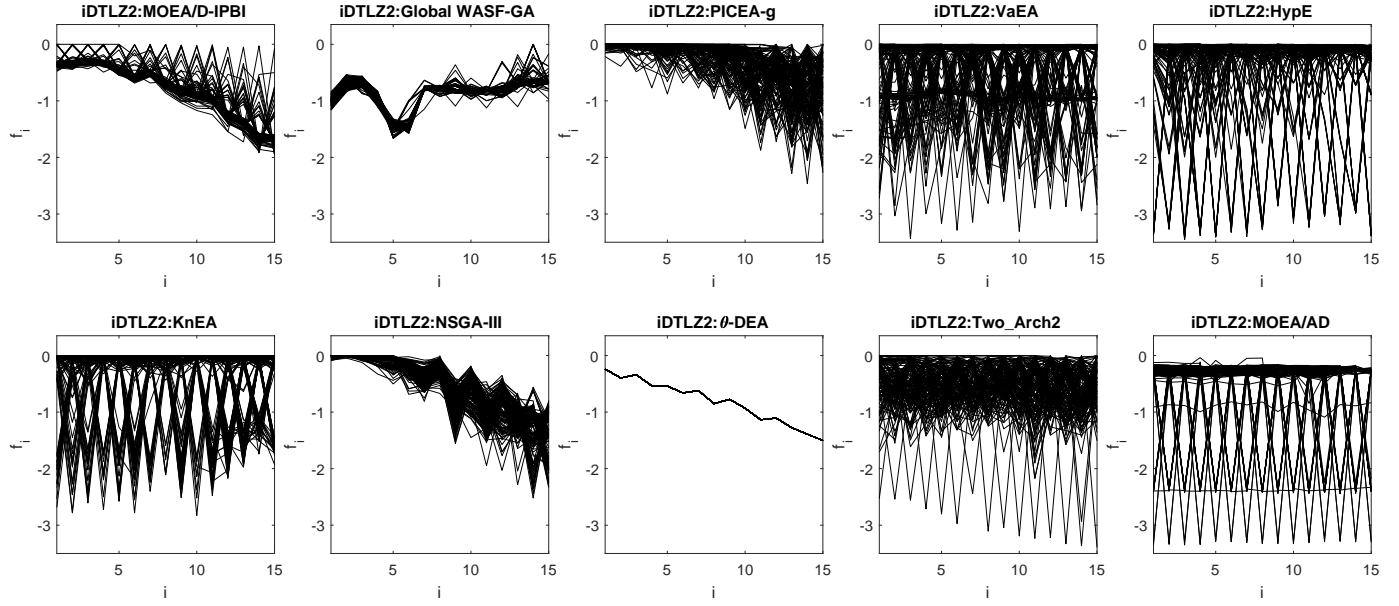


Fig. 130: Final solution sets on 15-objective DTLZ2⁻¹ test problem obtained by 10 algorithms in the run of median HV metric values with $\mathbf{z}^r = (2, \dots, 2)^T$.

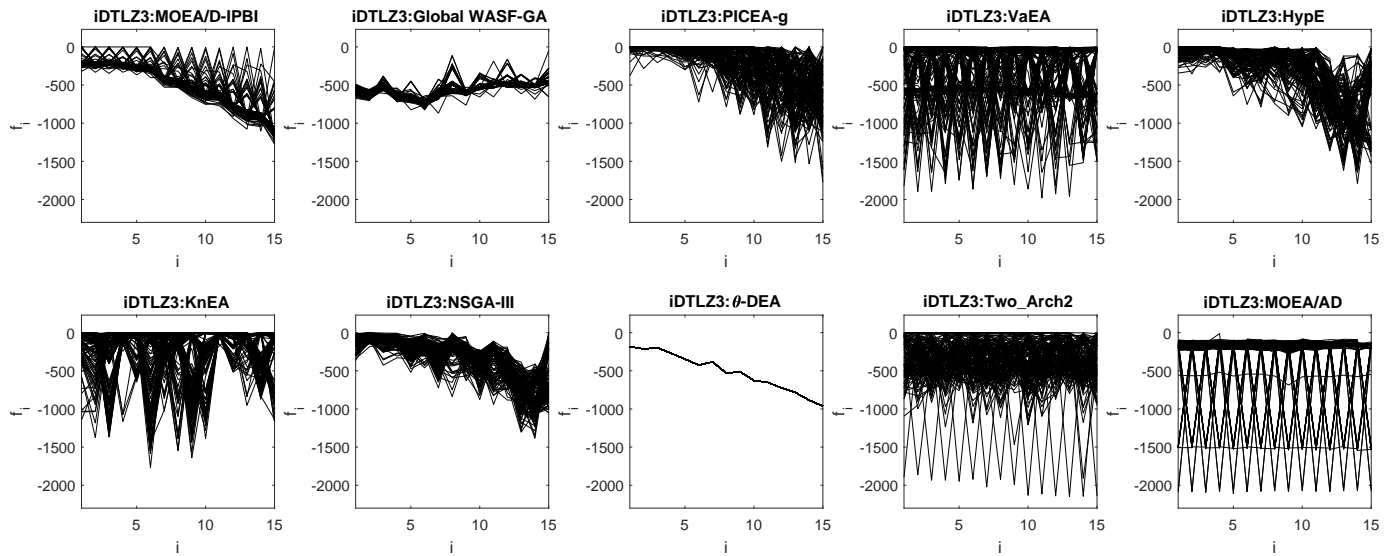


Fig. 131: Final solution sets on 15-objective DTLZ3⁻¹ test problem obtained by 10 algorithms in the run of median HV metric values with $\mathbf{z}^r = (2, \dots, 2)^T$.

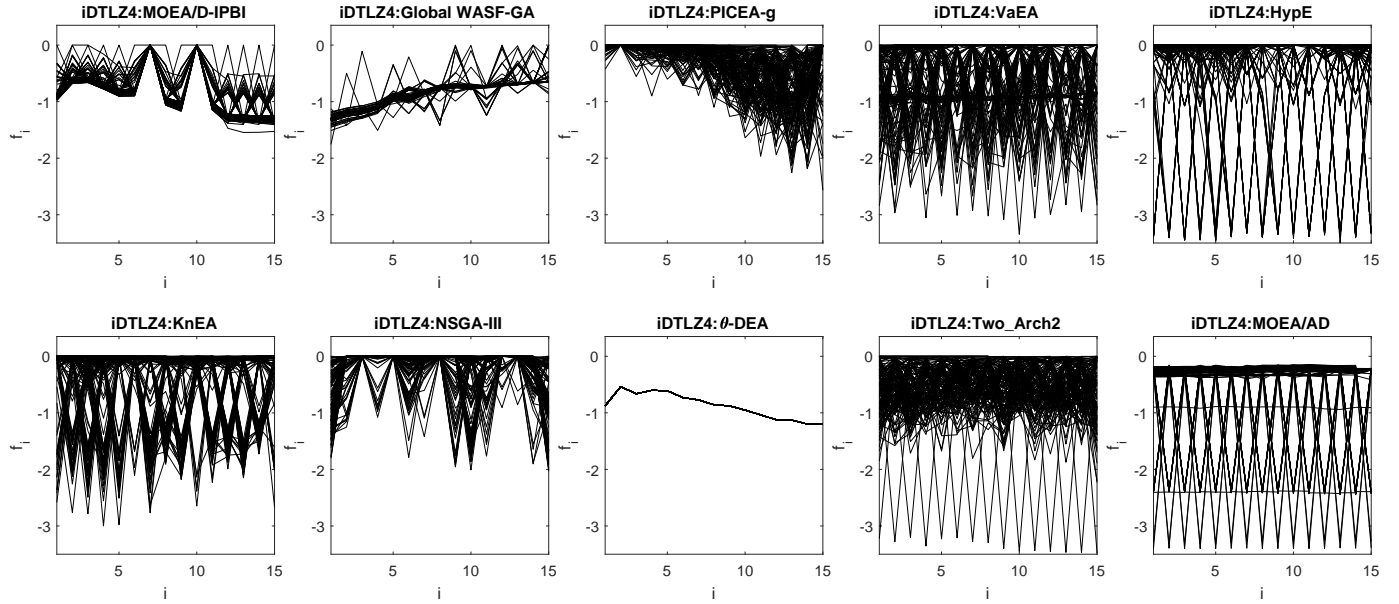


Fig. 132: Final solution sets on 15-objective DTLZ4^{-1} test problem obtained by 10 algorithms in the run of median HV metric values with $\mathbf{z}^r = (2, \dots, 2)^T$.

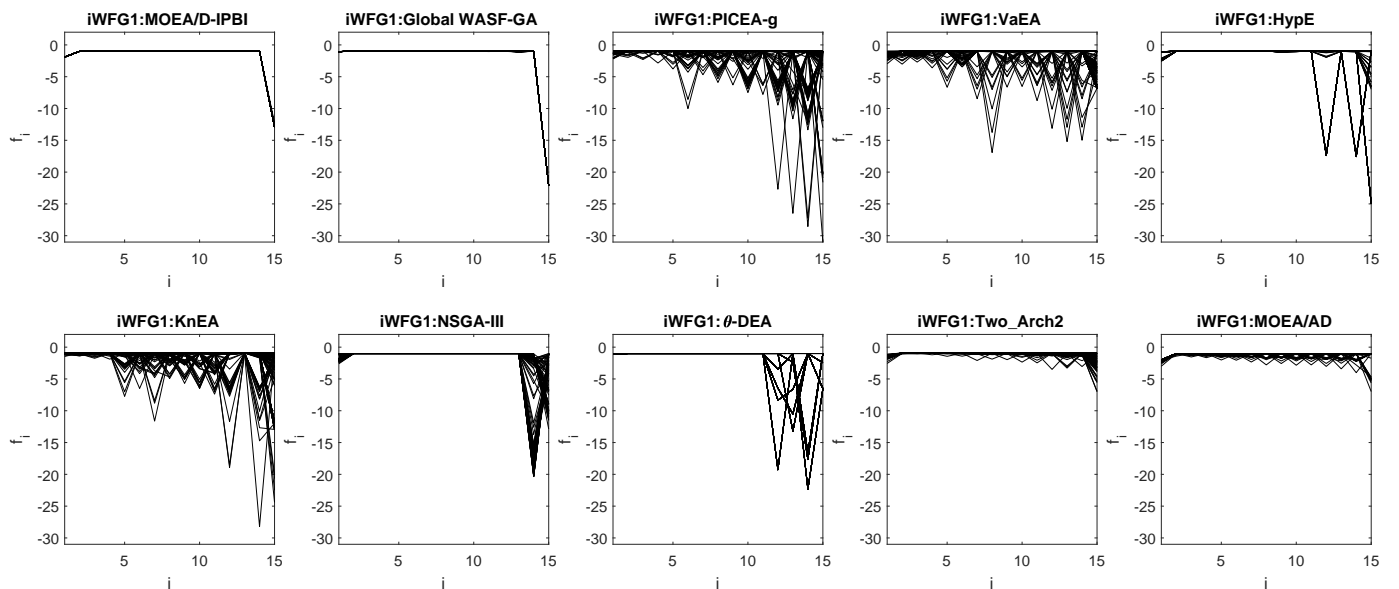


Fig. 133: Final solution sets on 15-objective WFG1^{-1} test problem obtained by 10 algorithms in the run of median HV metric values with $\mathbf{z}^r = (2, \dots, 2)^T$.

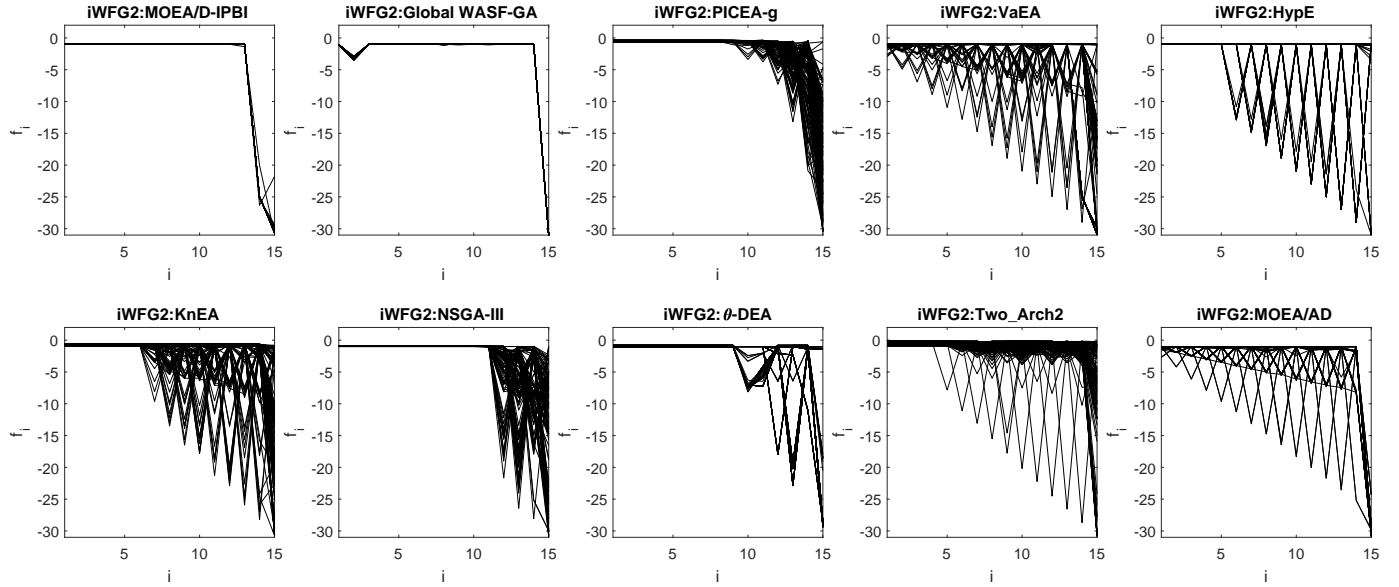


Fig. 134: Final solution sets on 15-objective WFG2^{-1} test problem obtained by 10 algorithms in the run of median HV metric values with $\mathbf{z}^r = (2, \dots, 2)^T$.

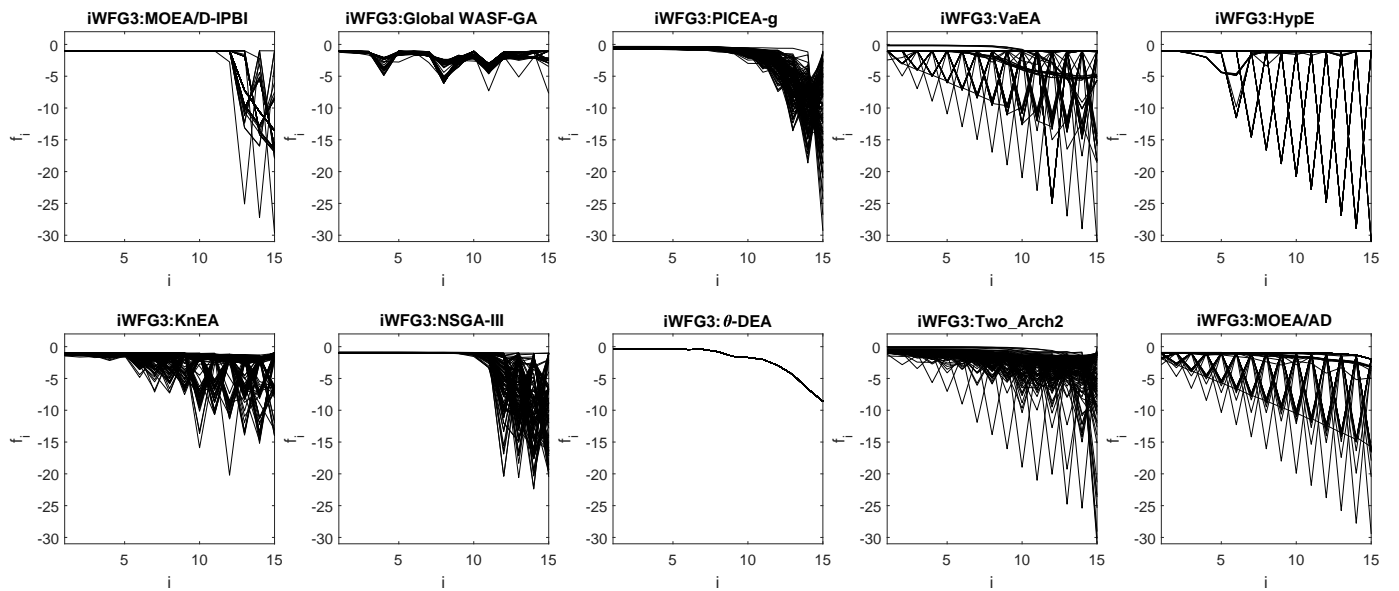


Fig. 135: Final solution sets on 15-objective WFG3^{-1} test problem obtained by 10 algorithms in the run of median HV metric values with $\mathbf{z}^r = (2, \dots, 2)^T$.

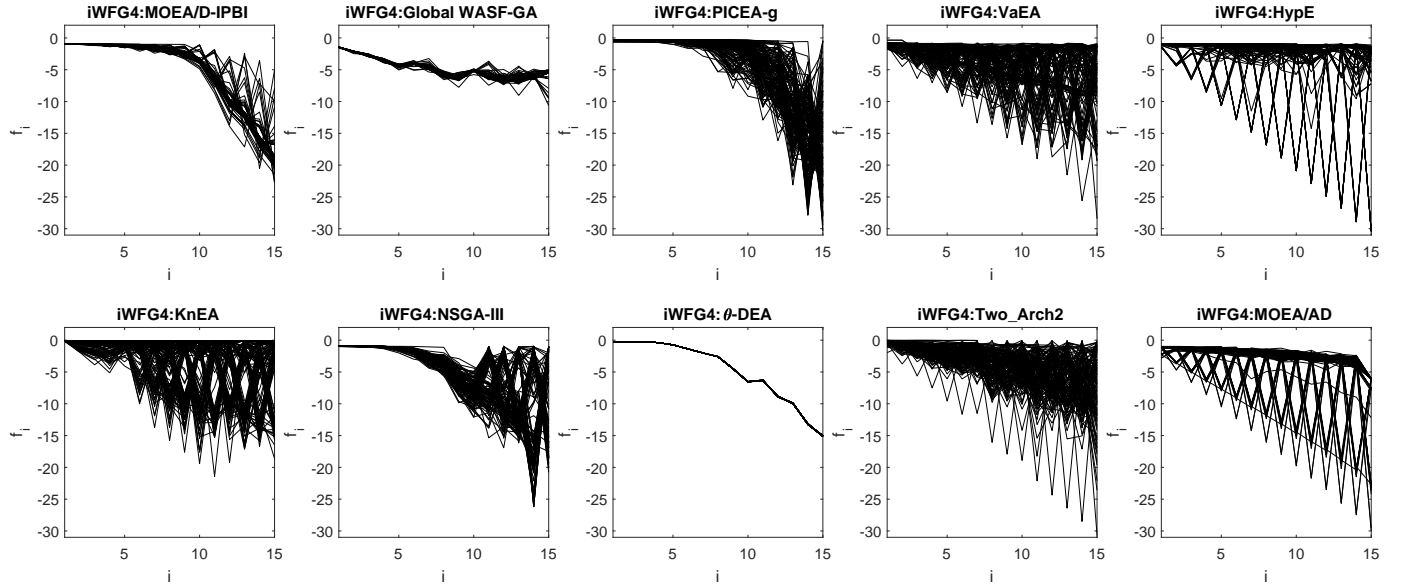


Fig. 136: Final solution sets on 15-objective WFG4^{-1} test problem obtained by 10 algorithms in the run of median HV metric values with $\mathbf{z}^r = (2, \dots, 2)^T$.

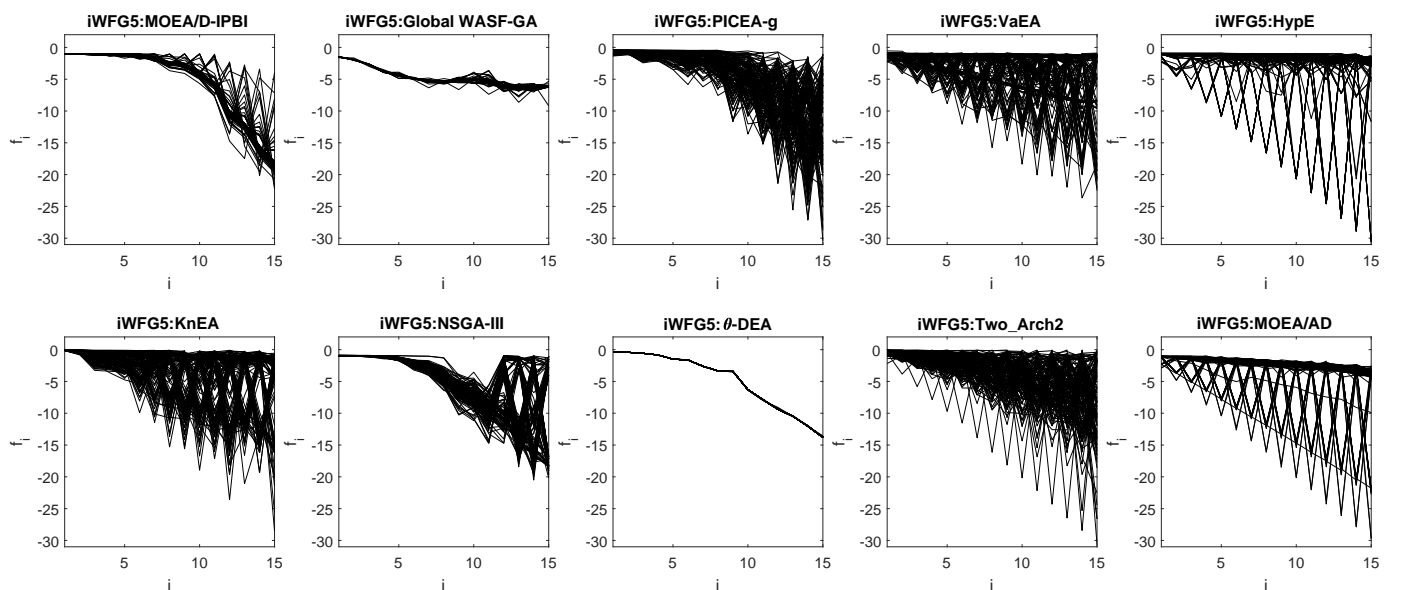


Fig. 137: Final solution sets on 15-objective WFG5^{-1} test problem obtained by 10 algorithms in the run of median HV metric values with $\mathbf{z}^r = (2, \dots, 2)^T$.

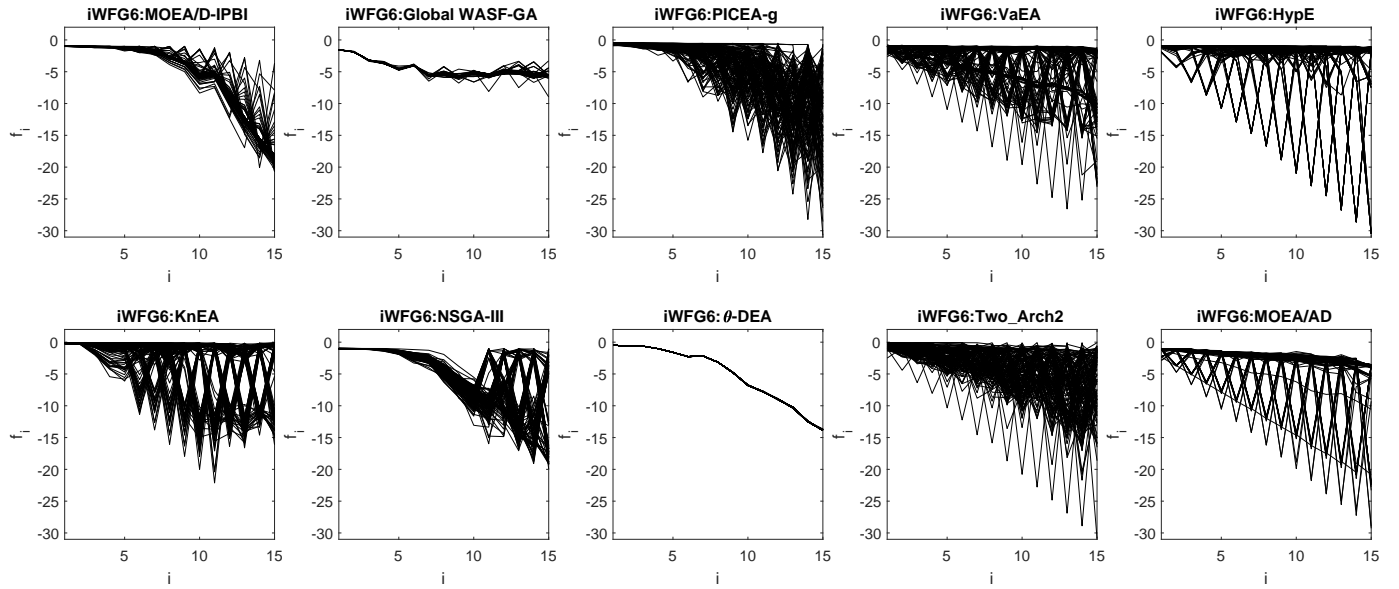


Fig. 138: Final solution sets on 15-objective WFG6^{-1} test problem obtained by 10 algorithms in the run of median HV metric values with $\mathbf{z}^r = (2, \dots, 2)^T$.

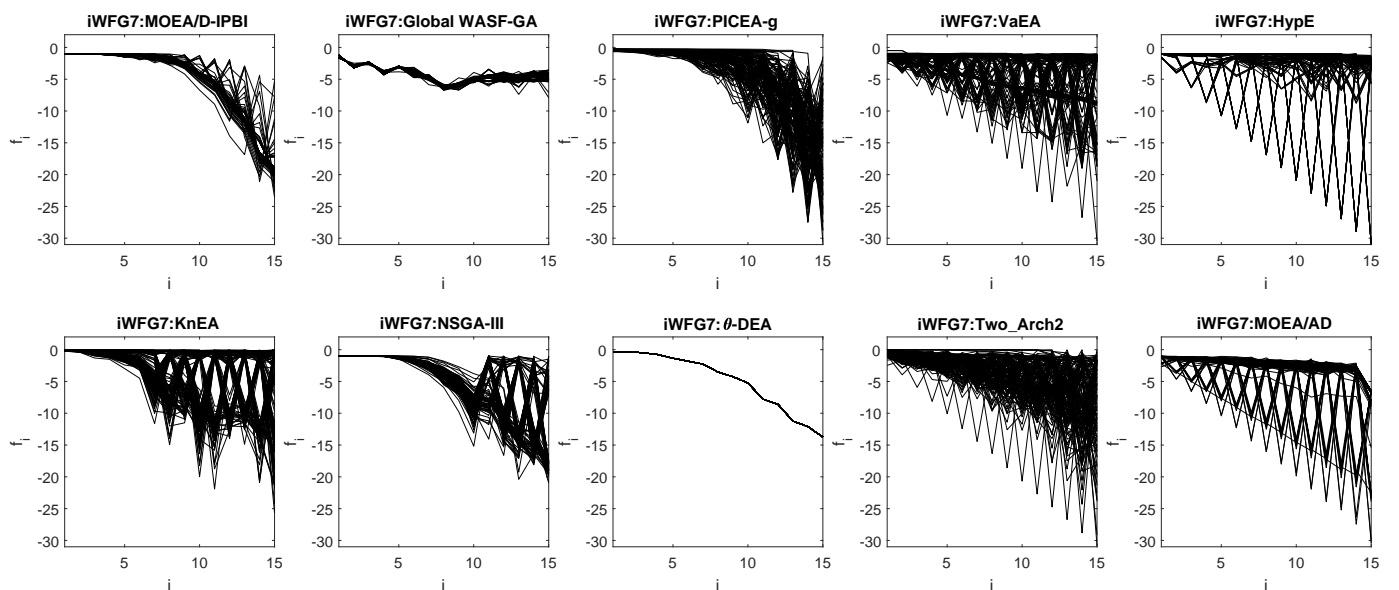


Fig. 139: Final solution sets on 15-objective WFG7^{-1} test problem obtained by 10 algorithms in the run of median HV metric values with $\mathbf{z}^r = (2, \dots, 2)^T$.

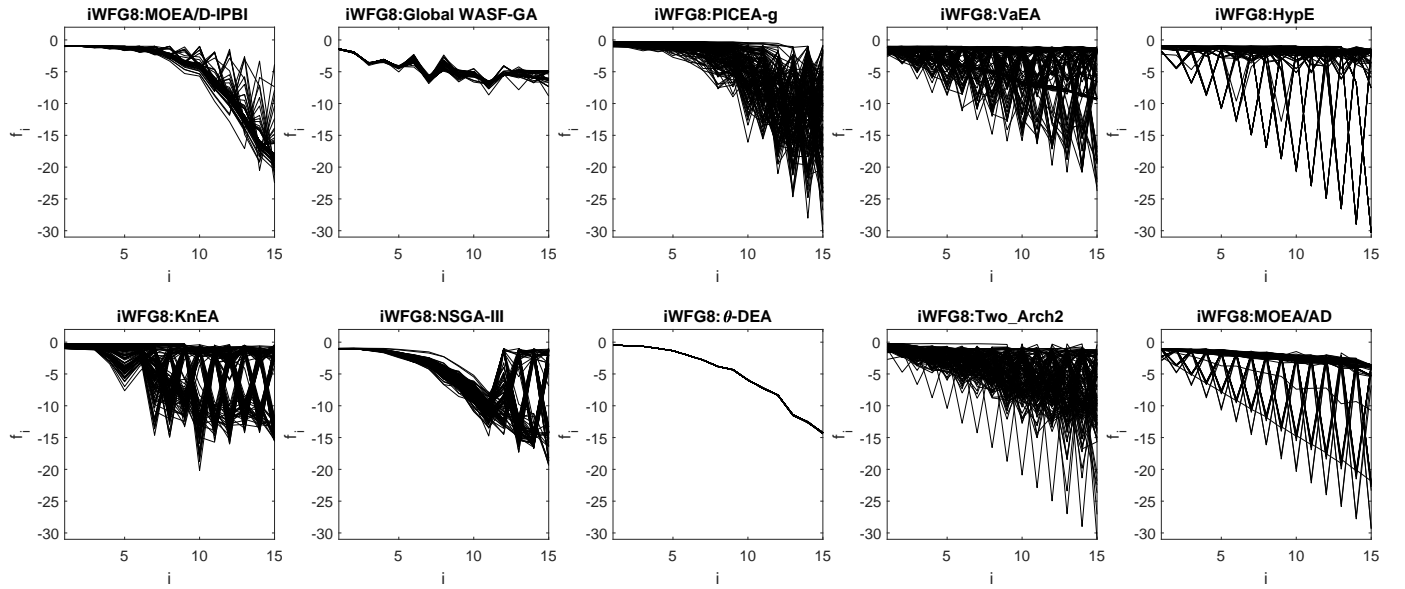


Fig. 140: Final solution sets on 15-objective WFG8^{-1} test problem obtained by 10 algorithms in the run of median HV metric values with $\mathbf{z}^r = (2, \dots, 2)^T$.

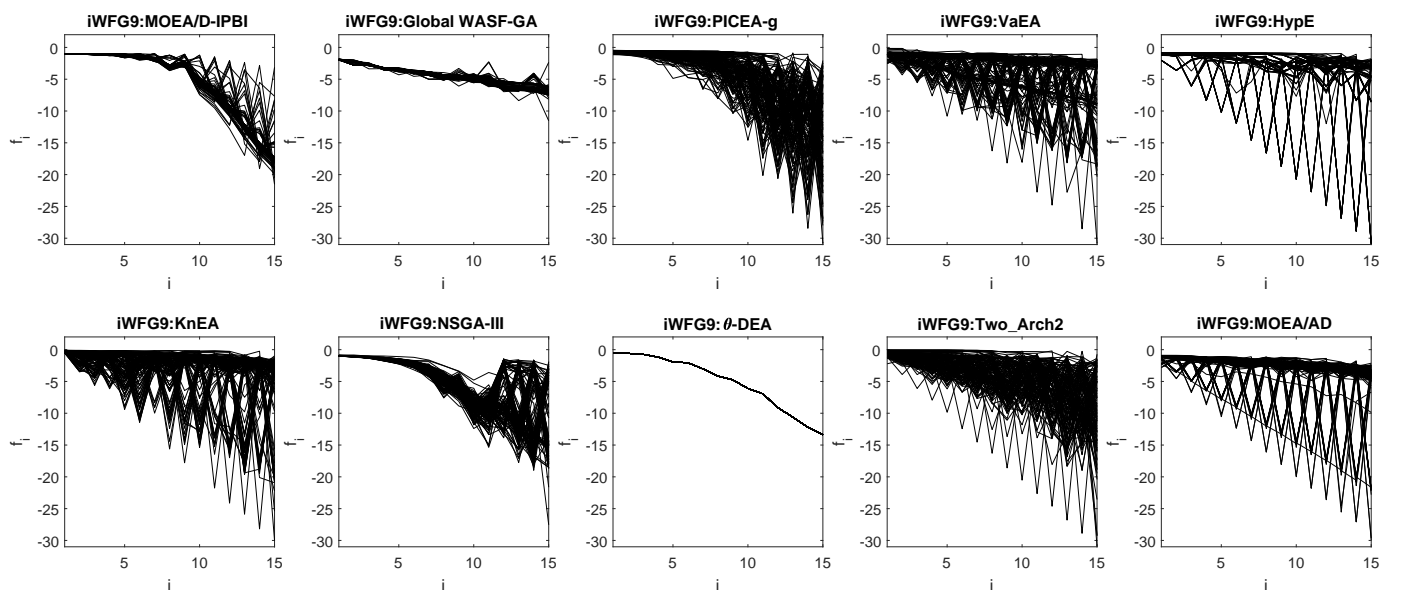


Fig. 141: Final solution sets on 15-objective WFG9^{-1} test problem obtained by 10 algorithms in the run of median HV metric values with $\mathbf{z}^r = (2, \dots, 2)^T$.

REFERENCES

- [1] H. Sato, “Inverted PBI in MOEA/D and its impact on the search performance on multi and many-objective optimization,” in *Genetic and Evol. Comput. Conference, GECCO ’14*, 2014, pp. 645–652.
- [2] H. Ishibuchi, Y. Setoguchi, H. Masuda, and Y. Nojima, “Performance of decomposition-based many-objective algorithms strongly depends on pareto front shapes,” *IEEE Trans. on Evol. Comput.*, vol. 21, no. 2, pp. 169–190, 2017.
- [3] Z. Wang, Q. Zhang, H. Li, H. Ishibuchi, and L. Jiao, “On the use of two reference points in decomposition based multiobjective evolutionary algorithms,” *Swarm and Evol. Comput.*, vol. 34, pp. 89–102, 2017.
- [4] K. S. Bhattacharjee, H. K. Singh, T. Ray, and Q. Zhang, “Decomposition based evolutionary algorithm with a dual set of reference vectors,” in *2017 IEEE Congress on Evol. Comput., CEC 2017, Donostia, San Sebastián, Spain, June 5-8, 2017*, 2017, pp. 105–112.
- [5] H. Ishibuchi, N. Akedo, H. Ohyanagi, and Y. Nojima, “Behavior of EMO algorithms on many-objective optimization problems with correlated objectives,” in *Proceedings of the IEEE Congress on Evol. Comput., CEC 2011, New Orleans, LA, USA, 5-8 June, 2011*. IEEE, 2011, pp. 1465–1472.
- [6] D. K. Saxena, J. A. Duro, A. Tiwari, K. Deb, and Q. Zhang, “Objective reduction in many-objective optimization: Linear and nonlinear algorithms,” *IEEE Trans. Evol. Comput.*, vol. 17, no. 1, pp. 77–99, 2013.
- [7] M. Wu, K. Li, S. Kwong, Y. Zhou, and Q. Zhang, “Matching-based selection with incomplete lists for decomposition multiobjective optimization,” *IEEE Trans. Evol. Comput.*, vol. 21, no. 4, pp. 554–568, 2017.